8-2018

Geomorphology of icy debris fans: Delivery of ice and sediment to valley glaciers decoupled from icecaps

R. Craig Kochel
Bucknell University, kochel@bucknell.edu

Jeffrey M. Trop
Bucknell University, jtrop@bucknell.edu

Robert W. Jacob
Bucknell University, rob.jacob@bucknell.edu

Recommended Citation
Kochel, R.C., Trop, J.M., and Jacob, R.W., (2018) Geomorphology of icy debris fans: Delivery of ice and sediment to valley glaciers decoupled from icecaps: Geosphere, v. 14, no. 4, p. 1710-1752.

Research Paper

GEOSPHERE

GEOSPHERE; v. 14, no. 4

https://doi.org/10.1130/GES01622.1

30 figures; 8 tables; 8 supplemental files

CORRESPONDENCE: kochel@bucknell.edu

CITATION: Kochel, R.C., Trop, J.M., and Jacob, R.W., 2018, Geomorphology of icy debris fans: Delivery of ice and sediment to valley glaciers decoupled from icecaps: Geosphere, v. 14, no. 4, p. 1710–1752, https://doi.org/10.1130/GES01622.1.

Science Editor: Shanaka de Silva

Received 18 October 2017
Revision received 10 January 2018
Accepted 12 April 2018
Published online 4 June 2018

[1]Supplemental Item A. Videos from helicopter showing site overviews. Please visit https://doi.org/10.1130/GES01622.S1 or the full-text article on www.gsapubs.org to view Supplemental Item A.

Geomorphology of icy debris fans: Delivery of ice and sediment to valley glaciers decoupled from icecaps

R. Craig Kochel, Jeffrey M. Trop, and Robert W. Jacob

Department of Geology and Environmental Geosciences, Bucknell University, Lewisburg, Pennsylvania 17837, USA

ABSTRACT

The pace and volume of mass flow processes contributing ice and sediment to icy debris fans (IDFs) were documented at sites in Alaska and New Zealand by integrating field observations, drone and time-lapse imagery, ground penetrating radar, and terrestrial laser scanning. Largely unstudied, IDFs are supraglacial landforms at the mouths of bedrock catchments between valley glaciers and icecaps. Time-lapse imagery recorded 300–2300 events reaching 15 fans during intervals from nine months to two years. Field observations noted hundreds of deposits trapped within catchments weekly that were later remobilized onto fans. Deposits were mapped on images taken three to four times per day. Most events were ice avalanches (58%–100%). Slush avalanches and/or flows were common in spring and fall (0%–65%). Icy debris flows were <5% of the events, observed only at sites with geomorphically complex catchments. Rockfalls were common within catchments; few directly reached a fan. Site selection provided a spectrum of catchment relationships between icecaps and fans. The largest most active fans occur below hanging glaciers or short chutes between the icecap and glacier and were dominated by ice avalanches, slush avalanches, and slush flows. Larger, complex catchments allowed temporary storage of ice and sediment that were later remobilized into ice and slush avalanches and debris flows. Unlike alluvial settings where larger fans are associated with larger catchments, there are variable relationships between IDF area and catchment area.

Exceptionally active and dynamic compared to alluvial fans, the studied IDFs exhibited annual resurfacing rates of 300%–>4000%. Annual contributions by mass flows ranged from 133,200 to 5,200,000 m³, representing 3%–56% of fan volume. Although ablation occurred, mainly during summers, significant ice transfer occurred through fan subsurface areas to adjacent valley glaciers. Icy debris fans annually contributed <1%–~24% of the mass of adjacent valley glaciers. Small glaciers (e.g., McCarthy Glacier, Alaska) showed minor thinning (<1 m/yr) compared to larger glaciers (e.g., La Perouse, Douglas, and Mueller Glaciers, New Zealand) that lost >5–10 m/yr over the hundreds of meters of valley glacier adjacent to the IDFs studied. Some IDFs lengthened in response to thinning of valley glaciers. Icy debris fans supplied significant ice and sediment to valley glaciers, slowing the rate of deglaciation. Results of this study have implications toward managing hazards and predicting glacial mass balance in alpine regions. For example, having quantitative information about the role of ice contribution from IDFs to valley glaciers may result in forecasting a lower rate of deglaciation than traditionally recognized for some glaciers decoupled from icecaps.

INTRODUCTION

Previous studies of deglaciating landscapes, formed during periods referred to as paraglacial (Church and Ryder, 1972), documented rapid development of alluvial fans and talus cones; however, the role of ice and ice-dominated mass wasting processes on landform evolution is less well documented. In deglaciating environments, it is common to find valley glaciers that are not directly connected to high-level icecaps but receive contributions of ice and sediment from the icecap and bedrock walls by mass wasting. Fan-shaped landforms, referred to as icy debris fans (IDFs; Kochel and Trop, 2012), occur at the base of escarpments separating the valley glaciers from the icecaps. Icy debris fans form at the mouths of small, incised bedrock catchments and prograde onto valley glaciers as supraglacial landforms (Fig. 1; refer to Supplemental Item A[1] for helicopter videos showing geomorphic settings of IDFs). Ice and sediment, sometimes stored temporarily along catchment channels, emerge through fan apexes and move onto the fans through a variety of mass flow processes, typically transforming along the flow path (Kochel and Trop, 2012). Icy debris fans are exceedingly active geomorphic environments, with >2000 depositional events reaching some IDFs annually (Reid, 2015). Most IDFs become thick enough to experience ice flow (deform) as small glaciers with active crevasse systems and deliver ice to subjacent valley glaciers (Kochel and Trop, 2012).

Dominantly fueled by ice avalanches, IDFs are especially active during early stages of the paraglacial phase of deglaciation (Kochel and Trop, 2012). Thus, transfer of ice from IDFs to valley glaciers may play an important role in the mass balance of valley glaciers, especially where valley glaciers have decoupled from their icecap region (Kochel and Trop, 2008, 2012). Most valley glaciers worldwide have receded and thinned in recent decades (Vaughan et al., 2013), including glaciers at our study sites in the Southern Alps of New Zealand (Chinn et al., 2005; Salinger et al., 2008) and Wrangell Mountains of Alaska (Das et al., 2014). The pace of change varied significantly between sites

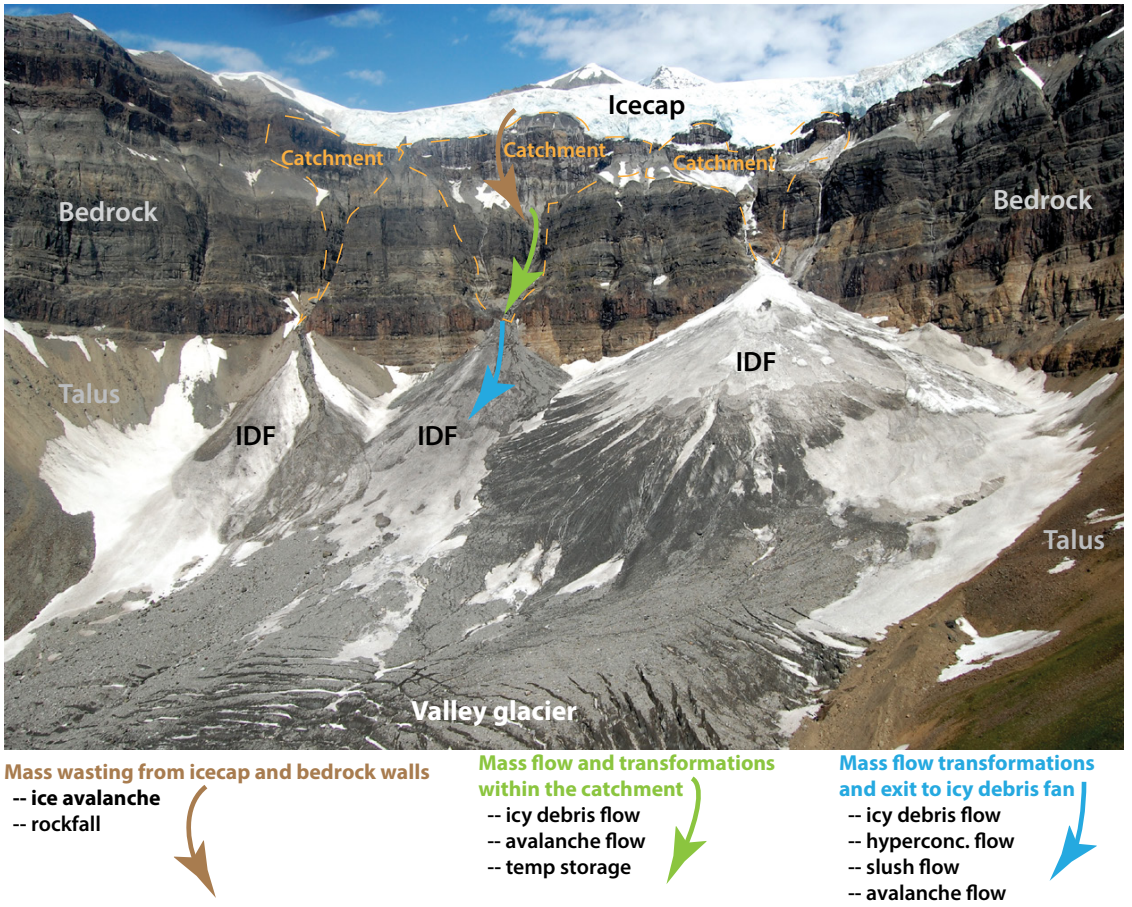

Figure 1. Geomorphic processes important to icy debris fans and their catchments. Mass wasting (brown arrow) delivers ice and sediment to catchments by calving and ice avalanches from the icecaps and rockfall from bedrock walls. Sometimes these materials undergo flow transformations, delivering mass flows directly to the fans. Ice and sediment are sometimes deposited in the catchments (green arrow) and stored temporarily as small icy debris fans (IDFs), icy talus, and talus cones. Subsequent avalanches and small outbursts (jökulhlaups) remobilize stored ice and sediment, resulting in a range of mass flow transformations (ice avalanches, slush flows, icy debris flows, and hyperconcentrated flows) that deliver ice and/or sediment to IDFs (blue arrow).

as a result of many factors, including glacier size and amount of debris production and debris cover (Chinn et al., 2014).

Kochel and Trop (2012) showed that IDFs differ from other landforms common in alpine hillslope settings, including talus cones, avalanche cones, reconstituted glaciers, rock glaciers, and alluvial fans. Unlike talus cones, IDFs consist dominantly of ice as opposed to sediment. Ice avalanches fall directly onto avalanche cones without the influence of a catchment (King, 1959; Alean, 1985a, 1985b; Owen and Derbyshire, 1989; Matthews and McCarroll, 1994; Decaulne and Sæmundsson, 2006, 2010; Masiokas et al., 2010). In contrast, avalanche material is typically transported to IDFs after landing in a catchment and transforming downslope into mass flows. Most avalanche cones completely ablate annually, unlike IDFs. Amorphous landforms known as reconstituted glaciers (King and Ives, 1956; Benn and Evans, 1998; Benn and Owen, 2002; Benn et al., 2003) form at the base of escarpments supplied by ice avalanches wasted from icecaps without focusing ice through a catchment. In contrast, IDFs are formed by ice avalanches cascading into discrete catchments where a variety of flow transformations may take place before emerging onto the fan apex. Icy debris fans differ from rock glaciers (i.e., Potter, 1972; White, 1976; Martin and Whalley, 1987; Giardino and Vitek, 1988; Hamilton and Whalley, 1995). Unlike rock glaciers, IDFs have a fan-shaped geometry resulting from frequent delivery of ice and sediment from a distinctive point-source (apex) fed by a small catchment. Icy debris fans are similar to alluvial fans except they are composed of ice and their depositional processes are ice-dominated mass flows (ice avalanches, slush flows, and slush avalanches) with subordinate sediment delivered by less common debris flow and/or hyperconcentrated flow processes (Kochel and Trop, 2012).

Event Log -- Douglas Neve-Glacier New Zealand -- January 2013			
January 6, 2013			
Time	**Location**	**Size**	**Notes**
0800	1	A	Apex
0807	2	A	Apex
0820	3	B	
0825	1	A	Upper midfan
0830	5-6	AA	Across fan – vid
0841	3	A	On fan
0850	0	B	
0854	0	C	
0855	2	C	
0857	2	C	
0912	2-3	B	
0922	6	B	
0924	4	C	Above
0926	3	C	Above
0929	4	C	Above
0935	5-6	C	Above
0940	4	B	

[2]Supplemental Item B. Table summarizing direct field-based observations of depositional events, including event type, size, and location. Please visit https://doi.org/10.1130/GES01622.S2 or the full-text article on www.gsapubs.org to view Supplemental Item B.

Whereas most alpine landforms have been well studied, IDFs are poorly understood beyond reconnaissance-scale field studies owing to their especially remote, rugged, and hazardous setting (Kochel and Trop, 2008, 2012). This study addresses four key questions to provide a better understanding of the quantitative aspects of IDF morphodynamics: (1) What is the nature, rate, and volume of IDF depositional processes throughout the year? (2) How does catchment morphology influence the nature of IDF depositional processes? (3) To what extent is the area and volume of IDFs changing? To what extent is the area and volume of valley glaciers adjacent to IDFs changing? (4) What is the linkage between IDFs and their associated valley glaciers, including the role of IDFs in valley glacier mass balance?

To answer these questions, we integrated several techniques during five field surveys in Alaska and New Zealand during 2013–2015, including: (1) direct field observations to document the nature and size of depositional processes and deposits; (2) time-lapse cameras to document the frequency and volume of new deposits; (3) repeat terrestrial laser scanning (TLS) surveys to quantify changes in IDF morphology and provide scales for time-lapse imagery; (4) ground penetrating radar (GPR) surveys to investigate subsurface architecture and linkage between IDFs and valley glaciers; and (5) drone and helicopter imagery to document catchment morphology not accessible by foot traverse. Details on these methods are introduced sequentially as data sets are presented. This paper reports the first quantitative observations of the nature and pace of depositional activity on IDFs, the area and volume of new deposits, and morphological and volumetric changes of IDFs and their associated valley glaciers. The new results, when integrated with previous reconnaissance-scale, non-quantitative field studies (Kochel and Trop, 2008, 2012), provide an improved understanding of IDF dynamics.

This study examines IDFs in the temperate subarctic Wrangell Mountains of Alaska (McCarthy Creek Glacier) and in the temperate mid-latitude Southern Alps of New Zealand (Douglas Glacier, Mueller Glacier, and La Perouse Glacier) (Fig. 2). Sites were selected to provide a range of catchment morphology and interaction with the valley glaciers. McCarthy Glacier provides a cirque setting where fan axes are parallel to the valley glacier axis. Also a cirque setting, IDFs at Douglas Glacier prograde approximately perpendicular to the valley glacier axis. Mueller Glacier IDFs occur below a hanging glacier and prograde approximately perpendicular to the valley glacier axis. Icy debris fans at La Perouse Glacier prograde approximately perpendicular to the valley glacier axis; however, unlike the other settings, the upper part of the valley glacier remains connected to an icecap.

DEPOSITIONAL PROCESSES ON ICY DEBRIS FANS

Overview and Methods

Field studies allowed us to directly observe and document active depositional processes and install time-lapse cameras. McCarthy Glacier, Alaska, was visited for week-long periods in July 2006, July–August 2010, July 2013, and June–July 2015. New Zealand sites (Mueller, La Perouse, and Douglas Glaciers) were visited for one- to two-day periods in August 2009 and June 2010, and for two-week periods in January 2013, March 2014, and March 2015, and a field photo-survey in December 2016.

Field work provided exceptional opportunities to carefully document the nature of depositional processes during and immediately after emplacement, characterize the sedimentology and morphology of deposits, and collect morphologic measurements of recent deposits (deposit length, width, and thickness). Our field time allowed us to directly observe >1445 events over 33 days (Supplemental Item B[2]) as they happened on IDFs and in their catchments, allowing us to observe downslope transformations in the nature of mass flows and determine how different processes can be distinguished based on their morphology and sedimentology. We also imaged new deposits daily from a helicopter and drone for geomorphic mapping. Preliminary estimates of deposit settlement and/or compaction and ablation were also made using stakes, but these do not represent a detailed ablation investigation.

Time-lapse cameras (nine total) were installed at all four sites during the 2013–2015 study period. Due to equipment malfunctions and rockfall damage, none of the cameras operated for the entire three-year deployment. Time-lapse cameras captured two to three images per day at each of the four sites for periods ranging from eight months to two years. Over 4000 images and hundreds of videos were used to analyze depositional activity. Time-lapse images were studied individually to classify and map each depositional event. Event type was interpreted based on comparisons of imagery with morphologies of active processes observed directly in the field. Given that small-scale events observed during field work are not visible on time-lapse cameras, the frequency and volume of deposits documented are conservative minimum estimates.

Icy debris fans are the geomorphic products (landforms) resulting from degradation of icecaps by ice-dominated mass wasting processes. Similar to alluvial fans in water-dominated settings, IDFs are conical depositional landforms that have sediment delivered to them through their apexes from a channel emerging from a small bedrock catchment. Unlike alluvial fans, IDFs are composed chiefly of ice, and their depositional processes are mainly ice-dominated mass flows. Material wasted from the icecap can be delivered directly to the IDF, or it may undergo flow transformations within the catchment en route to an IDF. Depositional processes include ice avalanches, slush avalanches, slush flows, icy debris flows, rockfalls, and occasional massive icy rock avalanches. Below we summarize our current understanding of each depositional process, integrating our previous and new field observations of active processes with time-lapse imagery.

Rockfall and Icy Rock Avalanches

Rockfall and rock avalanches are characterized by falling and sliding processes with sparse or no water. Rockfalls occur primarily within IDF catchments (Supplemental Item B [footnote 2]). Most rockfall deposits are stored temporarily within catchments on talus cones or along bedrock channels.

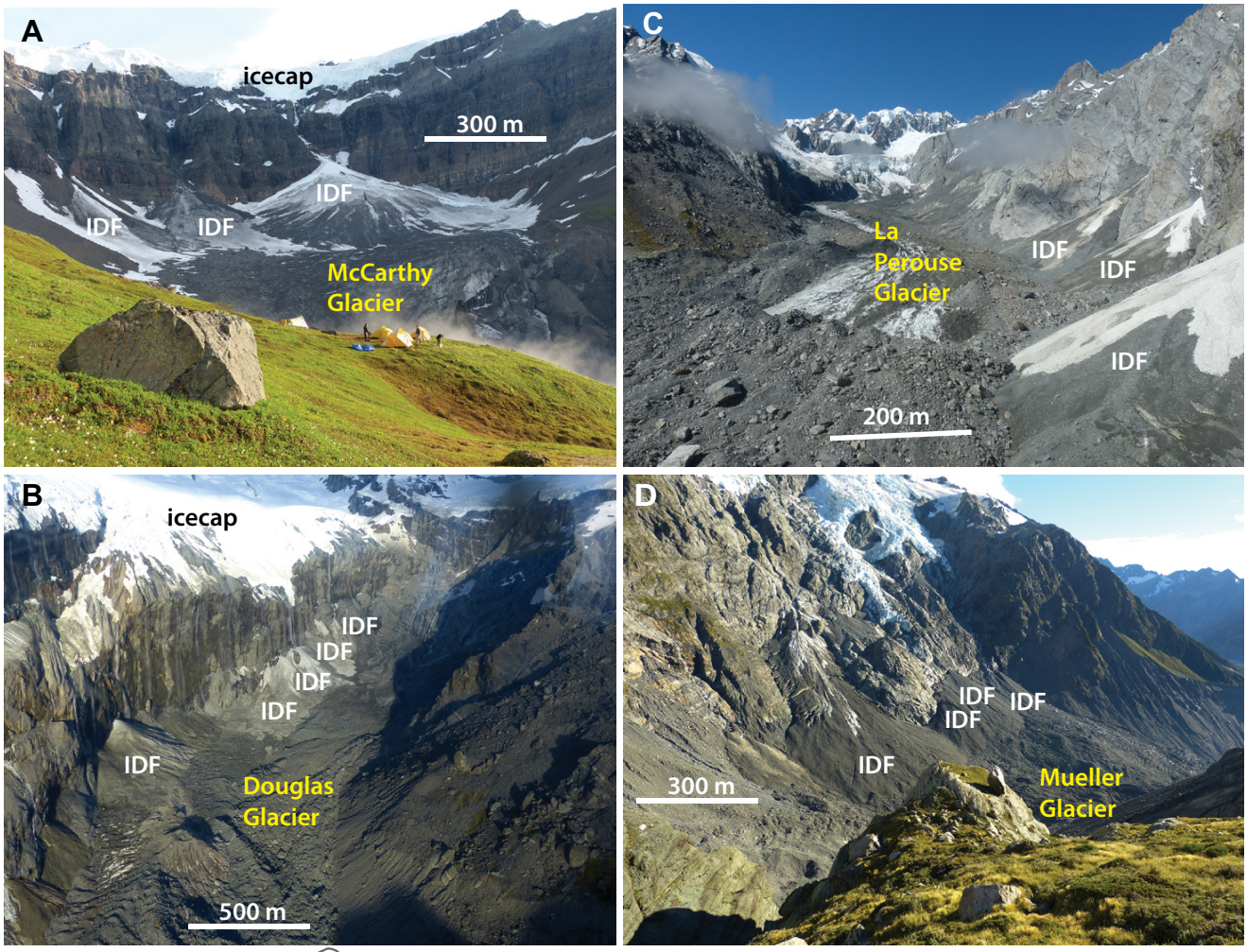

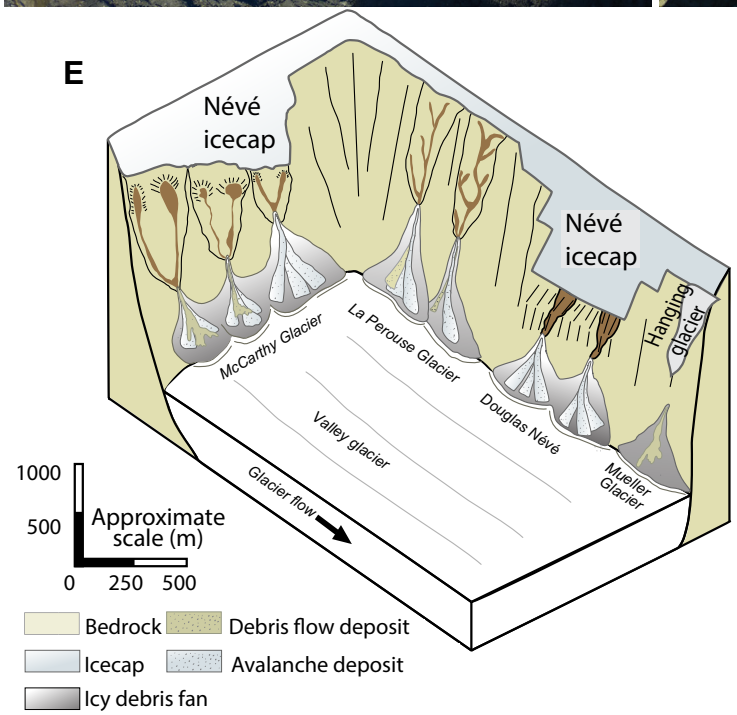

Figure 2. Geomorphic settings of icy debris fans discussed, showing the range of catchment styles and relationships to the valley glacier. (A) McCarthy Glacier icy debris fans (IDFs) (center) occur along the headwall of a cirque and prograde over a small cirque glacier. Note that the fan axis is parallel to valley glacier flow. Catchments are large and wide with a range of geomorphic complexity. (B) Douglas Glacier IDFs (left) occur along cirque sidewall directly below an extensive névé with narrow groove-like catchments. Note that the fan axis is approximately perpendicular to valley glacier flow. (C) La Perouse Glacier IDFs (right) occur along the lateral margin of a larger valley glacier. Catchments are extensive, steep, and elongated. Note that the fan axis is approximately perpendicular to valley glacier flow. (D) The large IDF at Mueller Glacier (left) occurs directly below a hanging glacier and has a limited catchment. Smaller fans have small but irregular bedrock catchments. Icy debris fans occur along the lateral margin of the glacier similar to La Perouse, but at the very distal part of the glacier. Note that the fan axis is approximately perpendicular to valley glacier flow. (E) Schematic showing the variation in catchments and relationships to the valley glaciers studied.

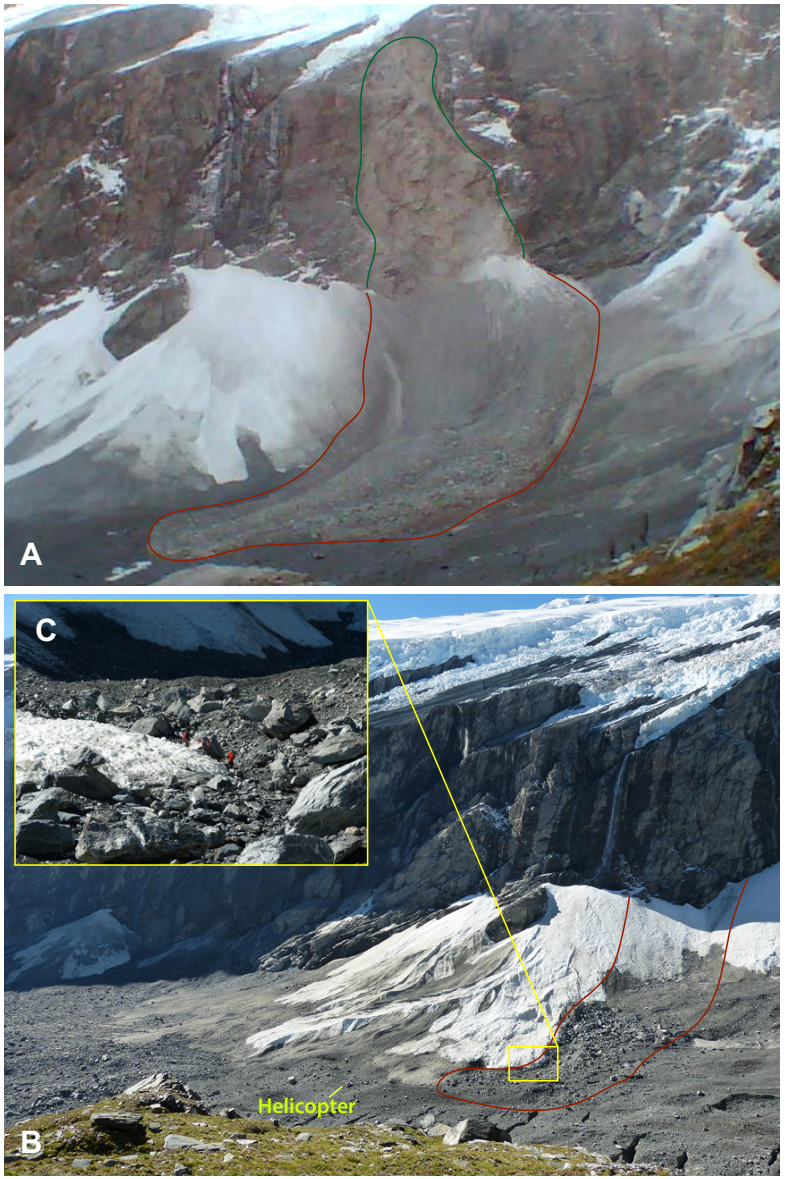

Figure 3. (A) Large rockfall from the bedrock wall above the boundary between Fans 3 and 4 at Douglas Glacier on 23 May 2013. The event was detected by seismometers >10 km distant. Upon hitting the fans, the material appears to have transformed into an icy rock avalanche. Green line outlines the source of the rockfall on the bedrock outcrop. (B) Photo of the same area taken in March 2014 showing the boulder lag from event after ice ablation (red boundary). Note the helicopter (yellow line) for scale. (C) Ground view of terminus of the ablated icy rock avalanche taken in March 2014.

Sediments are subsequently remobilized and transported to IDFs by a variety of flow processes, including ice avalanches, outbursts (jökulhlaups), hyperconcentrated flows, and debris flows. Infrequent rockfalls and rock avalanches land on IDFs; they typically entrain ice and continue across the fans as icy rock avalanches. A particularly large one occurred on Douglas Glacier, New Zealand (Fan 4; Fig. 3). This event, large enough to be recorded on regional seismometers operated by GNS Science (Reid, 2015), was similar to icy rock avalanches documented on the slopes of Aoraki and Mount Cook during our study (Hancox and Thomson 2013; Cox et al., 2015; for videos refer to http://blogs.agu.org/landslideblog/2013/01/23/; and http://blogs.agu.org/landslideblog/2015/11/23/).

Ice Avalanches

Ice avalanches fall into bedrock catchments where they become channelized and undergo flow transformations. During early stages of flow, poorly sorted angular ice clasts and minor sediment calve from the icecap and fall into the catchment. When ice and sediment interact with the bedrock channel, transformations to sliding and flow processes typically occur. Also, clasts become more rounded and better sorted during transfer downslope within the catchment, a process that continues downslope across the IDF surface. Ice avalanches move across IDFs via a mix of basal sliding and mass flow of ice clasts and minor sediment (Fig. 4A). In areas where sliding was observed, avalanche deposits were often arranged in longitudinal rows, similar to large ice avalanches documented in Tibet (van der Woerd et al., 2004). Sliding typically dominates in the proximal parts of IDFs, while debris flow–like processes (i.e., Bingham-type flow) dominate distal areas as the flow slows and comes to rest. Bingham plastic flow models, such as those for debris flows (Johnson and Rodine, 1984), are consistent with the presence of well-formed "boulder" levees (here mostly composed of ice clasts) along the margins of avalanches on IDFs; most levees have maximum thicknesses of ~2 to ~6 m (Fig. 4A). Similar to debris flows, the largest clasts (mainly ice) are deposited toward the top and lateral margins (typically forming levees) of the deposit (Figs. 4A and 4C). Outsized ice and sediment clasts typically run out beyond the levees, sometimes coming to rest beyond the IDF terminus. Unlike debris flows, ice avalanche termini are typically straight and steep (Figs. 4A and 4B). The straight fronts likely result from the lack of scour below the flow. Unlike channeled debris flows, the avalanche thickness is essentially constant, thus flow velocities do not vary substantially across the flow, resulting in similar runout for the clasts along the flow terminus. Most ice avalanche deposits have exceptionally high length/width ratios; the middle of most avalanche deposits we measured were ~1.5 to ~2.5 m thick (Table 1). The surface of ice avalanches typically consists of poorly sorted gravel-sized blocks of ice and sediment. The ice blocks, analogous to an agglomerate or welded breccia, consist of lumps of glacial ice within a matrix of finer-grained fragments of glacial ice and sparse sediment. Ice avalanche deposits are typically white (high albedo) because of their relatively low concentration of sediment (Fig. 4C).

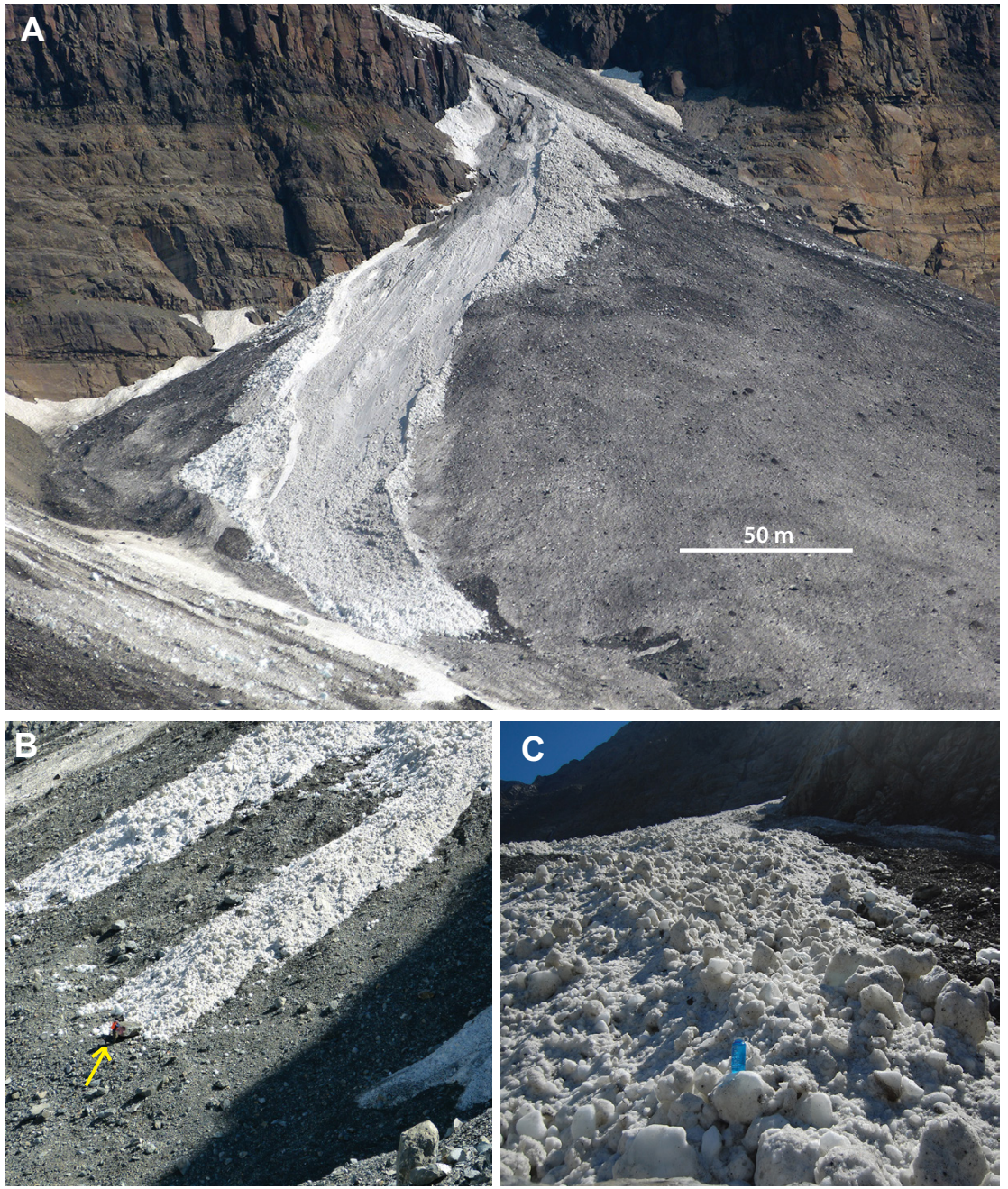

Figure 4. Ice avalanche morphology. (A) Large ice avalanche on Middle Fan at McCarthy Glacier moments after deposition on 24 June 2015. Note the abundant boulder-sized ice clasts, bright albedo, prominent levees, and straight terminus. Extensive levee overrun deposits on the outer bends are visible just below the fan apex after the avalanche emerged from the catchment. Note the darker surface on the remainder of Middle Fan, where sediment was concentrated by ice ablation in the weeks following earlier avalanches. The distal margin of West Fan is visible in the left foreground. (B) Recent (previous day or two) twin ice avalanche deposits near the terminus of Fan 1, at Mueller Glacier in March 2014. Note the person (near yellow arrow) for scale at the terminus of the avalanche on the right. (C) View up-fan from the base of the right avalanche in B (water bottle for scale).

TABLE 1. ICY DEBRIS FAN MORPHOLOGY

Icy debris fan	Length[a] (m)	Width[b] (m)	Fan area[c] (m^2)	Catchment area (m^2)[d]	Axial gradient (degrees)[d]	Convexity ratio[e]	Annual volume of new deposits (m^3)
McCarthy Glacier							
East Fan	590	530	259,800	47,600	25.1	0.12	714,000
Middle Fan	337	220	51,800	61,300	28.4	0.11	613,900
West Fan	350	160	59,200	91,500	30.0	0.10	190,200
La Perouse Glacier							
East Fan	265	250	96,000	222,700	26.7	0.08	133,300
Middle Fan	315	195	58,900	131,300	28.0	0.08	804,100
West Fan	215	200	59,800	210,200	29.2	0.09	
Douglas Glacier							
Fan 1	203	145	26,900	86,900	31.8	0.05	544,000
Fan 2	102	93	9900	17,100	41.3	0.07	125,800
Fan 3	201	175	35,000	53,500	33.2	0.07	857,500
Fan 4	275	260	117,600	92,500	25.1	0.06	1,493,000
Fan 5	300	210	81,300	101,200	21.3	0.04	254,300
Mueller Glacier							
Fan 1	415	325	162,100	58,400	31.0	0.09	5,203,200
Fan 2	250	102	33,400	13,500	31.3	0.09	391,800
Fan 3	265	190	45,300	31,600	30.2	0.06	973,400
Fan 4	270	185	23,900	33,600	24.0	0.06	39,000

[a]Length measured along fan axis.
[b]Width measured at mid-fan.
[c]Area estimated using terrestrial laser scanning data and RiScan in 2015.
[d]Area and gradient estimated using terrestrial laser scanning data, air photos, and Google Earth imagery.
[e]Elevation change across mid-fan profile/width.

[3]Supplemental Item C. Videos of ice avalanches. Please visit https://doi.org/10.1130/GES01622.S3 or the full-text article on www.gsapubs.org to view Supplemental Item C.

[4]Supplemental Item D. Videos of slush avalanches and slush flows. Please visit https://doi.org/10.1130/GES01622.S4 or the full-text article on www.gsapubs.org to view Supplemental Item D.

Within days, especially during summer months, ice avalanche deposits darken, concentrating sediment clasts in a surficial lag, sometimes as agglomerates of ice and sediment clasts, as the deposits compact and ablate (Fig. 5). Refer to Supplemental Item C[3] for videos of active ice avalanches.

Slush Avalanches and Slush Flows

During transitional seasons when significant snowfall occurs within IDF catchments, slush avalanches and slush flows (Rapp and Nyberg, 1981; Rapp, 1995) are common on some IDFs. Rapid melting of snow and ice, rainfall, or outbursts (jökulhlaups) prompts flow or avalanche of slush downslope. Both deposit types consist primarily of ice with minor sediment. Slush avalanches move by basal sliding and internal flow and are composed of much finer-grained clasts than ice avalanches. Similar to ice avalanches, slush avalanche deposits have relatively straight termini and are cloudy or opaque compared to the bright white high albedo of ice avalanches (Fig. 6A). Slush flows contain more abundant water and move as slushy flows with sparse sediment estimated at <10%. Slush flows are cloudy or opaque and exhibit elongate, digitate deposits with rounded termini (Fig. 6B). Similar to ice avalanches, slush avalanches and slush flows have high length/width ratios but are typically more elongate and narrow than most ice avalanches observed. Slush flows are exceedingly narrow and long (Fig. 6A). The maximum thickness of most slush avalanches and slush flows is estimated at <1 m; we observed several of these events during field work but were unable to directly measure any deposits. Slush flows were particularly common in winter and transitional months. For videos of active slush avalanches and slush flows, refer to Supplemental Item D[4].

Icy Debris Flows

Icy debris flows occur on some IDFs after rapid addition of water to catchments following large rainfall events or in association with outbursts (jökulhlaups) from the base of the icecap. Icy debris flows are lithic-dominated flows similar to debris flows except that they contain minor gravel-sized ice clasts (typically 5%–10%) remobilized from ice avalanche deposits previously stored in their catchments. Icy debris flows observed on West Fan at McCarthy Glacier in June 2006 occurred following a lag of several hours from outburst

Figure 5. Middle Fan at La Perouse Glacier in March 2014 showing a range of albedo reflecting the relative ages of recent ice avalanche deposits. The bright white deposits (left center) occurred the day the photo was taken. The slightly darker deposits on the left are two days old, and the deposits on the right half of the fan are four days old. Dark, lithic-rich zones in between show deflation lag resulting from several weeks of ablation since receiving new avalanche deposits. Fan is ~250 m wide near its base. Inset shows typical agglomerated clasts of avalanche deposits several days after deposition (example from Douglas Glacier Fan 4).

releases of water into the catchments (Kochel and Trop, 2008). This was interpreted as mixing of water and temporarily stored sediment and ice in complex subbasins within the catchments. In June 2015, icy debris flows observed at McCarthy Glacier emerged from Middle Fan catchment in the absence of rainfall; we speculate that the event resulted from an outburst (jökulhlaup) related to complex damming and/or channeling of water within the icecap. Icy debris flow deposits have dark albedo initially because of the high percentage of sediment (Fig. 7). Like slush flow deposits, they terminate in digitate lobes with rounded termini (Figs. 7A and 7B). Icy debris flow deposits typically have gravel-sized clasts in their levees.

In situations where there is enough water available, hyperconcentrated flows may occur. Flow character alternated between icy debris flow and hyperconcentrated flow numerous times during hour-long events on West Fan (July 2006) and Middle Fan (June 2015) at McCarthy Glacier. We interpret these variations as a result of mixing of sediment and ice clasts temporarily stored in bedrock pools prior to outbursts from the icecap followed by overtopping and downstream flows that vary in sediment concentration. Icy debris flows behave similarly to debris flows in other environments, including the development of standing waves and surges.

Icy debris flows, hyperconcentrated flows, and slush flows can erode IDF surfaces, creating concave channels along their flow paths, unlike ice avalanches, which do not substantially erode fan surfaces. We infer that the concavity of the channel contributes to the formation of lobate termini because central portions of the flow have greater flow depths than lateral zones. In contrast, ice avalanche and slush avalanche deposits (Fig. 6A) show little to no evidence of basal scour; hence, their deposits have similar depth across their cross section. We infer that the consistent depth across the flow results in the formation of notably straight termini. For a video of an active flow that transitions between debris flow and hyperconcentrated flow, refer to Supplemental Item E[5].

[5]Supplemental Item E. Videos of icy debris flows. Please visit https://doi.org/10.1130/GES01622.S5 or the full-text article on www.gsapubs.org to view Supplemental Item E.

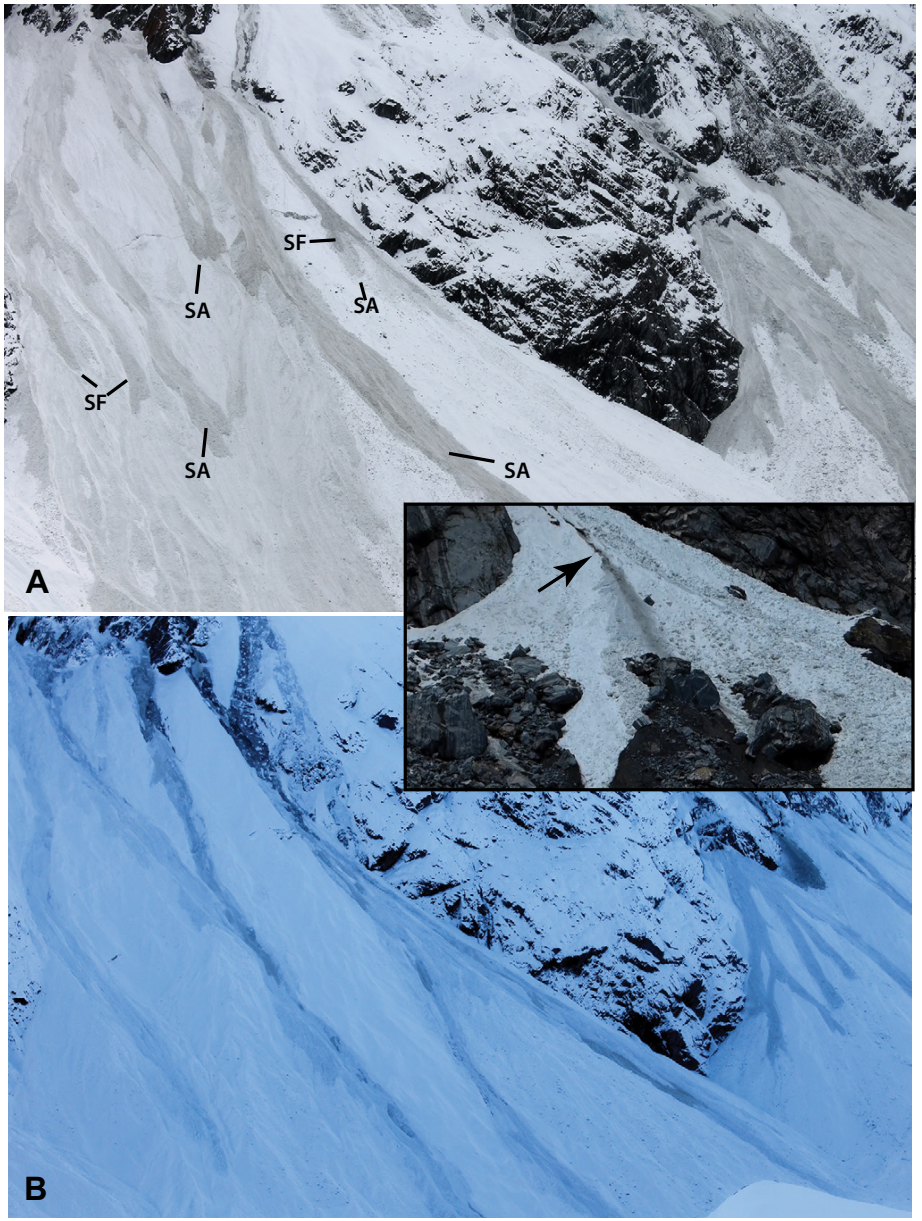

Figure 6. Slush avalanches (SA) and slush flows (SF) on Fan 1 at Mueller Glacier in July 2014. Note the dark-gray, cloudy nature of both types of deposits (A). Avalanches are generally wider with straight fronts. The more water-rich slush flows (B) exhibit lobate fronts and are generally thinner. Slush flows may also incise into underlying deposits due to turbulence during their flow. Inset from La Perouse Glacier in January 2013 shows incised channel (arrow).

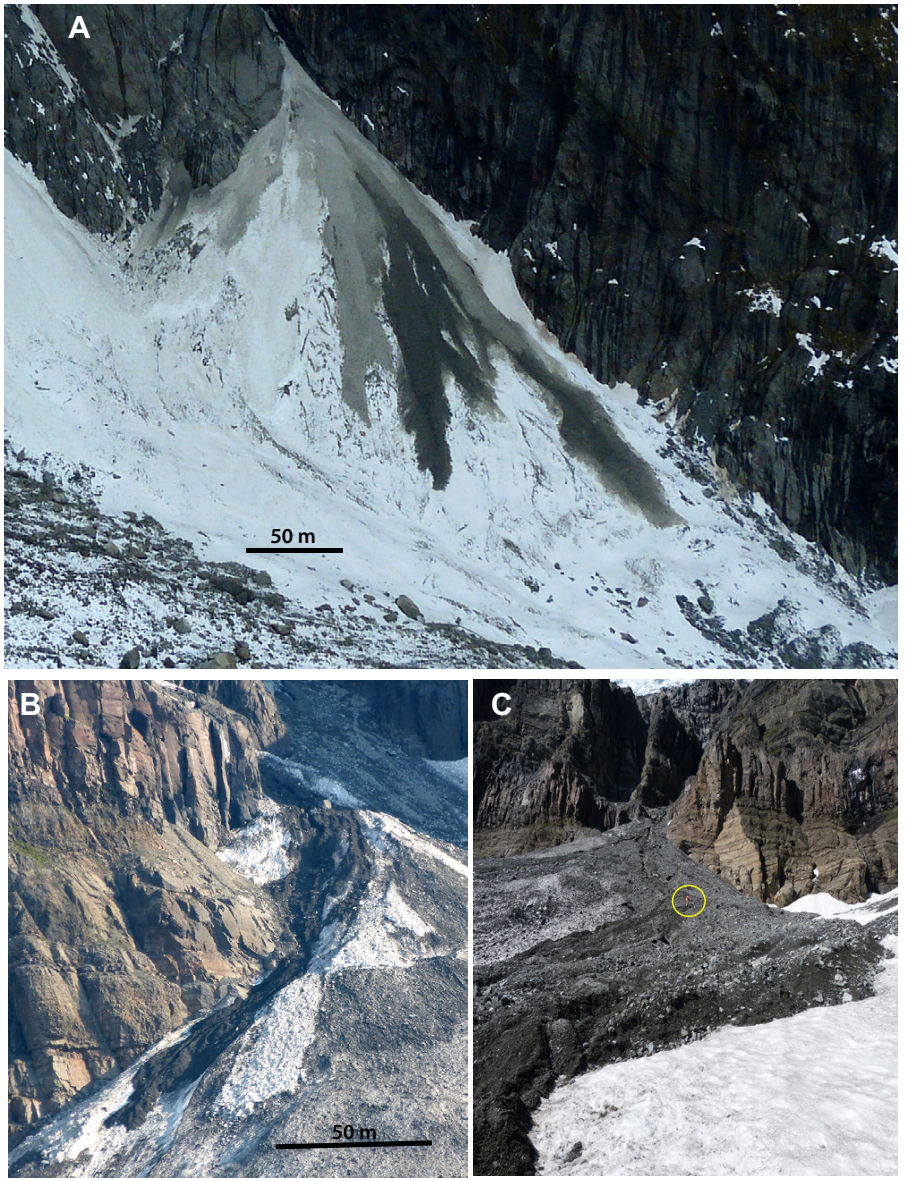

Figure 7. Icy debris flow deposits. (A) Recent icy debris flow deposit (darker, black albedo) on Middle Fan at La Perouse Glacier in December 2016. Note the digitate termini. Also visible are gray slush avalanche deposits on both sides of the debris flow. Note their straight termini. (B) Icy debris flow in June 2015 on Middle Fan at McCarthy Glacier. Note the black albedo and digitate morphology. (C) Large icy debris flow deposit on Middle Fan at McCarthy Glacier in July 2013, viewed from terminal area looking up-fan. Digitate lobes are farther down-fan off the photo. Person with red coat circled for scale midway up on the deposit. See Kochel and Trop (2008) for photos of ice clasts within the icy debris flows at McCarthy Glacier.

Conceptual Model of Depositional Processes

Figure 8 illustrates the continuum of processes observed delivering material to IDFs based on differing amounts of water, ice, and sediment. At the bottom of the conceptual ternary diagram are dry processes characterized by free-fall and sliding processes. Progressing toward the top of the diagram, processes incorporate increasing amounts of water and fluid flow. Discrete boundaries are not shown on Figure 8 owing to the transitional nature of processes. Our field observations show transformations in flow types can take place along the path of an individual event (i.e., sometime ice avalanches and rockfalls transition downslope into icy debris flows).

FREQUENCY AND VOLUME OF ICE AND SEDIMENT SUPPLY TO ICY DEBRIS FANS

The contribution of ice and sediment from icecaps and adjacent bedrock to valley glaciers via IDFs has not been evaluated previously. This study estimates the contribution of ice and sediment to valley glaciers delivered through IDFs via supraglacial depositional processes. Icy debris fans are remarkably active landforms, hosting hundreds to thousands of depositional events annually. Quantifying the contributions from IDFs is necessary to develop accurate mass balance estimates for valley glaciers.

Methods of Measuring Ice and Sediment Supply

To document depositional processes and rates, we used the following techniques: (1) direct field observations of depositional processes and drone and helicopter imagery of IDF and catchment regions not accessible by foot due to rugged terrain and rockfall and/or avalanche hazards; (2) time-lapse cameras documenting depositional processes; (3) repeat TLS ground surveys documenting surface elevation changes; and (4) GPR surveys along selected traverses to determine subsurface IDF architecture.

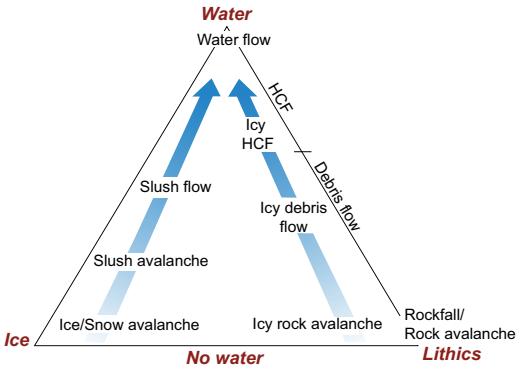

Figure 8. Ternary diagram for depositional processes observed on icy debris fans. Corners of the triangle represent increasing concentrations of water, ice, and sediment. The lack of discrete boundaries on the diagram reflects a continuum between major flow processes. During this study, it was not uncommon to observe differences in dominant processes as seasons change. Flow transformations also occurred during a single depositional event along the flow path. HCF—hyperconcentrated flow.

Field Observations and Time-Lapse Imaging

Field observations provided a basis for interpreting the nature and scale of depositional events in time-lapse images. Field-calibrated time-lapse imagery documented depositional events and allowed for a conservative estimation of the volume of ice and/or sediment delivered to IDFs over periods ranging from eight months to two years. Multiple time-lapse cameras were installed at all four sites; refer to Reid (2015) and Grune (2016) for camera locations. Time-lapse images were studied individually to map and classify each depositional event. Event type was interpreted based on comparisons of the imagery with morphology of >1400 events observed directly in the field (Fig. 9). After event type was determined, the area of the deposit was mapped directly on the photo using Adobe Illustrator. The scale in time-lapse images was determined using selected field measurements of deposits observed in the field and detailed bedrock calibration scales derived from TLS coverage (Fig. 10). We scaled multiple aerial zones for each fan using TLS measurements of unchanging bedrock features along fan margins. Given the ever-changing surface topography of the IDFs, we did not use TLS-based topography of the fans for scaling purposes; some fans experienced >100% resurfacing in one day from numerous depositional events (Table 2), as discussed in the section "Volume of Ice and Sediment Supply to Icy Debris Fans." Although daily TLS measurements would decrease errors associated with area estimates from photographs, daily TLS surveys are not practical in these especially remote, rugged settings prone to frequent precipitation.

Estimating deposit thicknesses from photographs introduces uncertainties. To constrain the error, we measured deposit thickness on tens of events in the field. Sampled ice avalanche deposits were consistently in the range of 1–3 m thick; so we applied the 2 m mean as the average thickness for volume estimations. Less frequent slush avalanches, slush flows, and debris flows were not measured directly, but field and drone observations indicated an average of 1 m, which we applied to volume estimates.

We also used the cameras to provide information about daily weather, allowing us to evaluate possible relationships between weather and depositional events. Photograph-based weather observations were supplemented with weather data obtained from the nearest weather stations (Fox Glacier, New Zealand; Mount Cook, New Zealand; McCarthy, Alaska). Refer to Reid (2015) and Grune (2016) for details of weather data.

Terrestrial Laser Scanning (TLS)

Repeat TLS surveys using light detection and ranging (LiDAR) technology provided scale for measuring active depositional events observed during field work and deposits mapped from time-lapse images (Fig. 10). Terrestrial laser scanning data also quantified changes in IDF volume during the course of this study. Repeat TLS surveys were completed at McCarthy Glacier in July 2013 and June 2015 and La Perouse Glacier and Douglas Glacier in January 2013 and March 2015. One TLS survey was conducted at Mueller Glacier in March 2015.

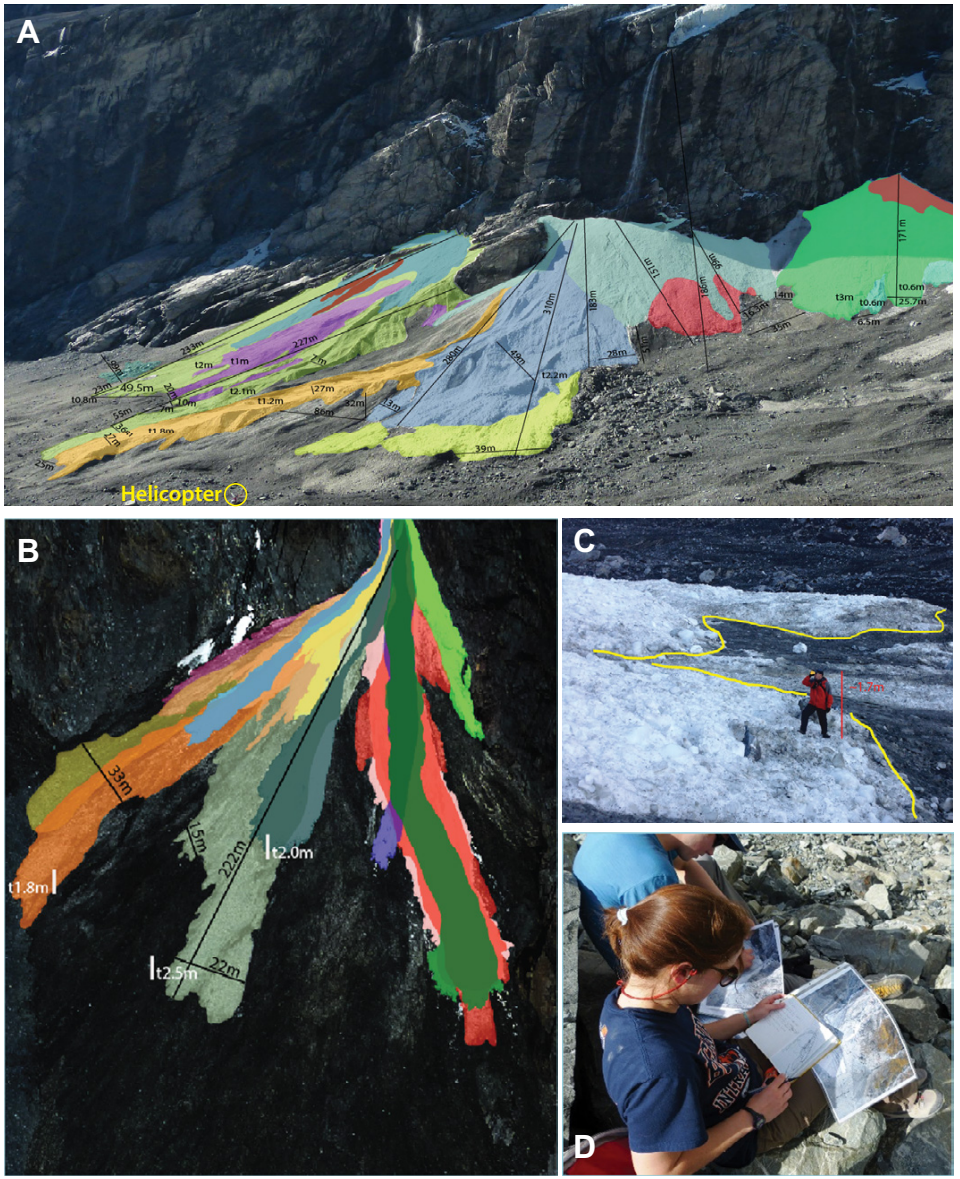

Figure 9. Field measurements of recent deposits on icy debris fans were done to calibrate image analysis and terrestrial laser scanning analysis and to obtain reasonable estimates of deposit thickness to be applied to deposits mapped on time-lapse images. (A) Recent deposits mapped on Fans 4–5 at Douglas Glacier in March 2014. (B) Recent deposits mapped on Middle Fan at La Perouse Glacier in March 2014. (C) Field mapping using Range Finder at the toe (delineated by yellow line) of a recent ice avalanche on Fan 4 at Douglas Glacier. (D) Mapping new ice avalanche deposits that occurred that day on to aerial photos taken from helicopter the previous day at La Perouse Glacier.

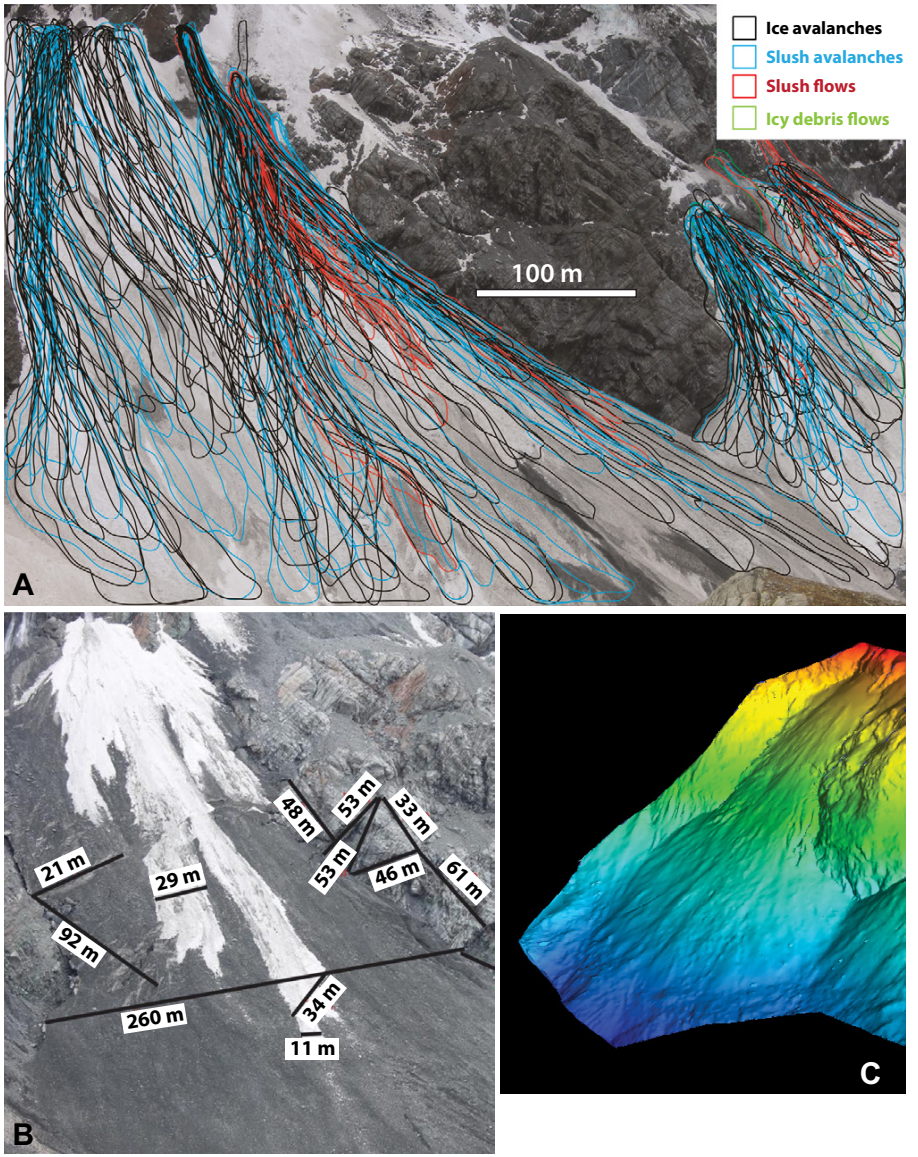

Figure 10. Scale calibration for new deposit mapping from terrestrial laser scanning (TLS) analysis. (A) Example of depositional events mapped at Mueller Glacier from images taken three times a day and digitized using Adobe Illustrator. Each event was interpreted for process based on deposit morphology and albedo, and their areas were calculated. This image shows cumulative deposits for the month of September 2014. (B) Example of 12 different scale bars used on different portions of the scene shown in A for calibrating deposit geometry. (C) TLS image of Mueller Glacier Fan 1 (~325 m across) showing topography viewed from a perspective looking up-glacier opposite from the view captured by the time-lapse camera in A and B. Warm colors—higher elevations; cool colors—lower.

TABLE 2. RESURFACING RATES BY NEW DEPOSITS ON ICY DEBRIS FANS

Icy debris fan	Area resurfaced (m^2) during time lapse	Percent fan area resurfaced during time lapse	Area resurfaced (m^2) prorated for one year	Fan area resurfaced prorated for one year (%)
McCarthy Glacier[a]				
East Fan	103,671,300	399	77,753,500	300
Middle Fan	71,484,000	1380	53,613,000	1035
West Fan	65,910,900	1114	49,433,200	836
La Perouse Glacier[b]				
East Fan	68,550,400	714	85,688,000	893
Middle Fan	120,269,400	2043	150,336,700	2554
West Fan	not imaged			
Douglas Glacier[c]				
Fan 1	31,092,600	1155	38,865,800	1444
Fan 2	5,902,900	598	7,378,600	748
Fan 3	120,462,300	3447	150,577,900	4308
Fan 4	261,080,800	2221	326,351,000	2776
Fan 5	146,739,300	1806	183,424,100	2258
Mueller Glacier[d]				
Fan 1	433,527,200	2675	520,232,600	3210
Fan 2	3,264,900	98	3,917,900	117[e]
Fan 3	81,117,100	1790	97,340,500	2148
Fan 4	4,494,300	188	5,393,200	226

[a]Time lapse at McCarthy Glacier: July 2013–June 2015.
[b]Time lapse at La Perouse Glacier: January 2013–September 2013.
[c]Time lapse at Douglas Glacier: January 2013–September 2013.
[d]Time lapse at Mueller Glacier: March 2014–March 2015.
[e]Low rate due to episodic fan slumping (fan active ~25% of the year).

UNAVCO collected the field data using a Riegl TLS system. Numerous positions on the ground were used to scan each IDF; individual scans were subsequently merged using RiScan software to create a three-dimensional cloud of data points. Terrestrial laser scanning surveys provide accurate topography useful in geomorphic mapping and enable maps to be produced showing detailed changes in topography and morphology (Kerr et al., 2009; Barnhart and Crosby, 2013; Picco et al., 2013). In spite of using multiple scan positions, minor data gaps exist on some IDFs due to inaccessibility either near crevasses or proximity to apex of IDF, convex topography, and low signal return of recent avalanche deposits. In addition, TLS data did not map the entire extent of some catchments.

Ground Penetrating Radar (GPR)

Ground penetrating radar profiles and soundings were completed along selected traverses at each IDF studied; at McCarthy Glacier in July 2013 and June 2015; at La Perouse and Douglas Glaciers in January 2013, March 2014, and March 2015; and at Mueller Glacier in March 2014 and March 2015. Ground penetrating radar data provide information on the subsurface architecture of the IDFs, which was used to aid in understanding the long-term evolution of the fans and to better constrain fan geometry in estimating fan volume. We used a Sensor and Software pulseEKKO Pro GPR system, employing bi-static antennas with center frequency of 100 and 200 MHz. In order to topographically correct the GPR profiles, we used a Trimble R8 RTK-GPS system with local base station. Ground penetrating radar soundings, known as wide-angle reflection and refraction (WARR), were collected and analyzed to determine the subsurface GPR signal velocity. The GPR signal velocity is used to translate the observed two-way travel time (TWTT) in GPR profiles to depth below the surface. In addition, differences in GPR signal velocities indicate changes in material (for example, compaction of ice) (Bradford et al., 2009). Refer to Jacob et al. (2017) for additional details of GPR data collection, analysis, and processing.

Frequency of Ice and Sediment Supply to Icy Debris Fans

Icy debris fan deposits were mapped on time-lapse photographs and are summarized on Figures 11–14 and Tables 3–6. The eight- to 24-month duration of time-lapse imagery allowed for estimation of the minimum annual

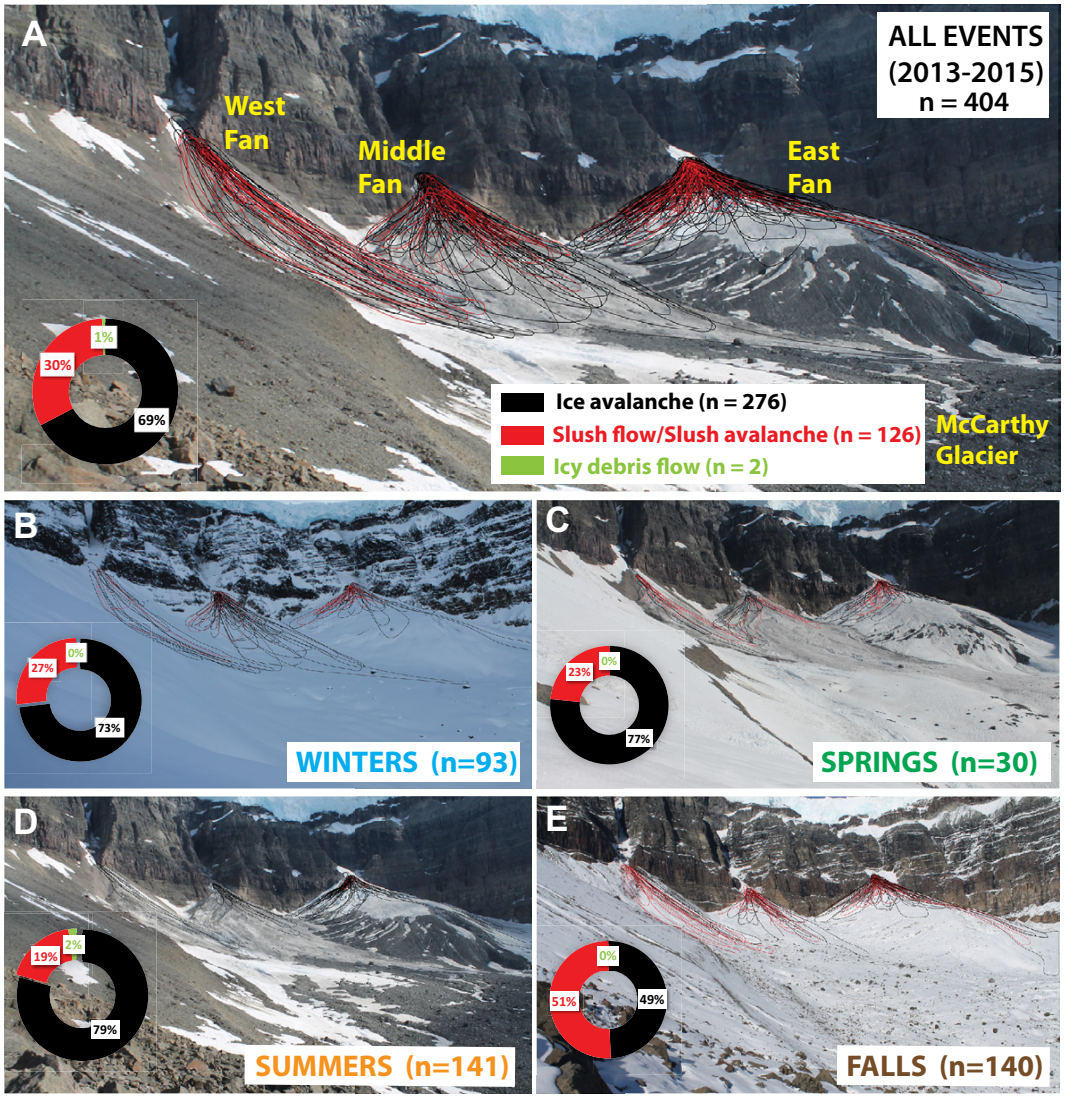

Figure 11. Summary mapping of deposits from time-lapse cameras at McCarthy Glacier from June 2013 to June 2015. (A) All 404 events cumulated. (B) Winter events. (C) Spring events. (D) Summer events. (E) Fall events.

frequency and volume of depositional activity. Videos of the time-lapse imagery can be viewed in Supplemental Item F[6]. In the following sections, we summarize the timing, nature, and patterns of depositional events. We do not provide quantitative temporal or spatial comparisons between sites given that cameras did not operate for the same durations at each site, and cameras only captured the largest events.

McCarthy Creek Glacier, Alaska

Time-lapse cameras at McCarthy Glacier operated for a two-year period from July 2013 to June 2015, collecting images three times a day. The camera was buried in snow for two several-month-long periods in late-winter to spring. New deposits were mapped on each image; refer to Grune (2016)

[6]Supplemental Item F. Time-lapse videos of deposits at icy debris fan sites. Please visit https://doi.org/10.1130/GES01622.S6 or the full-text article on www.gsapubs.org to view the Supplemental Item F.

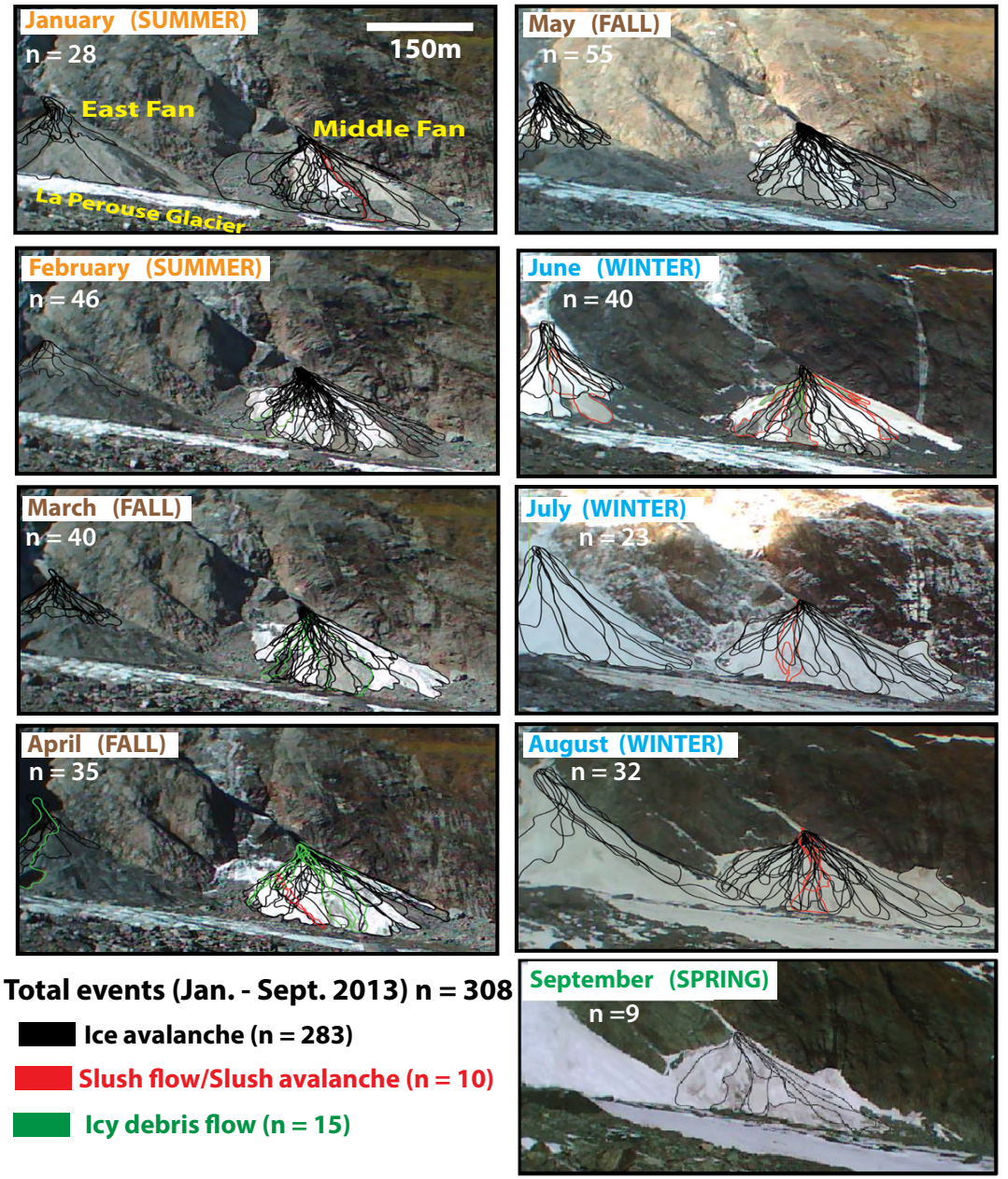

Figure 12. Summary mapping of deposits from time-lapse cameras at La Perouse Glacier from January 2013 to September 2013. Cumulative summaries for each month are shown.

for tables summarizing daily events. Figure 11 summarizes monthly events mapped from images. Area and volume estimates for these events are summarized in Table 3.

Deposition on McCarthy Glacier IDFs occurred throughout the year. Ice avalanches dominated 404 events imaged on the three IDFs, accounting for 69% of imaged events. Slush flows accounted for 30% of imaged events. Icy debris flows were rare, accounting for just 1%. East Fan, largest of the three fans, received more than half of the imaged events (232 deposits), with Middle Fan and East Fan receiving 113 and 55 deposits, respectively. The most active day occurred in August 2013, when East Fan received 23 ice avalanches, followed by 22 ice avalanches in September 2014 after large rainfall events (Grune, 2016). Debris flows were observed only on West and Middle Fans. No rockfalls were imaged on the fans. However, >175 rockfalls in fan catchments were observed during 22 days of field work, most above Middle and West Fans (Supplemental Item B [footnote 2]).

Figure 11 and Supplemental Item F-4 (footnote 6) illustrate seasonal variation of process dominance common at McCarthy Glacier IDFs. Ice avalanches dominated depositional events in winter and summer months, whereas slush flows and slush avalanches were more common in transitional months. Debris flows and hyperconcentrated flows occurred only in summer (Fig. 11D).

The high pace of depositional activity on McCarthy IDFs resulted in high resurfacing rates (Table 2). New deposits on Middle Fan covered ~1380% of the fan area during the two-year observation period; West Fan received new deposits amounting to ~1114% of its surface area, and East Fan received ~400% coverage by new deposits during that time.

La Perouse Glacier, New Zealand

Two time-lapse cameras at La Perouse Glacier recorded events on East and Middle Fans, taking two images per day during a nine-month period between January–September 2013. A camera recording activity on West Fan failed very early due to rockfall damage. Figure 12 shows monthly summaries of new deposits that reached the fans between January–September 2013. Table 4 summarizes area and volume estimates for these deposits. Refer to Reid (2015) for tables summarizing daily events.

During the nine-month period, 308 depositional events occurred on the two IDFs: 225 on Middle Fan and 83 on East Fan. Ninety-two percent of events were ice avalanches. The remaining 8% included icy debris flows, slush flows, and one rockfall. East Fan received only one icy debris flow and one slush flow while Middle Fan had several icy debris flows and slush flows. Depositional activity (resurfacing) on La Perouse Glacier fans was significant, covering >2000% of the fan surface at Middle Fan and ~700% of the fan surface on East Fan during the nine-month period (Table 2).

Although the fans received episodic deposits throughout the year, East Fan was considerably less active in the summer and experienced increased activity during the winter (Fig. 12; Supplemental Item F-1 [footnote 6]). Middle Fan

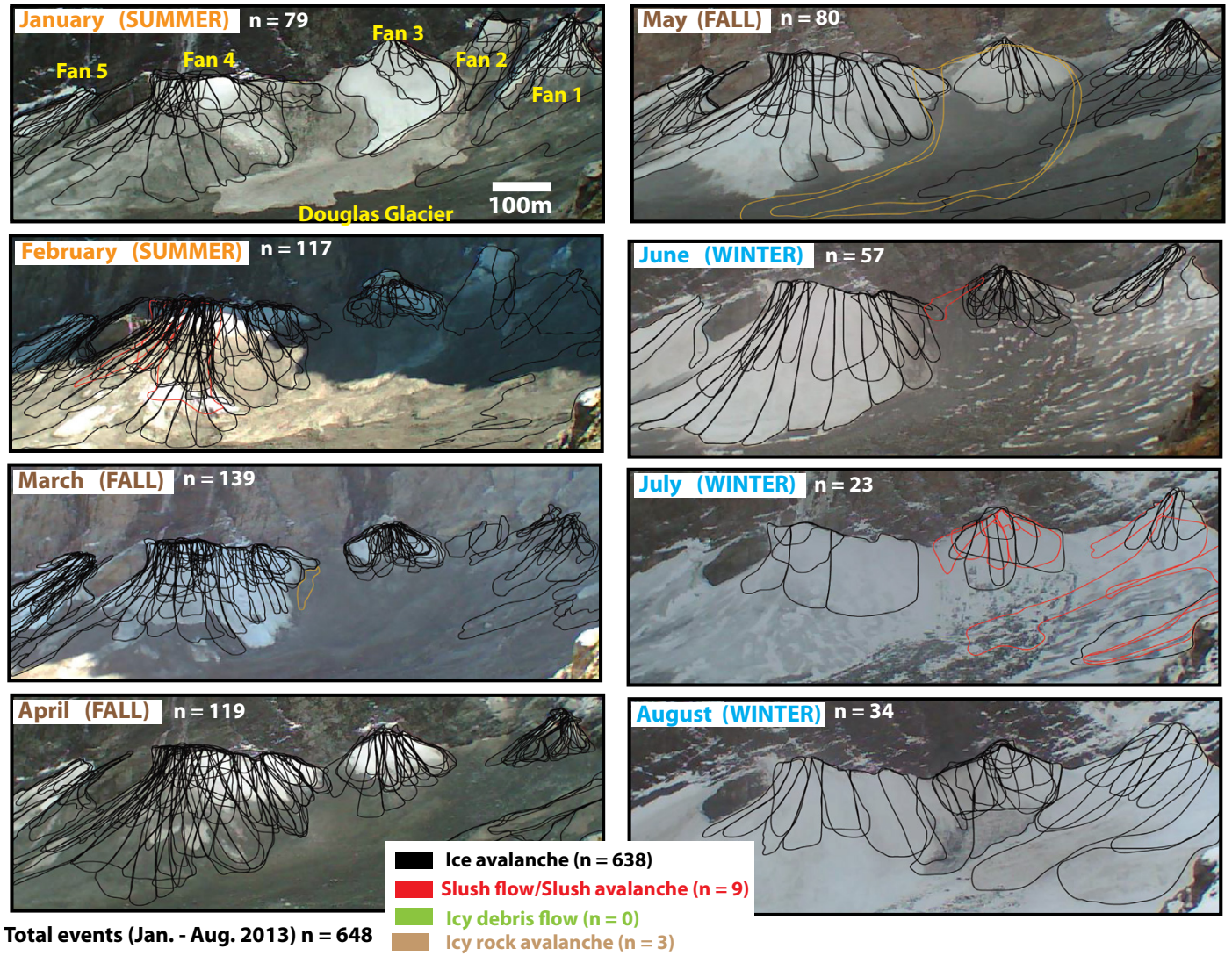

Figure 13. Summary mapping of deposits from time-lapse cameras at Douglas Glacier from January 2013 to August 2013. Cumulative summaries for each month are shown.

was active throughout the year. Although time-lapse imagery did not quantify activity on West Fan, field observations in March 2014 suggest that West Fan followed a pattern similar to East Fan. We also observed active events on West Fan during field work in June 2010, January 2013, March 2015, and December 2016 (Supplemental Item B [footnote 2]).

Field observations of fan catchments show that the terminal face of the icecap is more extensive above Middle Fan. We infer that the more extensive icecap face provides higher supply of ice avalanches throughout the year to the Middle Fan. Fewer ice avalanches may occur in East and West Fan catchments because they have less ice supply from the icecap. The increase in win-

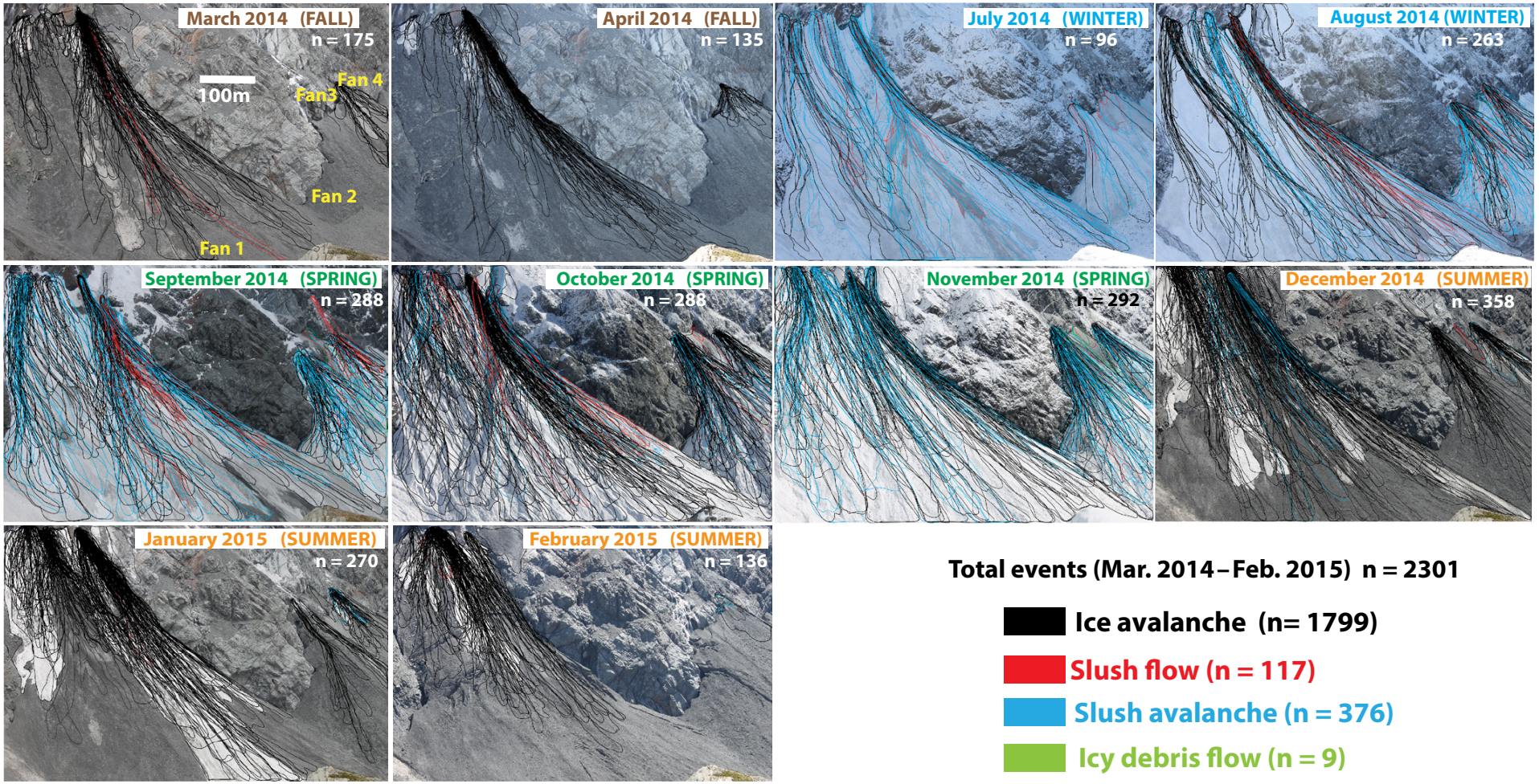

Figure 14. Summary mapping of deposits from time-lapse cameras at Mueller Glacier from March 2014 to March 2015. Cumulative summaries for each month are shown.

ter activity for East and West Fans probably results from mobilization of winter snow deposited in their catchments as snow avalanches, slush avalanches, and slush flows. The dominance of ice avalanches and slush flows is the result of the relatively simple catchment morphology. La Perouse fan catchments are extremely elongate and steep, with relief averaging >2000 m. These catchments offer little opportunity to store ice and/or sediment, hence, the limited occurrence of icy debris flows. However, a few icy debris flows were observed, likely resulting from mobilization of rockfall sediment during icecap outbursts or large rainfall events.

Douglas Glacier, New Zealand

One time-lapse camera at Douglas Glacier operated for an eight-month period, taking two images per day between January–August 2013 (Fig. 13; Table 5). A total of 648 depositional events were recorded and mapped on five IDFs and a ramp east of the fans where large avalanches were shed from the slope of Mount Sefton onto Douglas Glacier (Sefton events in Table 5). Refer to Reid (2015) for tables summarizing daily events. A second camera failed early due to rockfall damage.

TABLE 3. NEW DEPOSITS ON MCCARTHY GLACIER ICY DEBRIS FANS

Icy debris fan	Fan volume (m^3) (2015 TLS survey data)[a]	New deposit volume (m^3) (July 2013–June 2015)[b]	New deposit volume added (%) (July 2013–June 2015)[b]	New deposit volume (m^3) (prorated for one year)[c]	New deposit volume added (%) (prorated for one year)[c]
East Fan	25,360,000				
July 2013		5215		3911	
August 2013		50,012		37,509	
September 2013		26,119		19,589	
October 2013		84,934		63,701	
November 2013		0		0	
May 2014		21,928		16,446	
June 2014		31,721		23,790	
July 2014		106,189		79,642	
August 2014		70,282		52,712	
September 2014		101,918		76,439	
October 2014		46,734		35,051	
November 2014		55,185		41,389	
December 2014		99,926		74,945	
January 2015		59,738		44,804	
February 2015		67,404		50,553	
March 2015		0		0	
May 2015		53,345		40,009	
June 2015		71,329		53,497	
Total East		*952,000*	*3.8*	*714,000*	*2.9*
Middle Fan	2,441,000				
July 2013		0		0	
August 2013		3899		2924	
September 2013		13,737		10,303	
October 2013		24,422		18,317	
November 2013		33,673		25,255	
May 2014		0		0	
June 2014		17,423		13,067	
July 2014		27,314		20,486	
August 2014		18,746		14,060	
September 2014		10,504		7878	
October 2014		56,096		42,072	
November 2014		24,898		18,674	
December 2014		61,603		46,202	
January 2015		241,664		181,248	
February 2015		177,135		132,851	
March 2015		14,997		11,248	
May 2015		53,571		40,178	
June 2015		38,774		29,081	
Total Middle		*818,500*	*33.5*	*613,800*	*24.9*
West Fan	3,680,000				
July 2013		3047		2285	
August 2013		0		0	
September 2013		0		0	
October 2013		27,638		20,729	
November 2013		0		0	
May 2014		627		470	
June 2014		17,179		12,884	
July 2014		14,696		11,022	
August 2014		0		0	
September 2014		16,496		12,372	
October 2014		42,100		31,575	
November 2014		3471		2603	
December 2014		47,381		35,536	
January 2015		38,787		29,090	
February 2015		23,263		17,447	
March 2015		0		0	
May 2015		0		0	
June 2015		18,969		14,227	
Total West		*253,655*	*6.9*	*190,200*	*5.2*
Total McCarthy	*31,481,000*	*2,024,000*	*6.4*	*1,518,000*	*4.8*

[a]Volume estimated using terrestrial laser scanning data and RiScan (see Fig. 16) in 2015.
[b]Camera was occasionally inoperative during this time period, mainly due to snow cover or lack of solar charge.
[c]Annual volumes were prorated to a 12-month period using the ratio of deposits observed in imagery.

TABLE 4. NEW DEPOSITS ON LA PEROUSE GLACIER ICY DEBRIS FANS

Icy debris fan	Fan volume (m^3) (2015 TLS survey data)[a]	New deposit volume (m^3) (January–September 2013)	New deposit volume added (%) (January–September 2013)	New deposit volume (m^3) (prorated for one year)[b]	New deposit volume added (%) (prorated for one year)[b]
East Fan	3,618,100				
January 2013		8967		11,209	
February 2013		3913		4891	
March 2013		9619		12,024	
April 2013		5706		7,133	
May 2013		21,194		26,493	
June 2013		20,705		25,881	
July 2013		20,704		25,880	
August 2013		15,814		19,768	
September 2013		0		0	
Total East		*106,700*	*2.9*	*133,000*	*3.7*
Middle Fan	2,299,300				
January 2013		61,134		76,418	
February 2013		101,694		127,118	
March 2013		72,073		90,091	
April 2013		75,875		94,844	
May 2013		66,681		83,351	
June 2013		77,325		96,656	
July 2013		59,004		73,755	
August 2013		96,658		120,823	
September 2013		32,839		41,049	
Total Middle		*643,300*	*27.9*	*804,000*	*35*
Total La Perouse[c]	*5,917,400*	*750,000*	*12.7*	*937,000*	*15.8*

[a]Volume estimated using terrestrial laser scanning (TLS) data and RiScan (see Fig. 16) in 2015.
[b]Annual volumes were prorated to a 12-month period using the ratio of deposits observed in imagery.
[c]Camera data (to estimate volume) for only two of the three fans studied at La Perouse.

Depositional activity occurred throughout the year, but at a reduced pace during the coldest winter months (Fig. 13; Supplemental Item F-2 [footnote 6]). Large avalanches from Mount Sefton were most active during spring and early summer as seasonal snowfall was mobilized by spring rainfall and early summer snowmelt. Increases in depositional activity commonly followed large rainfall events, likely related to flow through crevasses stimulating icecap calving and elevated pore-water pressures of ice stored in bedrock catchment grooves. With the exception of one catastrophic rockfall and several slush flows, all depositional events were ice avalanches. A catastrophic rockfall on 23 May 2013 covered Fan 4 and the edge of Fan 3 with an extensive deposit of boulders (Fig. 4). The rockfall entrained significant ice from the fans, moving as an icy rock avalanche to the distal edge of Fan 4.

Depositional activity at Douglas Glacier was more frequent than that at La Perouse. Field event logs recorded more than 150 events in one day. Most events observed directly were too small to detect in time-lapse photos; only a small percentage of events were large enough to travel to the fan apex or beyond. Time-lapse imagery recorded only the largest events that deposited material on Douglas IDFs (Supplemental Item F-2 [footnote 6]). Time-lapse mapping data (Table 5) show that Douglas fans were extensively resurfaced by new deposits during the eight-month observation period; percentages of fan surfaces resurfaced were Fan 1 ~1150%, Fan 2 ~600%, Fan 3 ~3450%, Fan 4 ~2200%, and Fan 5 ~1800% (Table 2).

Mueller Glacier, New Zealand

Time-lapse cameras at Mueller Glacier captured activity for 12 months, taking three images per day from March 2014 to March 2015. The camera did not operate for a period of approximately two and a half months in winter during May–July. Figure 14 and Table 6 show events recorded by time-lapse imagery at Mueller Glacier. For details on this especially active IDF, refer to Supplemental Item G[7], which summarizes daily events recorded by the time-lapse camera. Supplemental Item F-3 (footnote 6) shows the video from time-lapse imagery.

Supplemental File G -- Depositional Events at Mueller Glacier (March 2014 - March 2015)

Fan 1					Fan 2				
Image #	Date	Time	Event #	Event Type	Image #	Date	Time	Event #	Event Type
16	3/8/2014	9:00 AM	1	AV	15	3/7/2014	3:00 PM	B-1	AV
16	3/8/2014	9:00 AM	2	AV	15	3/7/2014	3:00 PM	B-2	AV
16	3/8/2014	9:00 AM	3	AV	16	3/8/2014	9:00 AM	B-3	AV
16	3/8/2014	9:00 AM	4	AV	18	3/8/2014	3:00 PM	B-4	AV
16	3/8/2014	9:00 AM	5	AV	18	3/8/2014	3:00 PM	B-5	AV
16	3/8/2014	9:00 AM	6	AV	19	3/9/2014	9:00 AM	B-6	AV
16	3/8/2014	9:00 AM	7	AV	19	3/9/2014	9:00 AM	B-7	AV
16	3/8/2014	9:00 AM	8	AV	19	3/9/2014	9:00 AM	B-8	AV
17	3/9/2014	12:00 PM	9	AV	20	3/9/2014	12:00 PM	B-9	AV
20	3/9/2014	12:00 PM	10	AV	23	3/10/2014	12:00 PM	B-10	AV
23	3/10/2014	12:00 PM	11	AV	37	3/15/2014	12:00 PM	B-11	AV
23	3/10/2014	12:00 PM	12	AV	37	3/15/2014	12:00 PM	B-12	AV
23	3/10/2014	12:00 PM	13	AV	38	3/15/2014	3:00 PM	B-13	AV
24	3/10/2014	3:00 PM	14	AV	41	3/17/2014	9:00 AM	B-14	AV
24	3/10/2014	3:00 PM	15	AV	41	3/17/2014	9:00 AM	B-15	AV
24	3/10/2014	3:00 PM	16	AV	54	3/22/2014	9:00 AM	B-16	AV
24	3/10/2014	3:00 PM	17	AV	54	3/22/2014	9:00 AM	B-17	AV
24	3/10/2014	3:00 PM	18	AV	75	3/29/2014	9:00 AM	B-18	AV
24	3/10/2014	3:00 PM	19	AV	75	3/29/2014	9:00 AM	B-19	AV
24	3/10/2014	3:00 PM	20	AV	75	3/29/2014	9:00 AM	B-20	AV
25	3/11/2014	12:00 PM	21	AV	75	3/29/2014	9:00 AM	B-21	AV
25	3/11/2014	12:00 PM	22	AV	81	3/31/2014	9:00 AM	B-22	AV
25	3/11/2014	12:00 PM	23	AV	90	4/3/2014	9:00 AM	B-23	AV
25	3/11/2014	12:00 PM	24	AV	90	4/3/2014	9:00 AM	B-24	AV
25	3/11/2014	12:00 PM	25	AV	90	4/3/2014	9:00 AM	B-25	AV

[7]Supplemental Item G. Table summarizing Mueller Glacier depositional events. Please visit https://doi.org/10.1130/GES01622.S7 or the full-text article on www.gsapubs.org to view Supplemental Item G.

TABLE 5. NEW DEPOSITS ON DOUGLAS GLACIER ICY DEBRIS FANS

Icy debris fan	Fan volume (m^3) (2015 TLS survey data)[a]	New deposit volume (m^3) (January 2013–August 2013)	New deposit volume added (%) (January 2013–August 2013)	New deposit volume (m^3) (prorated for one year)[b]	New deposit volume added (%) (prorated for one year)[b]
Fan 1	1,081,400				
January 2013		71,540		89,425	
February 2013		73,140		91,425	
March 2013		29,220		36,525	
April 2013		37,030		46,288	
May 2013		72,728		90,910	
June 2013		26,418		33,023	
July 2013		39,082		48,852	
August 2013		86,220		107,775	
Total Fan 1		*435,400*	*40.3*	*544,200*	*50.3*
Fan 2	216,700				
January 2013		40,710		50,888	
February 2013		18,302		22,878	
March 2013		41,622		52,028	
April 2013		0		0	
May 2013		0		0	
June 2013		0		0	
July 2013		0		0	
August 2013		0		0	
Total Fan 2		*100,600*	*46.5*	*125,800*	*58.1*
Fan 3	1,534,500				
January 2013		80,632		100,790	
February 2013		61,620		77,025	
March 2013		67,396		84,245	
April 2013		59,358		74,198	
May 2013		202,426		253,033	
June 2013		61,162		76,453	
July 2013		55,618		69,523	
August 2013		97,794		122,243	
Total Fan 3		*686,000*	*44.7*	*857,500*	*55.9*
Fan 4	4,593,900				
January 2013		137,674		172,093	
February 2013		260,274		325,343	
March 2013		147,072		183,840	
April 2013		286,938		358,673	
May 2013		131,156		163,945	
June 2013		127,714		159,643	
July 2013		36,682		45,853	
August 2013		66,918		83,648	
Total Fan 4		*1,194,400*	*26*	*1,493,000*	*32.5*
Fan 5	3,145,900				
January 2013		30,772		38,465	
February 2013		32,566		40,708	
March 2013		64,016		80,020	
April 2013		30,640		38,300	
May 2013		36,538		45,673	
June 2013		8,908		11,135	
July 2013		0		0	
August 2013		0		0	
Total Fan 5		*203,400*	*6.5*	*254,300*	*8.1*
Total Douglas	*10,572,400*	*2,620,000*	*24.7*	*3,275,000*	*31*
Sefton[c]					
January 2013		*19,416*		*24,270*	
February 2013		*25,496*		*31,870*	
March 2013		*17,704*		*22,130*	
April 2013		*45,790*		*57,238*	
May 2013		*83,730*		*104,663*	
June 2013		*0*		*0*	
July 2013		*34,202*		*42,753*	
August 2013		*22,190*		*27,738*	
Total Sefton		*248,528*		*310,662*	

[a]Volume estimated using terrestrial laser scanning data and RiScan (see Fig. 16) in 2015.
[b]Annual volumes were prorated to a 12-month period using the ratio of deposits observed in imagery.
[c]Sefton deposits, although significant, were not included in the total for Douglas Glacier icy debris fan (IDF) contributions because they prograded directly onto the valley glacier but did not form IDFs given that they were not focused through canyons.

TABLE 6. NEW DEPOSITS ON MUELLER GLACIER ICY DEBRIS FANS

Icy debris fan	Fan volume (m^3) (2015 TLS survey data)[a]	New deposit volume (m^3) (March 2014–March 2015)[b]	New deposit volume added (%) (March 2014–March 2015)[b]	New deposit volume (m^3) (prorated for one year)[c]	New deposit volume added (%) (prorated for one year)[c]
Fan 1	13,432,100				
March 2014		278,943		334,732	
April 2014		219,420		263,304	
July 2014		309,859		371,831	
August 2014		408,720		490,464	
September 2014		489,371		587,245	
October 2014		658,202		789,842	
November 2014		622,163		746,596	
December 2014		682,148		818,578	
January 2015		428,593		514,312	
February 2015		238,560		286,272	
Total Fan 1		*4,336,000*	*32.3*	*5,203,200*	*38.7*
Fan 2	1,467,200				
March 2014		28,095		33,714	
April 2014		14,480		17,376	
July 2014		44,467		53,360	
August 2014		34,890		41,868	
September 2014		50,488		60,586	
October 2014		35,271		42,325	
November 2014		50,909		61,091	
December 2014		42,396		50,875	
January 2015		20,615		24,738	
February 2015		4845		5814	
Total Fan 2		*326,500*	*22.3*	*391,700*	*26.7*
Fan 3	3,249,700				
March 2014		0		0	
April 2014		0		0	
July 2014		30,192		36,230	
August 2014		134,179		161,015	
September 2014		129,680		155,616	
October 2014		175,124		210,149	
November 2014		203,013		243,616	
December 2014		114,966		137,959	
January 2015		23,825		28,590	
February 2015		209		251	
Total Fan 3		*811,200*	*25*	*973,400*	*30*
Fan 4	1,803,100				2
March 2014		0		0	
April 2014		0		0	
July 2014		0		0	
August 2014		14,332		17,198	
September 2014		0		0	
October 2014		0		0	
November 2014		1207		1448	
December 2014		11,912		14,294	
January 2015		0		0	
February 2015		5067		6080	
Total Fan 4		*32,500*	*1.8*	*39,000*	*2.2*
Total Mueller	*19,952,100*	*5,506,000*	*27.6*	*6,607,000*	*33.2*

[a]Volume estimated using terrestrial laser scanning data and RiScan (see Fig. 16) in 2015.
[b]Camera was occasionally inoperative during this time period, mainly due snow cover or lack of solar charge.
[c]Annual volumes were prorated to a 12-month period using the ratio of deposits observed in imagery.

More than 2300 depositional events were recorded on IDFs at Mueller Glacier, a pace more than twice as active as any other site studied (~3000 events prorated for one year). Two-thirds of the events recorded occurred on Fan 1. Ice avalanches dominated the events on all fans (1799 events) followed by slush flows (376 events) and slush avalanches (117 events). No icy debris flows were recorded on Fan 1 because it receives ice calved directly from the hanging Huddleston Glacier. A mix of avalanches, slush flows, and debris flows was observed on the smaller fans to the east (Fans 2–4). Fans 2–4 have more complex catchments that store rockfall sediment. Ice avalanches predominated during summer months, while slush avalanches dominated activity during spring and fall months (Fig. 14). Slush flows and ice avalanches were the dominant depositional process during winter months. Early summer was the most active period, dominated by ice avalanches. The most active month was December, when 345 ice avalanches were recorded (237 on Fan 1 alone). The highest one-day total was 27 ice avalanches on 19 December 2014, with 26 recorded on 10 January 2015. November (late spring) experienced the highest number of icy debris flows and slush avalanches, mostly during heavy rainfall events. The day with the most icy debris flows was 20 November 2014 (four events) after a heavy rain. Single debris flows occurred in September and February after large rain events. Slush avalanches peaked (34 events) on 4 November 2014 within a day after a large rainfall and snow mix. Other active slush avalanche days occurred in mid-September, associated with significant rainfall. The size of depositional events observed was largest on Fan 1. Fan 4 had the smallest event areas.

Activity on the various fans at Mueller Glacier varied seasonally in a manner similar to that observed at La Perouse Glacier. Fan 1, and to a lesser extent, Fan 2, were active throughout the year, but activity on the smaller eastern fans, particularly Fans 3 and 4 occurred primarily during transitional months and winter; they were relatively inactive during the summer. Fan 1 and part of the catchment to Fan 2 lie below the hanging Huddleston Glacier and are subject to ice avalanches year round. Their catchments are geomorphically simple, allowing ice to cascade directly to the IDFs. Fans 3 and 4 are small but have relatively complex catchments exposing significant areas of bedrock and have no hanging glacier above them. They appear to be fed primarily by ice falling from a relatively thin, discontinuous icecap and mobilization of snowfall and rockfall stored in their catchments during heavy precipitation events in late fall, winter, and early spring.

Mapping data in Tables 2 and 6 show that Mueller fans were extensively resurfaced by new deposits during the 12-month observation period. Given that the camera was not operational for approximately two and a half months during the winter, the minimum percentages of fan surfaces covered were Fan 1 ~2675%, Fan 2 ~98%, Fan 3 ~1790%, and Fan 4 ~188%.

Seasonal Patterns of Ice and Sediment Supply and Linkages to Weather

Integration of time-lapse imagery from all sites documents seasonal patterns in depositional processes. Depositional events on all IDFs studied occurred throughout the entire year. However, the pace and depositional process varied seasonally and were influenced by significant precipitation events. Figures 11–14 and Supplemental Item F-3 (footnote 6) show depositional activity at all sites throughout the year. The pace of activity and the dominant depositional process varied seasonally at most sites (Fig. 15). Based on time-lapse imagery, IDFs experienced a slower pace of depositional activity in the winter (Fig. 15). Peak activity rates occurred during transitional and summer months.

Process dominance varied seasonally at some locations. Ice avalanches occurred throughout the year but predominated during summer months at all sites (Fig. 15). At McCarthy Glacier, slush avalanches and slush flows were nearly equal to the pace of ice avalanches during winter and transitional months (Fig. 11). Many slush avalanches and slush flows likely originated from mobilization of snowfall within the catchments by rainfall events. Conversely, no slush flows or slush avalanches were observed at McCarthy during summer months. At Mueller Glacier, slush flows and slush avalanches dominated during winter and transitional months, while ice avalanches dominated in the summer. Icy debris flows, only observed at IDFs with larger, complex catchments (McCarthy-West and Middle Fans, La Perouse Fans, and Mueller Fans 2–4) occurred in summer or transitional months. Icy debris flows typically occurred following large rainfall, snowmelt, or rain on snow events but have also been observed during outbursts (jökulhlaups) from the base of icecaps. Icy debris flows remobilize avalanche and rockfall sediment stored within the catchments and transport it to the fans.

Enhanced depositional activity often (although not always) followed major rainfall events. For examples of depositional events following rainfall, refer to Reid (2015). Days with the largest number of events and with the highest areal coverage of fan surfaces often followed large rains. On several occasions, we witnessed notable increases in the pace of depositional activity following major rainfall events. For example, on 6 January 2013, we recorded more than 150 events at Douglas Glacier the day after >30 cm of rainfall (Supplemental Item B [footnote 2]). A much lower pace of activity ensued the rest of the week. These short-term increases in depositional activity may have a variety of explanations. First, there is evidence that rainfall may infiltrate through crevasses in the icecap and cause water outbursts (jökulhlaups) from its base (i.e., Kochel and Trop, 2008). Second, infiltrating water may elevate pore-water pressure at the base of the icecap, promoting sliding and accelerating calving at its terminus. Large rainfalls at Douglas Névé may elevate pore-water pressures below recently calved ice in the bedrock grooves, facilitating ice movement to the edge of the shelf where it avalanches onto the IDFs. Third, rainfall can mobilize recently accumulated snow in winter and transitional months within the catchments and trigger slush avalanches and slush flows. Finally, if rainfall rates are high enough, icy debris flows can result, remobilizing ice avalanche and rockfall sediment stored within the catchments. Although all types of depositional processes appear to be enhanced at times by major rainfall, the impact of rainfall appears most pronounced with icy debris flows, slush avalanches, and slush flows.

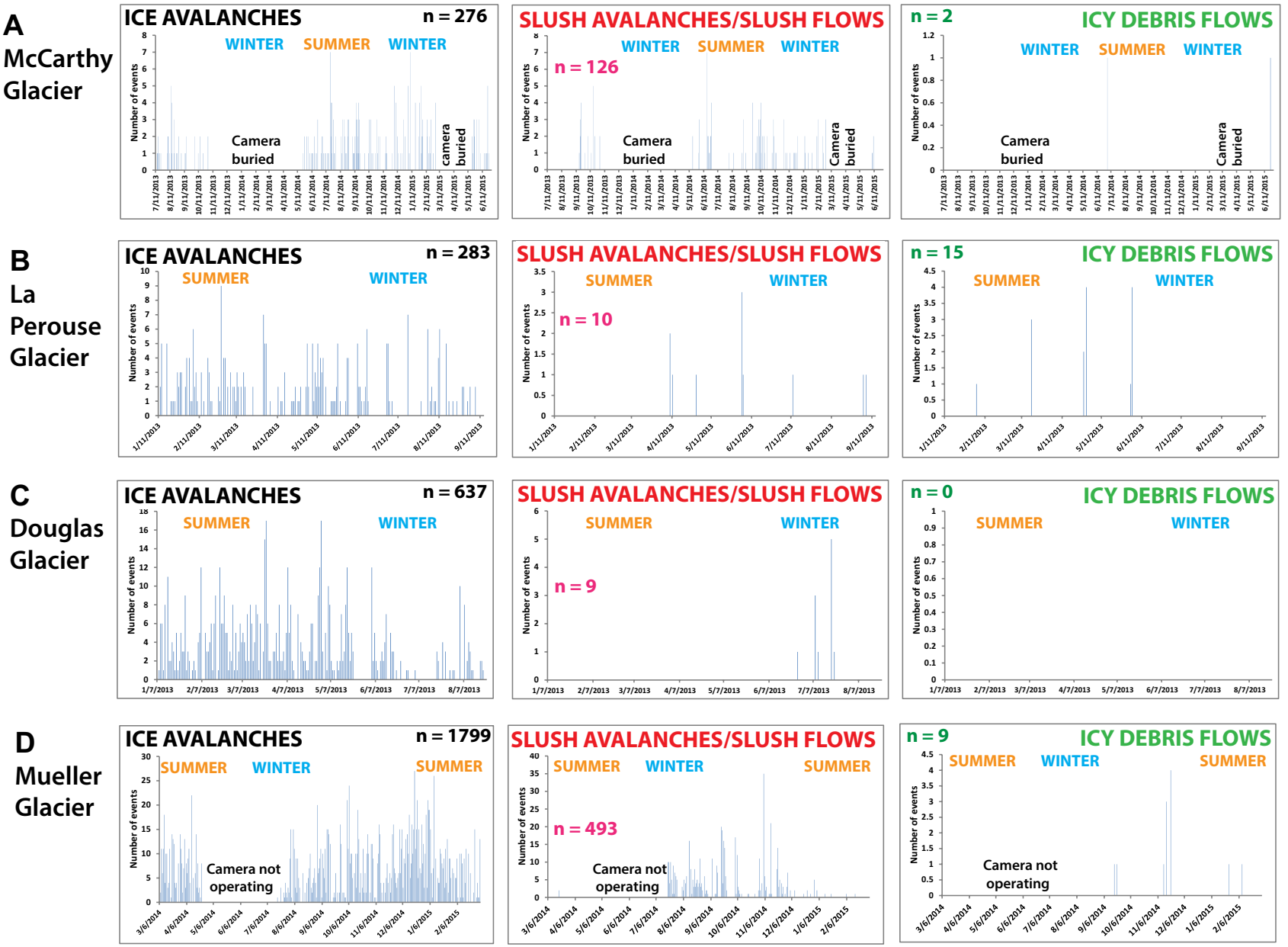

Figure 15. Histograms showing seasonal variation in depositional processes (ice avalanches, slush avalanches and slush flows, and icy debris flows) on icy debris fans. Data are summaries from all fans at each of the four sites; n values show the total number of events recorded by the time-lapse cameras. (A) McCarthy Glacier, Alaska; (B) La Perouse Glacier, New Zealand; (C) Douglas Glacier, New Zealand; and (D) Mueller Glacier, New Zealand.

Volume of Ice and Sediment Supply to Icy Debris Fans

Integration of time-lapse imagery together with TLS data allowed for conservative estimates of the minimum volume of ice and sediment deposited on IDFs (Tables 3–6).

McCarthy Glacier, Alaska

The volume of ice and/or sediment added to three IDFs at McCarthy Glacier in two years was estimated ~2,024,000 m^3, prorated to ~1,518,000 m^3 annually (Table 3). This volume amounts to ~8% of the volume of the IDFs over two years, or ~4% per year. Not accounting for ablation, the volume of material deposited annually on the McCarthy Glacier IDFs is estimated to be ~8%–14% of total McCarthy Glacier volume.

La Perouse Glacier, New Zealand

The estimated volume of ice and/or sediment added to two of the IDFs at La Perouse Glacier in nine months (Table 4) is ~750,000 m^3, prorated to ~937,000 m^3 annually; estimated to be <1% of the La Perouse Glacier volume. Down-valley glacier flow was estimated at ~250 m/yr judging from tracking movements of large boulders on the surface of the glacier visible time-lapse images oriented perpendicular to the glacier axis. Similar analysis of Google Earth images between 2006 and 2013 indicates average flow rates of ~173 m/yr for La Perouse Glacier.

Douglas Glacier, New Zealand

The estimated volume of material added to Douglas IDFs during the eight-month observation period (Table 5) is ~2,620,000 m^3, prorated to ~3,275,000 m^3 annually. This is estimated to be ~4%–7% of the volume of Douglas Glacier. Down-valley flow rates of Douglas Glacier were estimated from Google Earth imagery at ~32 m/yr during 2009–2013. Estimates from the time-lapse camera are ~35 m/yr.

Mueller Glacier, New Zealand

The estimated volume of material added to Mueller IDFs during a one-year observation period (Table 6) is ~5,506,000 m^3—~6,607,000 m^3, if prorated to a year for the period of camera failure. Although Mueller Glacier remains connected with tributary glaciers and icecaps up-glacier, the contribution of ice and sediment via IDFs likely represents a significant part of the budget for the terminal reach of Mueller Glacier, where thinning has exposed the glacier base in places, and large moulins expanded significantly in recent years. This annual contribution from IDFs is estimated to be ~20%–24% of the volume of the lower part of Mueller Glacier below the moulin.

Analysis of Google Earth imagery during 2006–2013 indicates no detectable down-valley movement of the terminal reach of Mueller Glacier, reflective of the nearly stagnant terminal zone. No detectable down-valley movement is observed from our time-lapse camera.

Ablation and Compaction of Icy Deposits

Significant ablation of ice, especially during summer months, impacts estimates of the volume of ice deposited on IDFs. Figure 6 illustrates morphologic and albedo changes due to summer ablation on IDF ice-rich deposits. Fresh ice avalanche deposits are typically bright white. Within days, the deposits compact, congeal, and darken as sediment clasts are concentrated as a surface lag. Relief on levees lessens as the surface topography is smoothed as ablation continues. Short-term estimates of summer ablation and compaction were conducted in La Perouse and Douglas Glaciers in March 2014 using ablation stakes pounded into the fans and measured over several days following depositional events (Reid, 2015). Deposits thinned ~40% during an especially warm four-day period. Ground penetrating radar shows a velocity decrease that occurred on an icy debris deposit during a four-day period; this decrease in velocity indicates a decrease in pore space attributable to compaction (Jacob et al., 2017). Based on our field observations, fresh deposits become increasingly compacted after deposition. Although our measurements were not extensive, field observations and interpretations of time-lapse photos suggest that ablation may account for ~20%—~25% volume loss of ice from newly deposited ice-rich deposits during summer months. We speculate that lower ablation rates occur during intervals of high-frequency activity when new deposits shield previously deposited material from ablation. Additionally, ablation rates in winter months are likely to be much lower than during summer months. We infer that ablation of ice-rich IDF deposits is unlikely to account for more than ~10%–15% reduction in volume contributed to the IDFs when extended over the year. Detailed studies are needed to fully quantify ablation, thereby improving volume contribution estimates. In summary, ablation of ice reduces the total volume of ice added to IDFs annually. Currently, the pace and volume of ice deposition exceed the pace of ablation resulting in volumetric additions to most IDFs (Table 7).

CHANGES IN ICY DEBRIS FAN VOLUME AND SURFACE TOPOGRAPHY (2013–2015)

Terrestrial laser scanning surveys made in 2013 compared to surveys in 2015 were used to investigate changes in elevation, surficial morphology, and IDF volume at all sites except Mueller Glacier (where only a 2015 survey was made). Icy debris fan volumes were estimated using the following techniques on the TLS point cloud in RiScan Pro software (Fig. 16). Fans were outlined (Fig. 16A) and selected to create a smaller point cloud (Fig. 16B), capturing data

TABLE 7. VOLUME CHANGES IN ICY DEBRIS FANS (2013–2015)[a]

Icy debris fan	Volume[a] (2015) (m^3)	Volume change (2013–2015)[e] (m^3)	(%)
McCarthy Glacier[b]			
East Fan	25,360,000	+700,000	+2.8
Middle Fan	2,441,000	–683,700	–21.9
West Fan	3,680,000	–1,200,000	–24.6
La Perouse Glacier[c]			
East Fan	3,618,100	+397,100	+12.3
Middle Fan	2,299,300	+229,700	+11.1
West Fan	2,121,400	+191,200	+9.9
Douglas Glacier[c]			
Fan 1	1,081,400	+62,700	+6.2
Fan 2	216,600	–12,600	–5.5
Fan 3	1,534,500	+115,200	+8.1
Fan 4	4,593,900	+890,600	+24.0
Fan 5	3,145,900	+784,700	+33.2
Mueller Glacier[d]			
Fan 1	13,432,100		
Fan 2	1,467,200		
Fan 3	3,249,700		
Fan 4	1,803,100		

[a]Volume surveyed by terrestrial laser scanning (TLS) ground surveys.
[b]June 2013–June 2015.
[c]January 2013–March 2015.
[d]Estimated from photo analysis and TLS survey in March 2015.
[e]Calculated from TLS data using RiScan Pro (see Fig. 16).

limited to the IDFs. People and large boulders were removed using the "data filtering" tool in the RiScan software. A regularly spaced mesh was created by triangularly interpolating between observations (Fig. 16C) to morph the point cloud into a complete mesh without data gaps (Fig. 16D). The "smooth and decimate" tool in the RiScan software was then applied to the triangulated mesh to remove remaining anomalies and decrease the mesh size (Fig. 16E) and create a digital elevation model (DEM) of the IDF. A horizontal reference plane was inserted at the base of the elevation of the IDF DEM (Fig. 16F). This insertion assumes that the fan sits on top of the glacier as defined by the horizontal plane, which is unlikely; thus, some overestimation of fan volume is expected. This method, however, provides a consistent methodology for calculating fan volume among different sites between surveys. The final step in calculating IDF volume was to use the RiScan software "volume tool," which integrates the total elevation difference between the base plane and the IDF DEM (Figs. 16G and 16H).

Differences in surface elevations between the 2015 and 2013 DEMs from the TLS surveys were computed to produce maps of differential surface elevation change of individual IDFs and adjacent sections of valley glaciers (Fig. 17). As a quality control procedure, we compared portions of the differential surface elevation data to RTK-GPS data generated simultaneously during the field work.

McCarthy Glacier, Alaska

Between 2013 and 2015, the volume of the Middle and West Fans at McCarthy Glacier decreased by ~22% to ~25%, while East Fan volume increased ~3% (Table 7). East Fan grew chiefly by aggradation in the proximal region, amplifying its convexity (Fig. 17A). These changes are consistent with time-lapse camera data that show >50% of the events reaching the three fans occurred on the East Fan (Fig. 18). The exposed terminal face of the icecap is twice as extensive above the East Fan as it is above the Middle or West Fans (Fig. 19A), providing more opportunity to supply ice to East Fan. Meanwhile the convexity diminished slightly on Middle Fan and substantially on West Fan (Fig. 19B). Middle Fan remained relatively stable, losing overall elevation slightly and gaining material in few areas. Aggradation occurred mainly along preferred avalanche tracks on Middle Fan along its western and mid-fan areas. In contrast, West Fan lost substantial material (commonly ~3–6 m) across most of its area. The only area of aggradation of West Fan was the mid-fan zone where ice avalanches and icy debris flows accreted distal of the fan-head trench.

Only a portion of McCarthy Glacier was able to be compared in the differential TLS analysis, preventing estimates of volume change. The TLS data document minor deflation (averaging ~1–2 m) of the glacier (Fig. 17A). Localized linear zones of enhanced deflation (up to ~9 m) occurred on the central distal part of East Fan and the adjacent part of the glacier. This area has a dendritic surface drainage that extends from the East Fan terminus onto the glacier and into a large moulin. The amount of deflation at McCarthy (1–2 m) is lower than glaciers studied in New Zealand (up to tens of meters) (Fig. 17). The lower amount of deflation at McCarthy is interpreted to partly reflect a higher ratio of material contributed from IDFs compared to the volume of McCarthy Glacier.

La Perouse Glacier, New Zealand

The volume of the three IDFs at La Perouse Glacier increased ~10%–12% (Table 7). Figure 17B shows that while La Perouse Glacier experienced extensive deflation (in most places ~6–10 m) East and Middle Fans experienced extensive aggradation (more than 5 m across large areas) and volume increase. In spite of the deflation, West Fan elevation remained relatively unchanged because it experienced ~10% volume increase as a result of distal lengthening of the IDF. With the exception of a large axial crevasse that opened, East Fan experienced ~4–12 m of aggradation over half its middle-distal region. Similarly, Middle Fan experienced ~2–10 m of aggradation over most of its surface during the two-year period (Fig. 17B). In contrast, West Fan at La Perouse was characterized by areas of aggradation and loss. We infer that the inter-fan differences reflect less connectivity of West Fan with the icecap terminus.

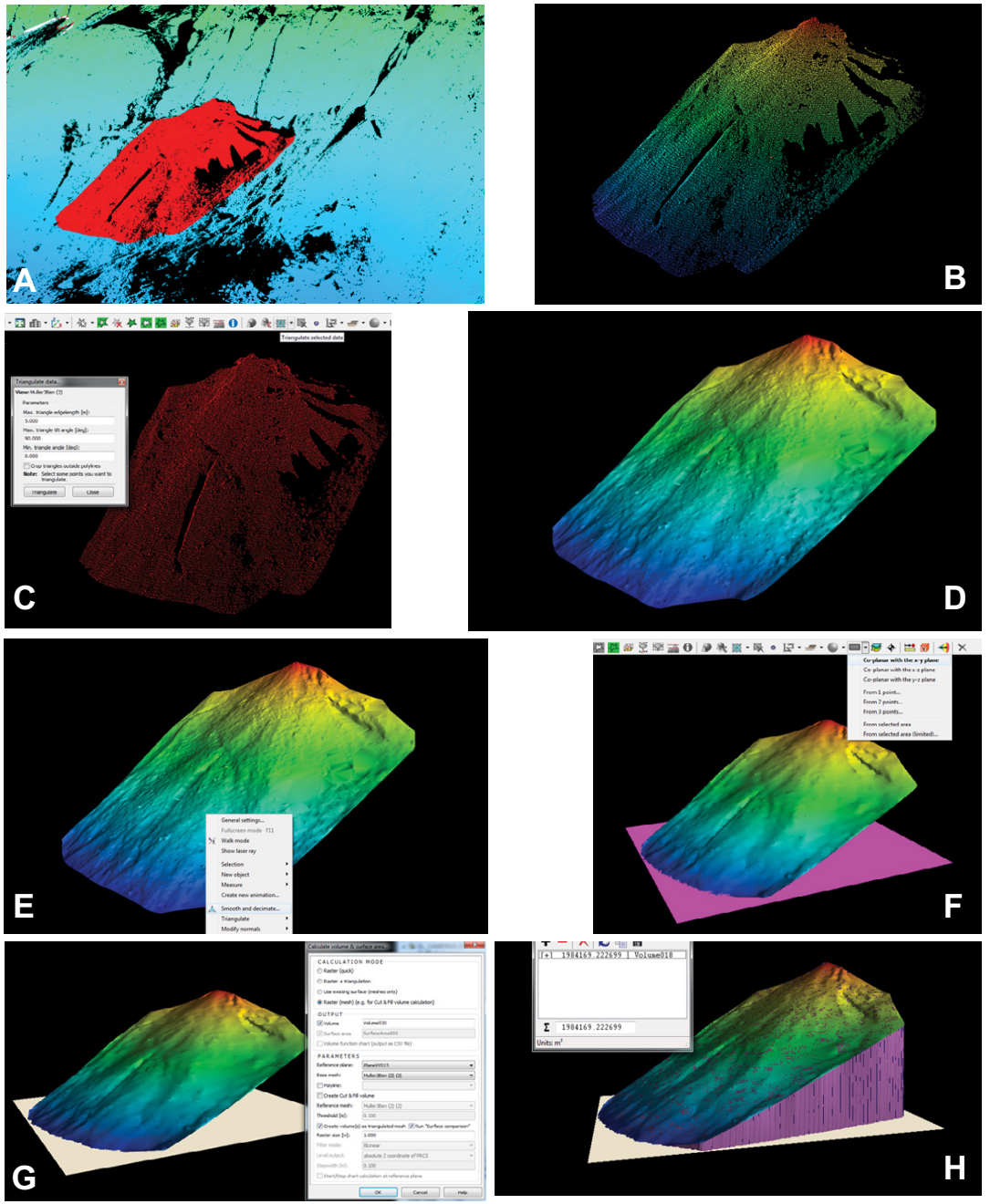

Figure 16. Estimate of volume of icy debris fans from terrestrial laser scanning (TLS) analysis using RiScan Pro software. (A) Delineation of target fan on TLS merged scan image. (B) Capture of fan to create polydata. (C) Data filtering to remove vegetation and people from the point cloud. (D) Triangulated mesh to removed data gaps in the point cloud. (E) Smoothing and decimation to remove anomalies from the point cloud. (F) Insertion of horizontal base plane to calculate fan volume. (G and H) Use of volume tool to estimate fan volume above the base plane.

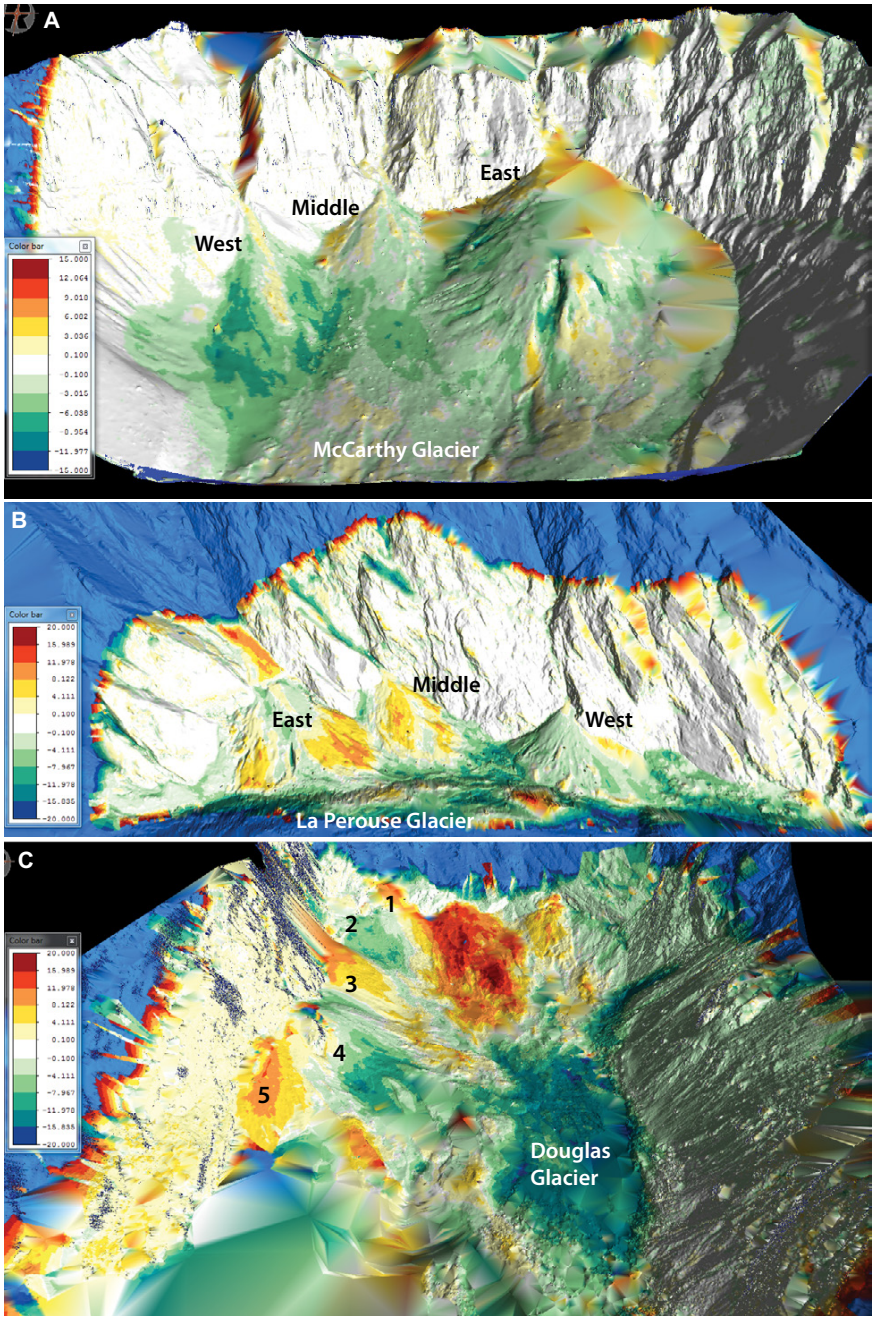

Figure 17. Elevation changes on icy debris fans and associated valley glaciers between terrestrial laser scanning (TLS) surveys in 2013 and 2015. See text for methods. Scale of surface elevation change is in meters. Warm colors represent net gain in surface elevation; cool colors represent net loss in surface elevation. Scale ranges are: McCarthy: –16 m to +15 m; La Perouse: –20 m to +20 m; Douglas: –20 m to +20 m. Fans are labeled in black, glaciers in white. Blue areas on the uppermost slopes are areas beyond reliable TLS coverage. (A) Surface elevations at McCarthy Glacier indicated overall minor thinning (deflation), generally between 1 and 3 m. One exceptionally rapid area of thinning was just below the central-distal part of East Fan where a moulin has been developing. Icy debris fans showed a variety of responses during the two years. East Fan experienced thickening in its proximal region and maintained a nearly constant elevation to slight loss over much of the remainder of the fan. Middle Fan experienced minor elevation losses over much of its distal area but experienced gains along the western third and much of the proximal region. West Fan showed elevation losses except along an axial corridor that was aligned with the fan-head trench. (B) Icy debris fans at La Perouse experienced elevation gains during the survey period, especially on East and Middle Fans. West Fan showed mixed results, with slight losses or maintaining a balance on much of its surface while experiencing gains on its western 15%. La Perouse Glacier experienced thinning, with elevation losses averaging ~10 m and more in places. (C) Most Douglas Glacier fans experienced elevation gains during the survey period. Most notable were increases of >5 m on Fans 3 and 5 and along the area receiving avalanches from Mount Sefton (rear of image to the right of Fan 1). A notable exception was Fan 2, which experienced elevation loss (3–5 m), but this was the fan that episodically slumped onto the glacier during winter months. Similar to La Perouse Glacier, Douglas Glacier experienced thinning, with elevation losses between 5 and 10 m along its northern half (closer to the fans) and >10 m along its southern half (right).

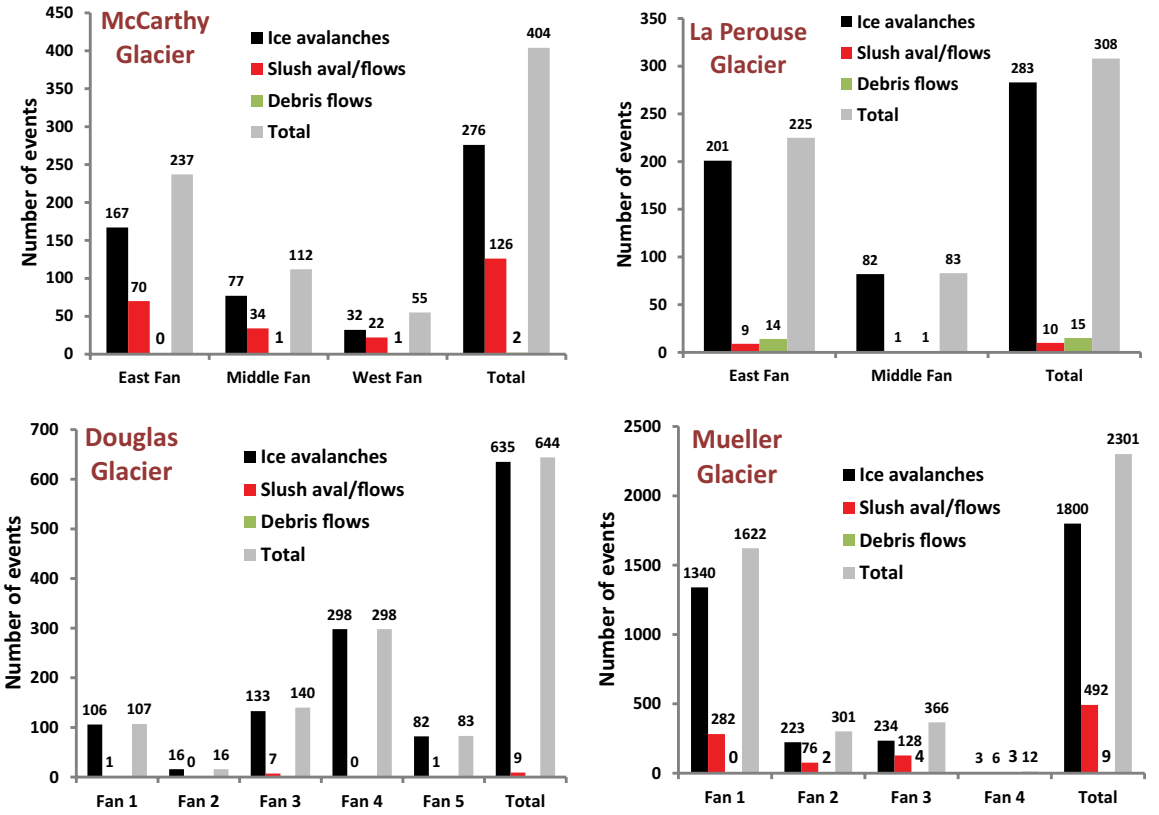

Figure 18. Variation in process dominance between fans related to differences in catchment morphology based on analysis of time-lapse photography. See Figures 11–14 and Supplemental Item F (footnote 6) for time-lapse imagery and videos. Dates of imagery vary between sites. McCarthy Glacier: June 2013 to June 2015; La Perouse Glacier: January 2013 to September 2013; Douglas Glacier: January 2013 to August 2013; Mueller Glacier: March 2014 to March 2015. Note the absence of debris flows at fans with simple catchments (Douglas Fans 1–5, Mueller Fan 1, and McCarthy East Fan). Fans with simple catchments receive only ice avalanches and slush avalanches and/or slush flows. Fans with larger, more complex catchments receive all types of deposits (McCarthy West and Middle, La Perouse Fans, and Mueller Fans 2–4).

Although La Perouse Glacier experienced extensive deflation between 2013 and 2015 (Fig. 17B), there are zones of apparent aggradation. One notable aggradation zone appears on the glacier near the toe of West Fan in Figure 17B. This location does not actually reflect aggradation on the glacier but is an artifact of down-glacier transport of a major rockfall deposit (ca. 2006–2010) that insulated the glacier and was not within the scanned area in 2013. A similar, but less extensive rockfall in front of East Fan likely explains this area of little topographic change on the glacier.

Douglas Glacier, New Zealand

Figure 17C shows complexity in topographic changes for Douglas Glacier and its IDFs. Aggradation occurred on Fans 1, 3, and 5, as well as the up-glacier zone east of the IDFs that received large avalanches from the western slope of Mount Sefton. Fans 2 and 4 showed mixed topographic change. Most of Fan 5 and most of the area off the slope of Mount Sefton experienced ~10–20 m of aggradation during the survey period (Fig. 17C). A similar amount of aggradation occurred in the proximal half of Fan 3, while its distal portion had ~3–6 m of aggradation. Fan 4 accreted between ~3–6 m in the proximal zone, while much of the remaining two-thirds of the fan experienced ~2–8 m of elevation loss. Aggradation occurred along the eastern margin of Fan 4, reflecting a large rock-ice avalanche that emerged onto the fan on 23 May 2013. Fan 2 showed behavior different from other fans (Fig. 17C). Fan 2 was active only during the summer in 2013. After March, deposition ceased on Fan 2, and the fan slumped onto the glacier, demonstrating that small IDFs can be ephemeral. Subsequent field observations in 2014 and 2015 suggest that episodic slumping continues to occur. Fan 1 experienced aggradation (~4–20 m) along its proximal region but showed loss of up to ~6 m in its proximal region along the west toward Fan 2. We infer that the anomalous elevation loss in the area of Fan 2 and western parts of Fan 1 may be indicative of amplified deflation of the underlying Douglas Glacier in this area. This area of Fan 2 showed losses in a zone otherwise characterized by elevation gains (Fig. 17C).

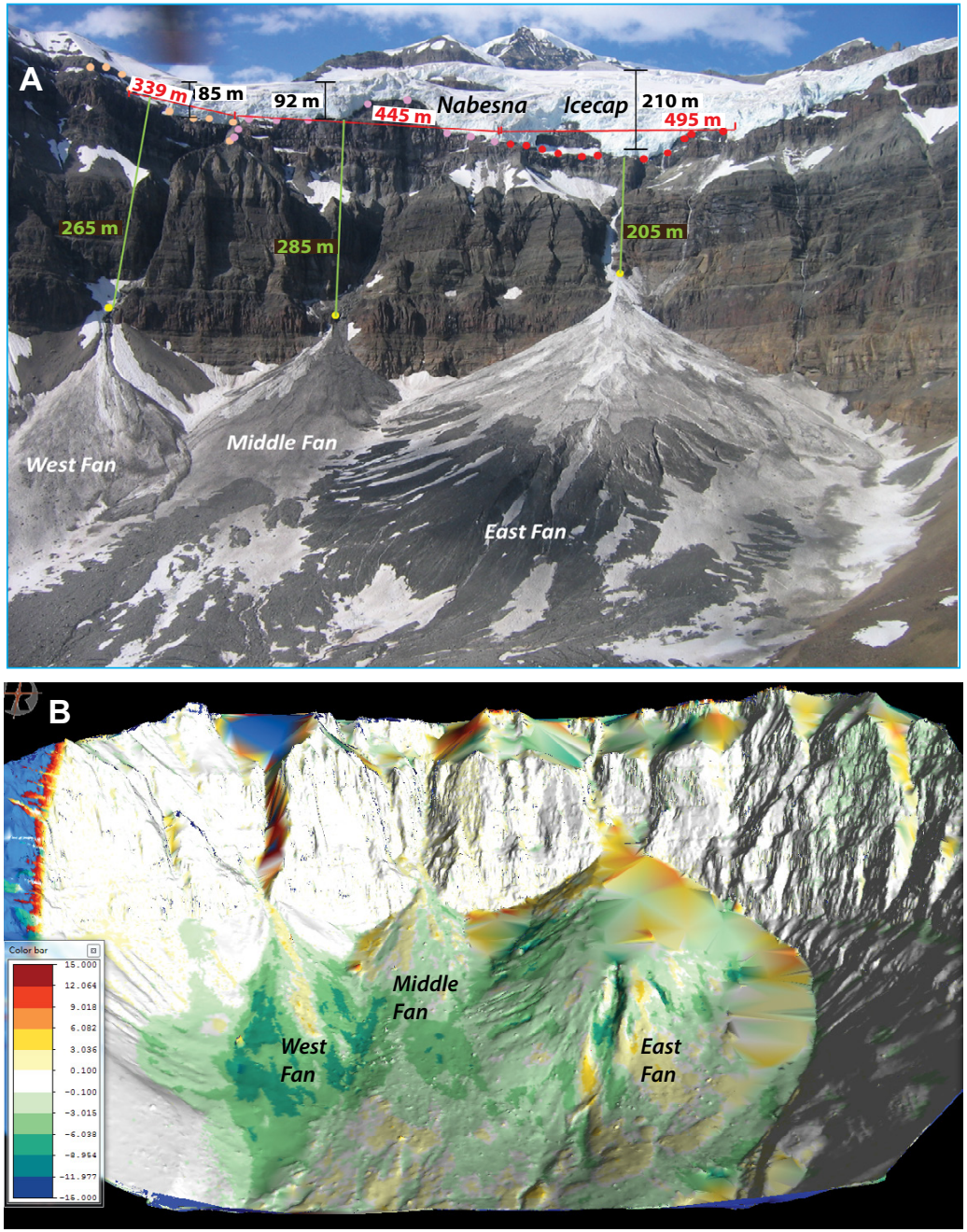

Figure 19. Influence of connection to icecap and catchment morphology on the size of icy debris fans at McCarthy Glacier. (A) Morphology of the Nabesna Icecap terminus above the fan catchments. The exposed area of the icecap is much more extensive above East Fan than above the others, resulting in higher pace and volume of ice avalanches to East Fan. Additionally, the less complex geomorphology of East Fan catchment facilitates more efficient delivery of ice to the fan. In contrast, the limited exposure of ice above West and Middle Fans, combined with increased opportunity for storage within their complex catchments, results in lower delivery rates to those fans. (B) Digital model of changes in fan elevations from terrestrial laser scanning surveys in June 2013 and June 2015. Scale of surface elevation change is in meters. Warm colors represent net gain in surface elevation; cool colors represent net loss in surface elevation (ranges from –16 m to +15 m). Note slight overall growth of East Fan and smaller areas of recent deposition on West and Middle Fans.

Differential topographic analysis of TLS data on Douglas Glacier shows that it experienced deflation during 2013–2015 (Fig. 17C). The south part of the glacier, which is beyond the normal runout of avalanches, lost ~15–20 m elevation, similar to La Perouse Glacier. Most other areas experienced ~6–10 m deflation. Only the sections influenced by avalanche runout from IDFs and the area influenced by Mount Sefton avalanches gained elevation, except for a few areas insulated by extensive rockfall debris in the west-central part of the survey region.

Mueller Glacier, New Zealand

Differential topographic analysis at Mueller Glacier is limited due to the lack of a repeat TLS survey. However, repeated field observations and photographs together with Google Earth imagery document topographic changes. The lower reaches of Mueller Glacier deflated, receded, and formed a moulin in the region where the distal fans were positioned during the 1980s. As discussed in the section "Frequency of Ice and Sediment Supply to Icy Debris Fans," Fan 1 (Fig. 14) experienced exceptionally high depositional rates during the observation period. Repeat photographs from 2009 to 2016 with a scale calibrated using the 2015 TLS data on Mueller Glacier show that it experienced ~65 m of deflation adjacent to the IDFs during the seven-year period. As a result of substantial glacier deflation, Fan 1 appears to be detaching from the glacier and hanging above the valley glacier.

ROLE OF CATCHMENT MORPHOLOGY ON DEPOSITIONAL PROCESSES

The nature of depositional processes varied considerably between IDFs (Figs. 11–14). Ice avalanches dominated depositional events observed or imaged on all IDFs—ranging from 68% to 99% of events. Slush flows and slush avalanches accounted for 1%–31% of events. Icy debris flows comprised 0%–5% of events. The relative proportions of types of depositional processes on specific IDFs were influenced by the size and geomorphic complexity of their catchments. We define the catchment as the area between the terminus of the icecap and the fan apex, however an undetermined area within the icecap contributes water that emerges from the base of the icecap. Geomorphically complex catchments have bends, steps in the longitudinal profile, bedrock basins, changes in width, and tributaries. These features allow for temporary storage of ice and sediment wasted from the icecap and catchment walls. Icy debris fans located below large and geomorphically complex catchments exhibited the greatest diversity of depositional processes, including avalanches, slush flows, and icy debris flows. Catchments with smaller and less complex catchments mainly funnel ice to IDFs as avalanches.

Figure 20 shows the spectrum of catchment geomorphology exhibited by the IDF sites studied. The simple, less developed end of the catchment geomorphic spectrum is represented by Fan 1 at Mueller Glacier and all fans at Douglas Glacier. Fan 1 at Mueller is fed by direct calving from the hanging Huddleston Glacier. Ice avalanches are nominally channeled through poorly incised chutes in the bedrock directly to the fan apex. As a result, Mueller Fan 1 received only ice avalanches, slush avalanches, and slush flows; no debris flows were observed. Very small amounts sediment reached the fan. All five fans at Douglas Glacier were similarly dominated by ice avalanches and occasional slush flows with minor sediment. Ice that calved from Douglas Névé (icecap) slid down linear channels cut into the bedrock just below the icecap (névé) (following the dominant bedrock foliation) and cascaded directly onto fan apexes. Short, simple, less incised catchments provided little opportunity to incorporate sediment. The East Fan at McCarthy Glacier has a larger catchment, but it is also geomorphically simple with two linear chutes that converge on a central chute leading to the fan apex. Avalanches readily moved down this ramp-like feature to the East Fan with little opportunity to store sediment in the catchment. The high frequency of avalanches keeps much of the catchment bedrock ice covered. Therefore, East Fan was also dominated by ice avalanches, slush avalanches, and slush flows. No debris flows have been observed in more than a decade of observations at East Fan.

Catchments above IDFs at Mueller and La Perouse Glaciers represent the middle of the geomorphic complexity spectrum (Fig. 20). Fans 2–4 at Mueller Glacier received ice calved from various icecaps and hanging glaciers; however, the ice was funneled through channels that are slightly more incised and sinuous. The slight increase in geomorphic complexity for Mueller Fans 2–4 results in a setting where more accumulation of sediment from bedrock walls can be episodically remobilized into icy debris flows. Several small icy debris flows were recorded by the time-lapse camera over the course of a year.

La Perouse catchments have large areas but are extraordinarily elongated along the dominant foliation plane of the bedrock. Catchment lengths exceed 1500 m and are moderately incised. Abundant bedrock exposure occurs along these catchments, yielding occasional rockfalls. Sharp bends, common along catchment segments where joints and foliations intersect, provide limited areas for temporary storage of rockfall debris that can be later mobilized by mass flows, including icy debris flows. Although there are steps in the axial profile along joints and foliation planes, the steepness of the catchments reduces long-term storage of material. La Perouse catchment gradients range from ~45° to ~52°, whereas other catchments studied have ~33° to 44° gradients. As a result, La Perouse IDFs were dominated by ice avalanches, but slush flows and debris flows also occurred.

The geomorphically complex end of the catchment spectrum is represented by West Fan and Middle Fan at McCarthy Glacier (Fig. 20). These IDFs are fed by comparatively large, deeply incised, and geomorphically complex catchments based on aerial surveys from helicopters and drones (Fig. 21). The West and Middle McCarthy catchments bifurcate into first-order tributaries that extend along joints and less resistant bedrock units. Longitudinal profiles along valley axes show steps and variations in grade and width.

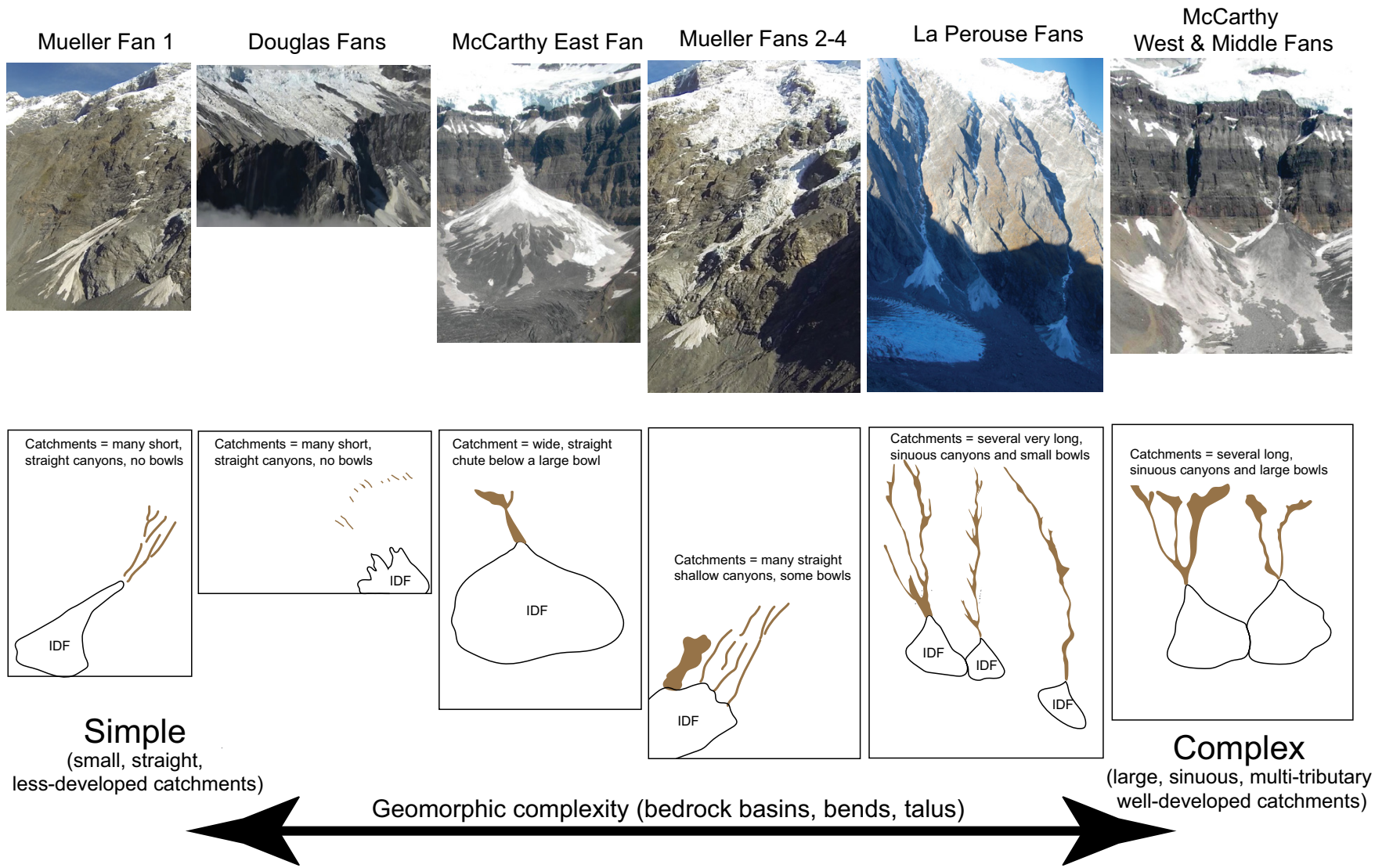

Figure 20. Spectrum of catchment geomorphic complexity at icy debris fan sites. Simplest catchments with small areas, minor incision, and limited bends and storage spaces are on the left. Catchments with greater geomorphic complexity—larger area, stepped axial profiles, bedrock basins, bends, and abundant spaces to store ice and sediment are on the right. Fan 1 at Mueller Glacier has virtually no catchment, delivering ice directly to the fan apex by ice avalanching and slush flows from hanging Huddleston Glacier. The catchments above icy debris fans (IDFs) at Douglas Glacier have slightly more geomorphic complexity. They are simple grooves and/or channels cut into the bedrock shelf below the icecap, just large enough to funnel ice into discrete channels before it avalanches onto fan apexes. Only ice avalanches and slush avalanche and/or flows can develop here. East Fan at McCarthy has a large but simple catchment. It is a straight, ramp-like shape with limited bedrock exposure, hindering extensive storage of material in the catchment. During this study, only ice avalanches and slush avalanche and/or flows were observed on East Fan at McCarthy. Fans 2–4 at Mueller Glacier have slightly more complex catchments; channels and/or grooves are slightly cut into bedrock along foliation and joints, providing access to occasional rockfall and providing limited storage sites, allowing for some development of debris flows. La Perouse catchments exhibit moderate geomorphic complexity. La Perouse catchments are very long (hundreds of meters) and narrow with modest but limited space to store rockfall and avalanche material. Most events here are ice avalanches and slush avalanches and/or flows, but occasional debris flows occur. West and Middle Fans at McCarthy have extensive, deeply incised and geomorphically complex catchments. Storage areas in these catchments are abundant, allowing mixing of ice, water, and sediment to yield the full range of icy debris fan depositional processes, including debris flows.

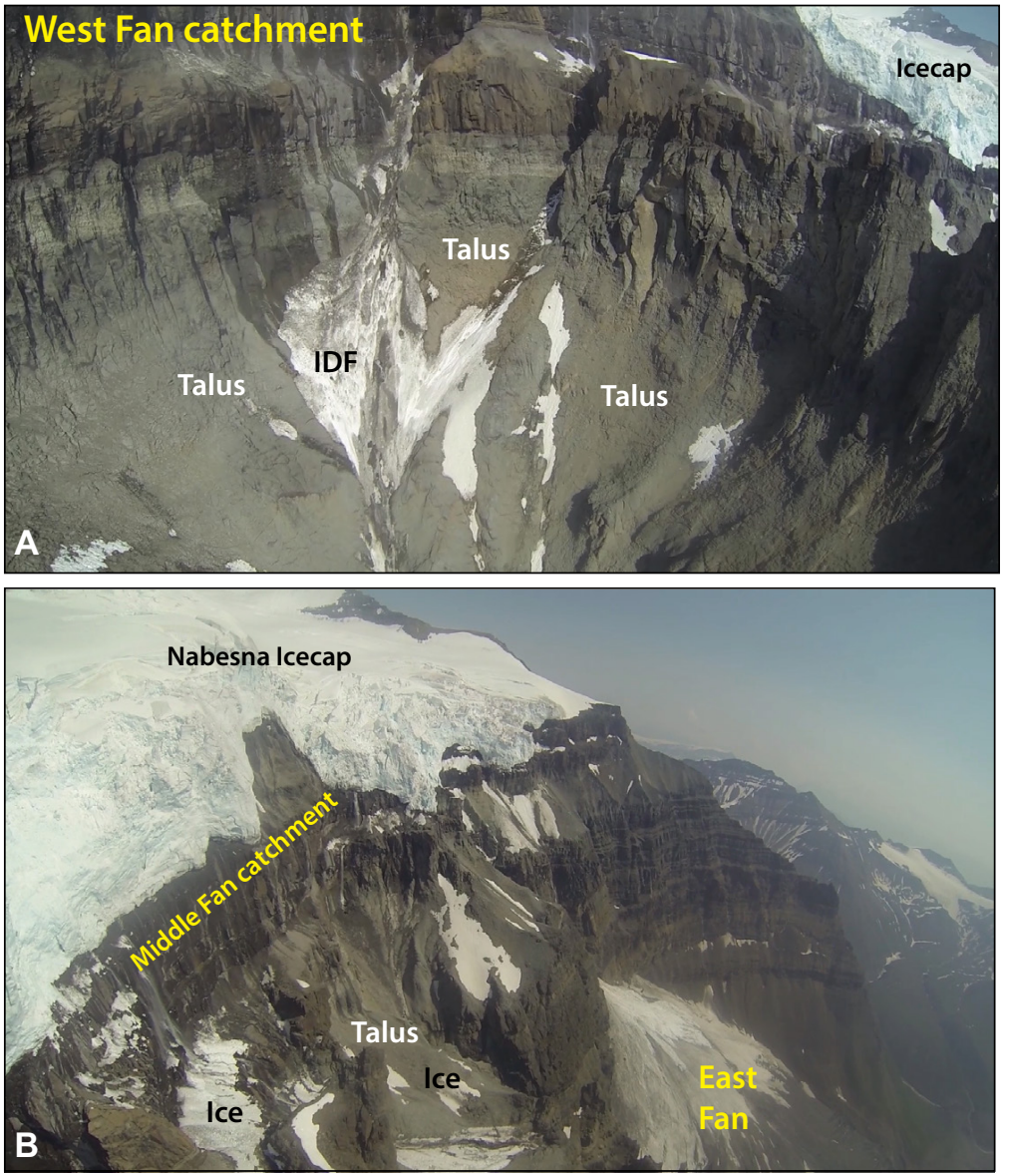

Figure 21. Drone photos of upper regions of icy debris fan (IDF) catchments at McCarthy Glacier showing geomorphic complexity and abundant storage of ice and sediment wasted off of the Nabesna Icecap and bedrock walls. (A) West Fan catchment showing small IDFs and talus stored temporarily high up above the fans in the catchment within bedrock basins and ledges. (B) Temporary storage of talus and avalanche materials in the upper parts of Middle Fan catchment. Field observations documented dozens of rockfalls and avalanches daily. Refer to Supplemental Item B (footnote 2) for field observations showing that most deposits do not reach the IDFs and thus are temporarily stored in the catchment.

This geomorphic complexity provides multiple locations within these catchments for temporary storage of ice and sediment. We observed icy debris flows shortly following outbursts (jökulhlaups); we infer that ice and sediment previously stored in the catchments were remobilized sediment, resulting in icy debris flows. Consequently, West and Middle Fans at McCarthy received deposits from a mix of all processes that contribute material to IDFs. In addition, the West and Middle Fan catchments contain small bedrock basins, talus cones, and avalanche cones. We infer that much of the sediment remobilized into icy debris flows onto the fans originated from rockfall and ice avalanche events restricted to catchments.

There is also a positive relationship between dominance of depositional process type and the degree of connectivity and area of the icecap exposed above their catchments. The terminal face of the icecap exposed above East Fan on McCarthy Glacier has twice the area as the icecap face above West and Middle Fans (Fig. 19). Thus, we expect that seasonal variability in depositional processes on IDFs likely reflect a greater area of icecap exposure—for example, the Middle Fan at La Perouse Glacier compared to the East Fan (Supplemental Item F-1 [footnote 6]).

The influence of catchment morphology is reflected in variability in depositional processes between sites documented in our time-lapse imagery. Larger, geomorphically complex catchments exhibited the highest proportions of sediment-rich mass flow processes (icy debris flows and hyperconcentrated flows—0.5% at West and Middle Fans at McCarthy Glacier; 5% at East and Middle Fans at La Perouse Glacier; and 1% at Fans 2 and 3 at Mueller Glacier). Geomorphically simple catchments exhibited the highest proportion of ice-rich mass flow processes (ice avalanches and slush flow and slush avalanches—100% at Fans 1–5 at Douglas Glacier, Fan 1 at Mueller Glacier, and East Fan at McCarthy Glacier). The proportions of ice avalanches to slush flow and slush avalanches varied with size of geomorphically simple catchments. The smallest simple catchments yielded (Fans 1–5 at Douglas Glacier) 99% ice avalanches and 1% slush flow and slush avalanches; the medium-sized simple catchment (Fan 1 at Mueller Glacier) yielded 83% ice avalanches and 17% slush flow and slush avalanches; the largest simple catchment (East Fan at McCarthy Glacier) yielded 70% avalanches and 30% slush flow and slush avalanches.

ICY DEBRIS FAN MORPHOLOGY AND COMPARISON TO ALLUVIAL FANS

From the air, IDFs appear similar to alluvial fans with their conical shape radiating from a mouth of a bedrock canyon. With most axial gradients ~22°–33° (Table 1), IDFs are steeper than alluvial fans, which are typically <15°. Axial fan gradients exhibit a profile similar to alluvial fans in that they have a progressive decrease in the longitudinal gradient with no measureable step across the apex region. Transverse profiles across IDFs vary considerably between fans, but generally display greater convexity than alluvial fans. Fans with the highest frequency and volumes of ice avalanches have greatly enhanced convexity, to such an extent that the longitudinal profile is locally convex (East Fan at McCarthy Glacier, Fig. 22). This enhanced convexity creates a bulge large

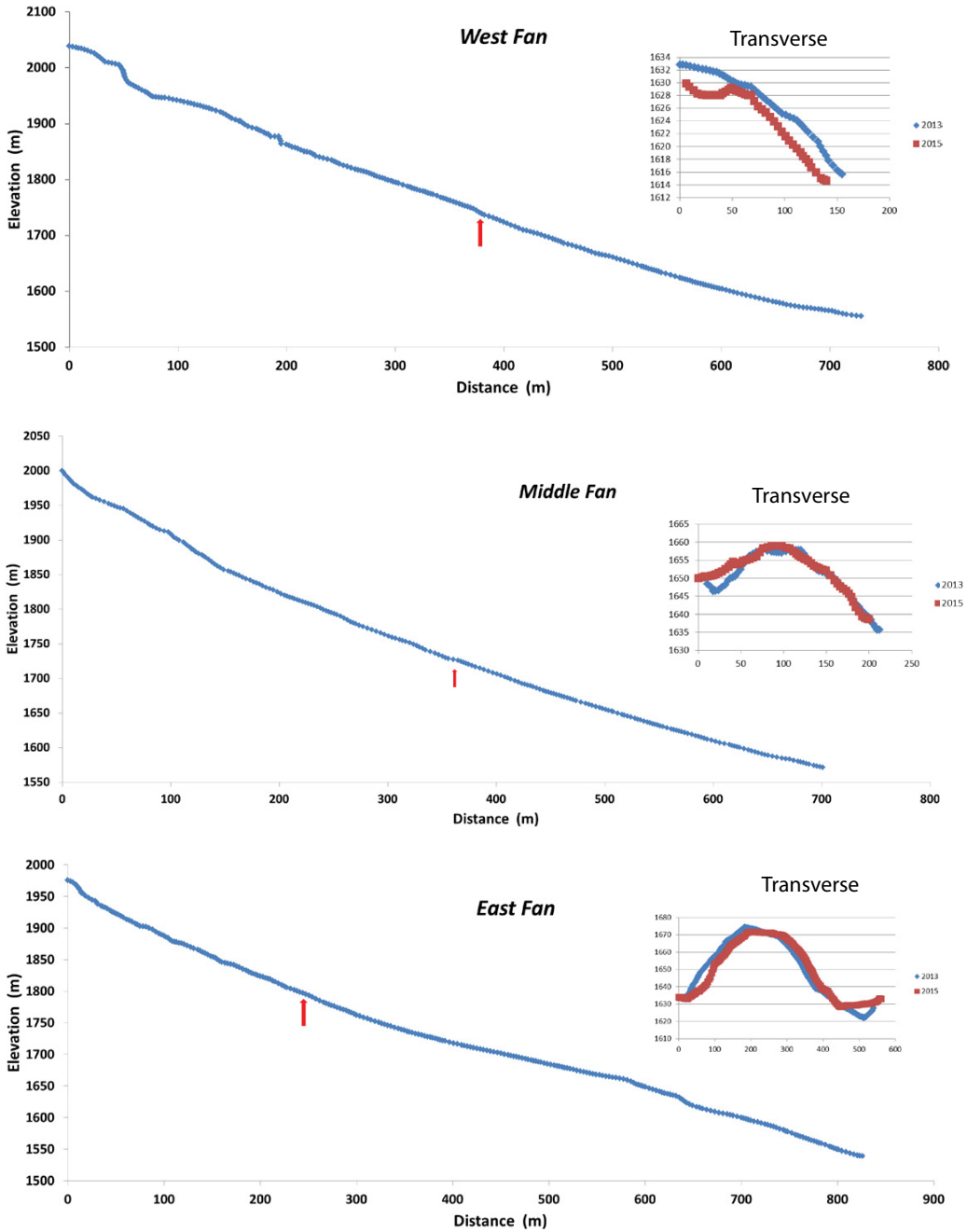

Figure 22. Axial (taken near apex to distal region) and transverse profiles (taken at the mid-fan region) of icy debris fans (IDFs) at McCarthy Glacier. Red vertical lines represent the location of the fan apex. Transverse profile across East Fan exhibits enhanced convexity, which reflects higher pace of ice delivery to East Fan. Data were extracted from terrestrial laser scanning surveys in 2013 and 2015.

enough to divert new avalanches to the lateral fan margins. Convexity ratios of IDFs range from 0.06 to 0.16 (Table 1) compared to those of alluvial fans, for example, in southern California that are typically <0.03, with some as low as 0.007 (Bull, 1964; Blair and McPherson, 1994). Fans with lower depositional frequency generally display less convexity (West and Middle Fans at McCarthy Glacier on Fig. 22).

Relationships between catchment area and IDF fan area are complex. Unlike the well-established positive relationship between alluvial fan area and catchment area (Bull, 1964; Ritter et al., 2011), IDF size shows variable relationships to catchment area (Table 1; Fig. 23). For example, Douglas Glacier IDFs show a positive relationship, whereas McCarthy Glacier IDFs exhibit an inverse relationship (Table 1; Fig. 23). Icy debris fan area and frequency and/or

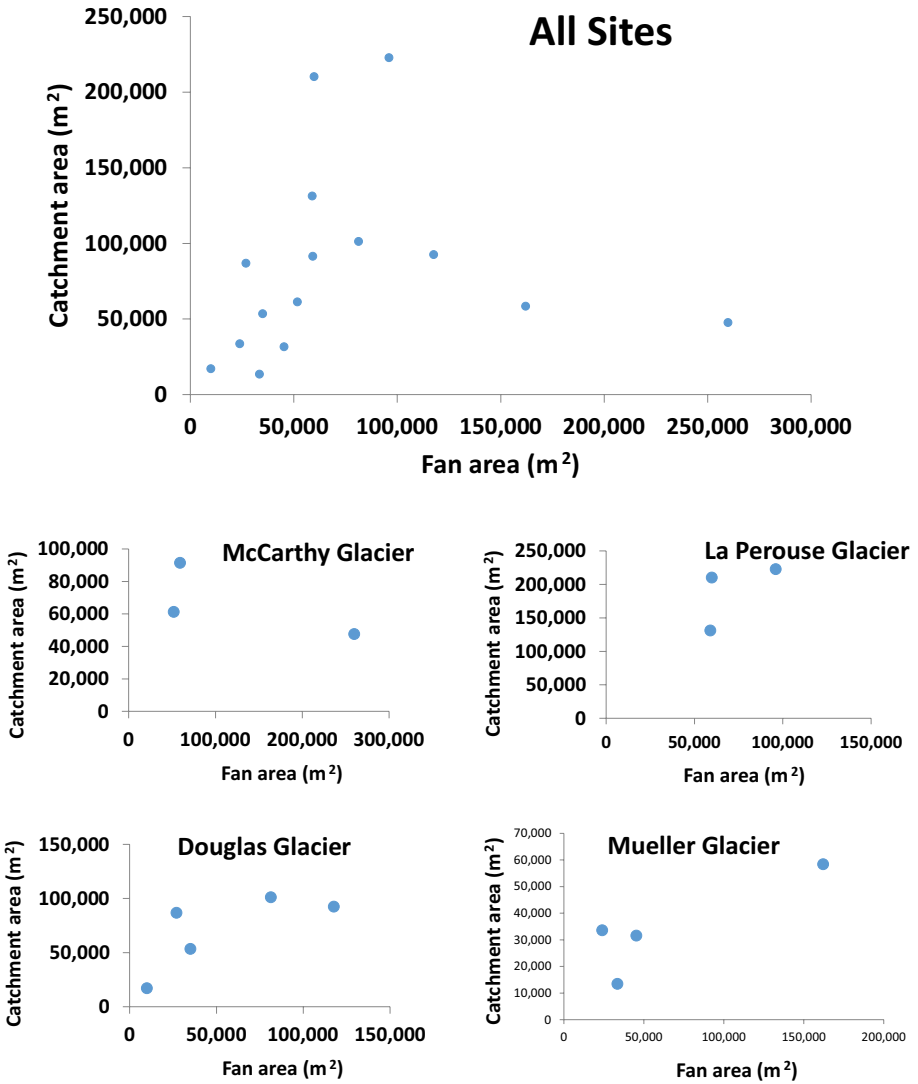

Figure 23. Relationships between fan area and catchment area. Top plot shows all 15 fans studied. Note the large scatter in the relationship. The four plots below show data from fans within each of the four study sites. Most sites show a positive relationship between fan area and catchment area, albeit somewhat variable. The exception is at McCarthy Glacier where an inverse relationship exists.

volume of depositions exhibit a more consistent positive relationship (Fig. 24). We interpret these relationships, together with our depositional event data, to indicate that the exceptionally high frequency of deposition on IDFs compared to alluvial fans adds complexity to the relationship between fan area and catchment area.

Similar to alluvial fans, IDFs may exhibit episodic fan-head trenches. Slush flows and hyperconcentrated flows commonly erode proximal areas of IDFs, forming trenches. Direct observations of slush flows suggest that turbulence in these relatively warm waters promoted erosion of ice debris fan surfaces, exporting ice and sediment down-fan. Subsequent ice avalanches typically refill these small fan-head trenches within days to weeks. A large, long-lasting fan-head trench has been observed on West Fan at McCarthy Glacier (Fig. 25) since the beginning of our observations in 2006. We interpret this as suggesting that the West Fan formed on top of the talus apron and was later incised by large

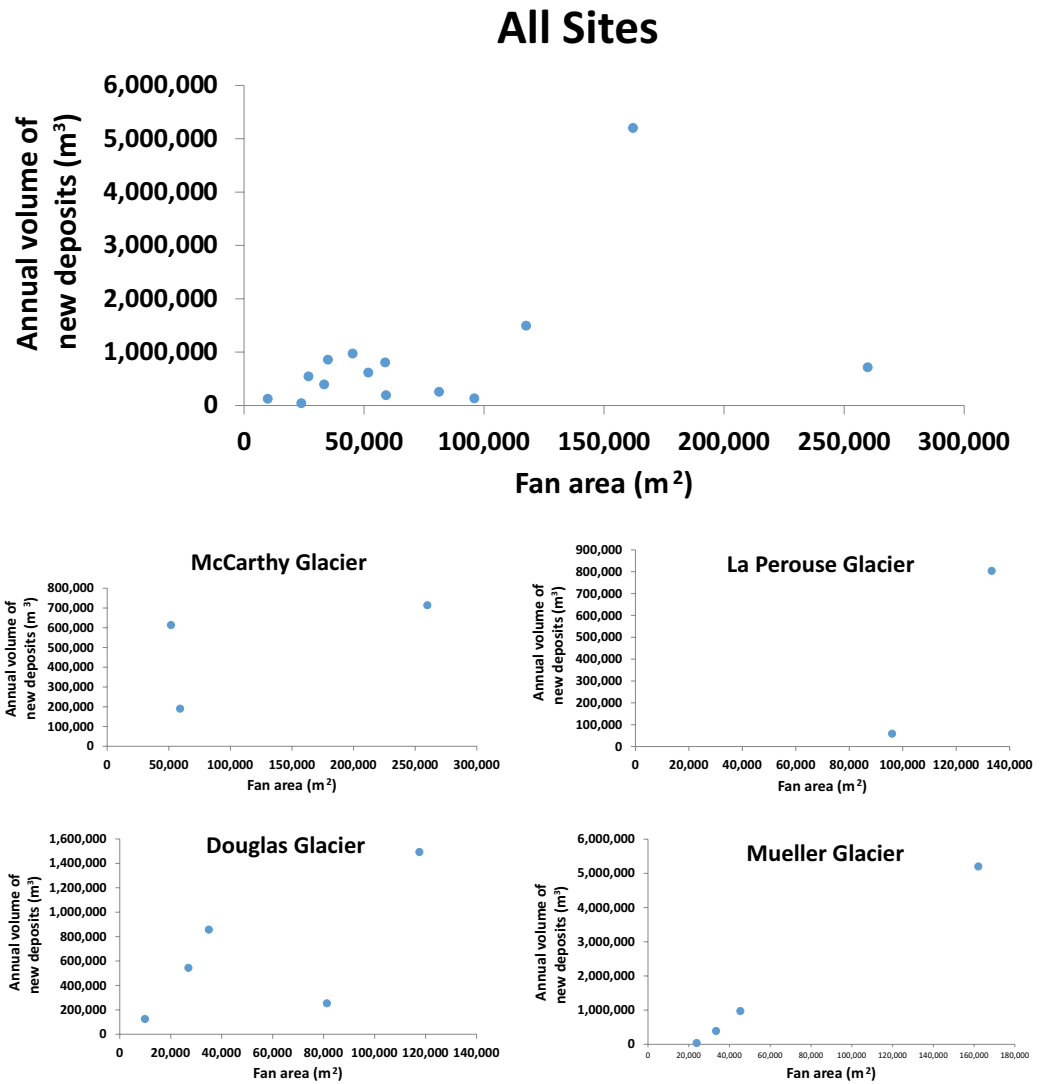

Figure 24. Relationships between fan area and annual depositional volume of new ice and sediment. Upper plot shows data from all 15 fans; lower plots show within-site data from each of the four sites studied. There is a positive relationship, but considerable scatter exists.

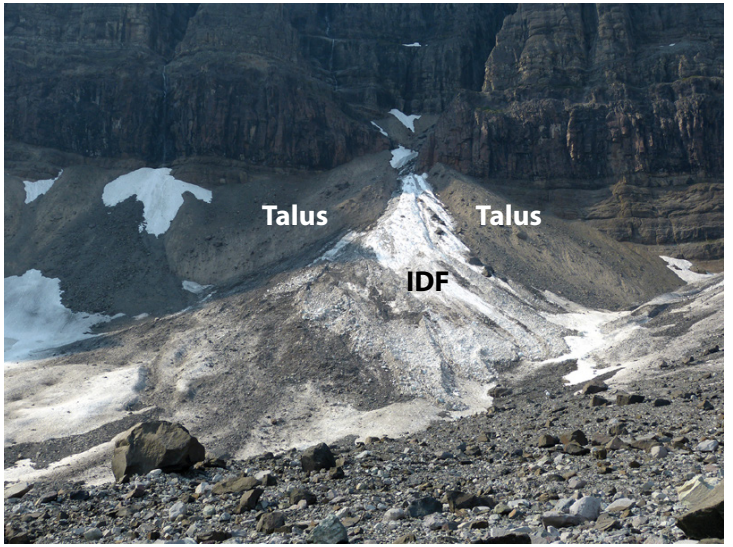

Figure 25. Photograph of fan-head trench on West Fan at McCarthy Glacier. Most mass flow deposits reaching the fan travel through an incised fan-head trench before splaying out onto mid-fan and distal-fan areas. Note extensive talus on both sides of fan-head trench. IDF—icy debris fan.

debris flows and ice avalanches. It appears that the pace of activity through the fan-head trench has prevented its refilling.

Icy debris fan sediment deposits are also different than their alluvial counterparts. Ice is the dominant component of IDF materials. Fresh ice avalanche deposits, which dominate IDF deposits, contain ~95%–98% ice clasts, with <5% clastic sediments. After days of ablation, clastic sediments may account for up to 50% of the materials visible on a surface lag. Below this lag, however, clastic materials rarely exceed 5% by volume. Icy debris flow deposits, which are far less abundant, may be >90% clastic in composition. No clast imbrication or stratification has been observed within IDF deposits, but it is important to note that excavation into these surfaces is nearly impossible, limiting observations to areas incised by hyperconcentrated flows and slush flows and large crevasses. Figure 26 illustrates a surface sediment lag and dominance of ice in subsurface exposures along IDF crevasse walls (also shown in Supplemental Item H[8]).

One of the most substantial differences between IDFs and alluvial fans is the region impacted by depositional activity on fan surfaces annually. Resurfacing area was determined by mapping the new deposit area of each event and dividing that area by the surface area of the fan. Icy debris fan surfaces were totally resurfaced during single depositional episodes numerous times in one year (Fig. 27), illustrating their exceptionally high rates of deposition. Large areas of alluvial fans are typically inactive annually; we are unaware of studies documenting resurfacing of alluvial fans more than several tens of percent. In contrast, IDFs experience resurfacing rates of >100% to >3000% annually (Table 2).

Valley glaciers underlying IDFs may change rapidly over shorter time periods (i.e., tens of meters of elevation change over several years) in comparison to alluvial fan basin floors. Thus, there is a complex dynamic between the frequency of material delivered to the fans and changes in the elevation of the underlying valley glacier. This complexity results in variable individual relationships in the evolution of IDF geometry and their adjacent valley glacier. In all sites studied, valley glaciers thinned during the past decade; annual rates varied from <2 m (McCarthy) to >10 m (Mueller, La Perouse, and Douglas). The volume and elevation at some IDFs increased; on other IDFs, the fan elevation decreased while volume increased. Icy debris fan volume may increase while losing elevation overall, if IDF depositional rates exceed the rate of valley glacier thinning. Icy debris fans have been observed to increase their length along the fan axis (at the fan toe) in some situations where the glacier thinned rapidly (e.g., Fan 1 at Mueller extended >100 m during 2010–2016).

In summary, IDFs differ significantly from alluvial fans dominated by streamflow or debris flow processes. Icy debris fans, composed chiefly of ice and deposits emplaced by ice-dominated mass flow processes, represent either a new class of alluvial fans dominated by ice or an entirely new geomorphic class of landforms.

LINKAGE BETWEEN ICY DEBRIS FANS AND VALLEY GLACIERS

Observations of depositional activity at all four study sites document large annual contributions of ice and sediment to IDFs, in some cases >50% of the volume of the IDF based on our time-lapse imagery (Tables 3–6). As a result, most sites show annual increases in IDF volume judging from repeat TLS measurements (5%–33% at all fans except McCarthy Middle and West Fans), and some of this material is transferred to valley glaciers. Analysis of time-lapse photography of Fan 1 at Mueller Glacier shows observable flow of ice and/or sediment on the fan surface to the glacier (Supplemental Item F-3 [footnote 6]). The down-fan flow rate observed during March 2014–March 2015 was ~220–250 m/yr. This rate is high enough to transport material more than half the distance to the glacier in one year, given that the IDF is ~480 m long along its axis.

Ground penetrating radar data from McCarthy IDFs document subsurface features consistent with accumulation and deformation, i.e., internal brittle deformation and ductile glacial flow of layered deposits in a down-fan direction (Fig. 28). There is a change in the characteristics of the GPR reflections with depth below the surface of the IDF (Fig. 28B). Shallow GPR reflections indicate layers, which we interpret to be produced by the episodic deposition followed by ablation (Fig. 28B). Ground penetrating radar data show that these subsurface layers thin toward the IDF toe and also indicate crevasses within these layered deposits that imply vertical movement within the fan (Fig. 28B). Below the deepest reflector that extends laterally for >100 m (solid line on Fig. 28B)

[8]Supplemental Item H: Drone video of crevasse and stratification in La Perouse. Please visit https://doi.org/10.1130/GES01622.S8 or the full-text article on www.gsapubs.org to view Supplemental Item H.

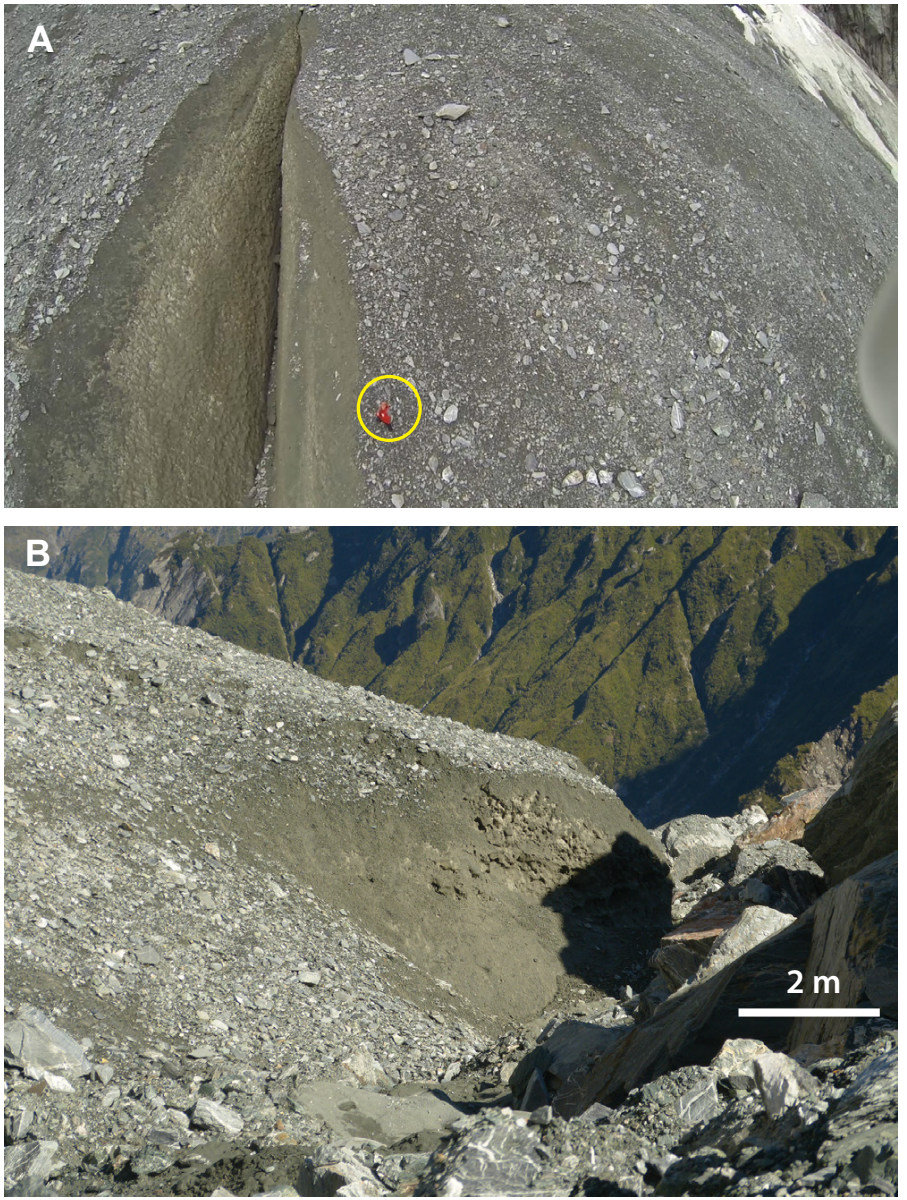

Figure 26. Internal stratigraphy of the distal parts of icy debris fans (IDFs) at La Perouse Glacier. (A) March 2015 drone photo into a large crevasse on East Fan (person in red for scale). (B) Oblique ground view of distal edge of Middle Fan where the toe has slumped along the margin of the rapidly thinning valley glacier. Both photos show the thin character of the surface ablation lag concentrated at the surface above an ice-rich material in the fans. Crude bedding dipping down-fan can be seen, but it is not well developed.

the characteristics of the GPR reflections include multiple diffractions (profile distances between 320 and 400 m, Fig. 28B) or weaker reflecting horizons with greater depth (profile distances greater than 400 m). We interpret these diffractions to be either large lithic clasts (i.e., boulders) or additional crevasses that terminate below the IDF surface. We infer that the weaker reflecting horizons and the crevasses observed in the layered deposits are produced by the IDF deposits transitioning and flowing into the valley glacier. Consistent with this interpretation, GPR data also indicate crevasses (some of which are visible at the surface) that imply vertical movement within the fan (Fig. 28B) (Supplemental Item F-3 [footnote 6]). These surficial and subsurface features support the interpretation of subsurface ice flow from the fans to the valley glaciers.

Figure 29 shows a schematic cross section highlighting the transfer of ice and sediment from icecaps through IDFs to valley glaciers. Several observations indicate that IDFs transition progressively into subjacent valley glaciers. For example, several large IDFs (in particular, East Fan at McCarthy, West Fan at Mueller, and La Perouse Fans) have extensive arcuate crevasses indicative of internal brittle deformation. The arcuate geometry of some crevasses along with time-lapse videos showing downslope flow toward the valley glacier are consistent with internal ductile flow as well (Supplemental Item F-3 [footnote 6]). Once thick enough, IDFs begin to exhibit glacial flow. The GPR data (Fig. 28) reveal changes in the orientation of the reflectors consistent with the progressive rotation of strata through time aided by extensional crevasses. Moreover, time-lapse imagery documents growth of extensional crevasses and extensional slumping of surface deposits (Supplemental File F-3). Collectively, our surface and subsurface data sets indicate that ice and sediment accumulates at the surface, becomes compacted as it is rapidly buried by new deposits, and experiences flow at tens of meters depth. In this sense, IDFs act as tributaries to the valley glaciers and are part of the glacial system. The continuum of ice and sediment transport from the IDFs through the subsurface to the valley glacier provides large volumes of ice to the annual mass budget of the valley glacier.

We have shown that even accounting for up to 10%–15% loss of deposited ice by ablation, the studied IDFs should be growing to accommodate the exceedingly high depositional rates unless ice and/or sediment is flowing from their basal regions into the underlying valley glaciers. The lack of substantial growth of IDFs is interpreted as evidence of extensive flow of ice and/or sediment from the IDFs into the valley glaciers. Although there are uncertainties in estimating the volume of valley glaciers as well as ablation, our estimates suggest that flow of ice and/or sediment from IDFs is variable, ranging from <1% to >20% of glacial volume annually (Table 8). The contributions of ice and/or sediment are highest where valley glaciers are decoupled from icecaps, ranging from ~4%–24% at McCarthy, Douglas, and Mueller Glaciers. Notably, our estimates of volume contributions are conservative minimum estimates. Our time-lapse imagery did not capture all IDFs per glacier, except at McCarthy Glacier. In addition, the cameras only captured relatively large events; field observations demonstrate that many smaller events routinely contribute ice and/or sediment. Thus, IDFs can represent a critical supply of ice to valley glaciers, especially those decoupled from icecaps.

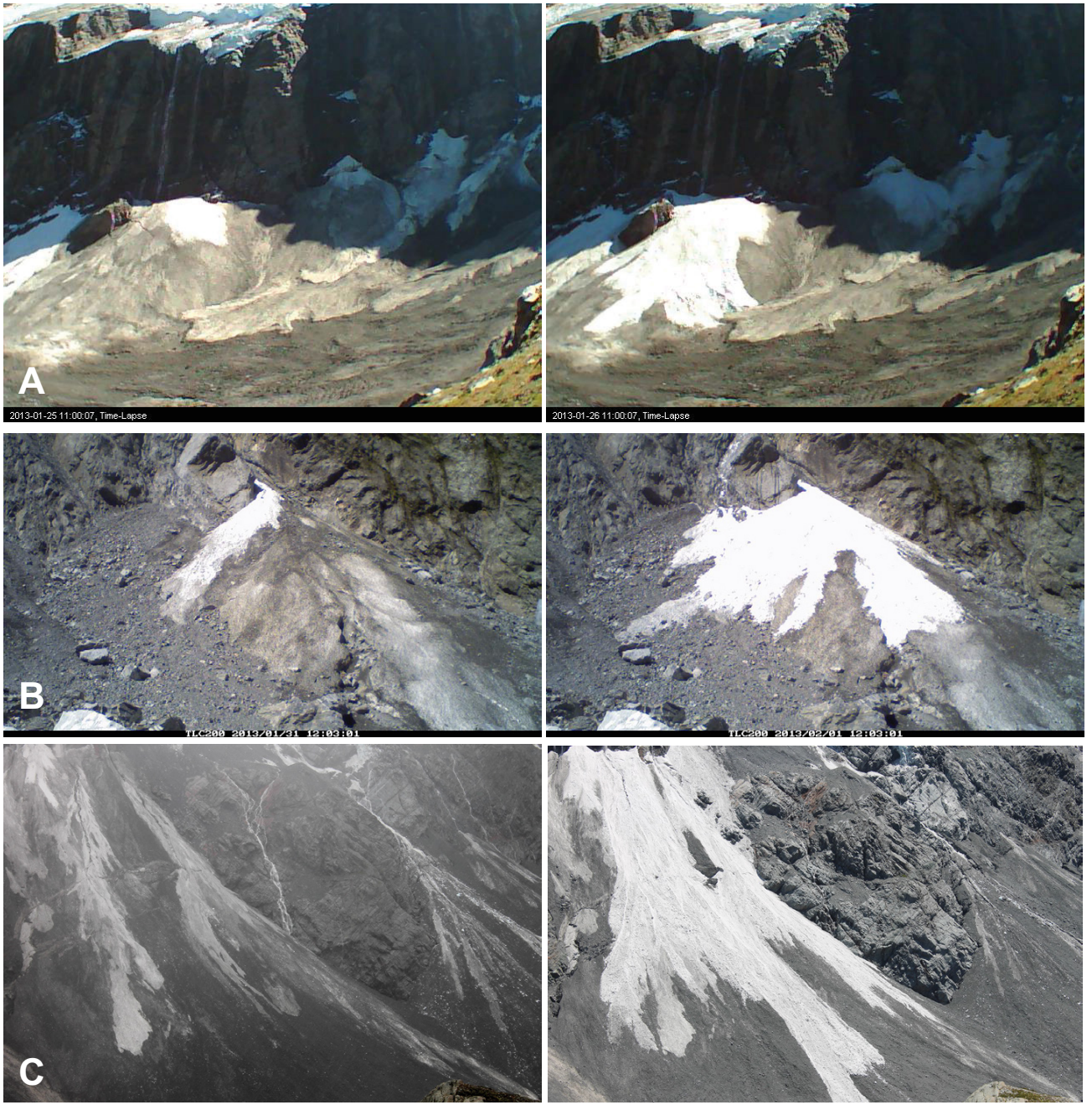

Figure 27. Examples of extensive resurfacing (coverage of the fans) by new deposits during one depositional episode over the course of less than 24 h. (A) 80% coverage by ice avalanches on Fan 4 at Douglas Glacier from 1/25/2013 to 1/26/2013. (B) 85% coverage by ice avalanches on Middle Fan at La Perouse from 1/31/2013 to 2/1/2013. (C) 65% coverage by ice avalanches of Fan 1 at Mueller Glacier from 12/30/2014 to 12/31/2014.

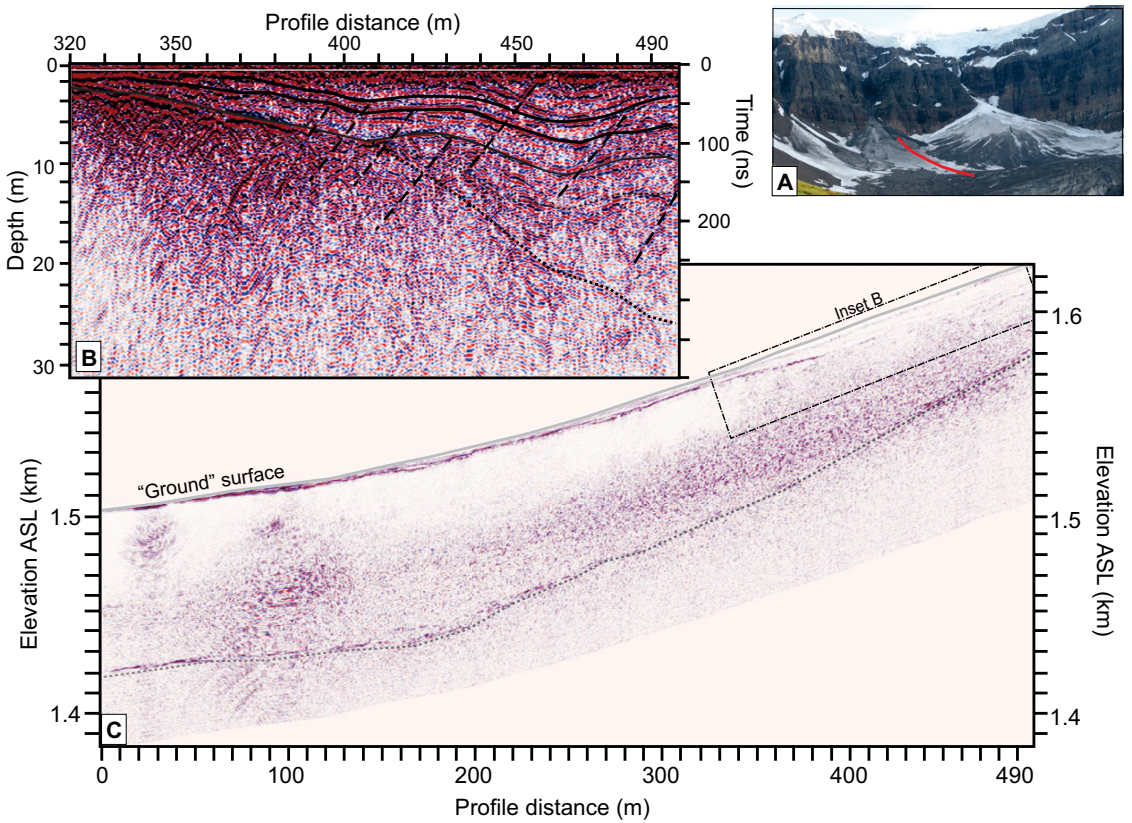

Figure 28. Ground penetrating radar (GPR) profile parallel to the axis of Middle Fan at McCarthy Glacier extending from the glacier onto the icy debris fan (IDF). (A) Ground photo showing the location of GPR profile (red line). (B) Unmigrated GPR profile on the IDF showing details of area denoted by black rectangle in (C). Note that elevations are not displayed. Depth based on wide-angle reflection and refraction (WARR) sounding on IDF providing a normal moveout (NMO) velocity of 0.158 m/ns and two-way travel time (TWTT) of 435 ns. Solid line denotes prominent reflection separating layered reflections interpreted as IDF deposits above and more abundant hyperbolic reflections below interpreted as either crevasses or boulders (lithic clasts). The dotted lines denote reflections that become less defined with depth. (C) Migrated and elevation-corrected GPR profile extending from glacier (left) up onto mid-fan area (right) using same NMO velocity. Elevations from RTK-GPS were used to display ground surface elevations, above sea level (ASL). The black dotted line connects prominent reflectors at depth interpreted to be the bedrock interface. We interpret a fan thickness of 45 m at mid-fan and a glacier thickness of 82 m.

Repeat TLS surveys quantify net changes in IDF topography and volume (Fig. 17) but fail to document the excessively high rate of depositional activity on the studied IDFs. Integrating daily imagery along with less frequent TLS surveys demonstrates that IDFs are extremely dynamic landforms. While TLS surveys provide a more precise measurement than time-lapse imagery, daily TLS measurements throughout the year are not practical in a remote, roadless, rugged setting. Thus, much of our knowledge of the IDF dynamics would be lost by not integrating daily imagery (i.e., the nature and pace and volume of mass wasting). For example, TLS surveys showed that Fan 3 on Douglas Glacier, New Zealand, increased by just 8% volume during a two-year period despite the addition of a photography-estimated addition of 56% (>857,500 m^3) deposited by 140 events in one year. An even more striking example, TLS surveys show that Middle Fan in McCarthy, Alaska, decreased in volume by 22% during a two-year period despite addition of a photography-estimated 34% volume of ice and sediment (>818,500 m^3) deposited by 126 events (Fig. 18; Tables 5 and 7). In summary, integration of time-lapse imagery with less frequent TLS surveys is needed to document net changes in IDF topography and volume and the frequency and volume of material added to the IDF and transferred to the valley glacier.

SUMMARY AND CONCLUSIONS

Icy debris fans are previously overlooked, transitional supraglacial landforms linking icecaps to valley glaciers. Icy debris fans occur at the mouths of small, incised bedrock catchments where ice from decoupled icecaps and sediment from bedrock walls accumulate. Icy debris fans are common landforms in rugged alpine terrain between degrading icecaps and valley glaciers. A survey using Google Earth imagery identified IDFs in diverse rugged settings worldwide (Fig. 30). Ice-dominated mass wasting from icecaps, through bedrock catchments, to IDFs, and finally flow to glaciers represent an important geomorphic process dominating the transfer of ice and sediment in alpine regions undergoing deglaciation.

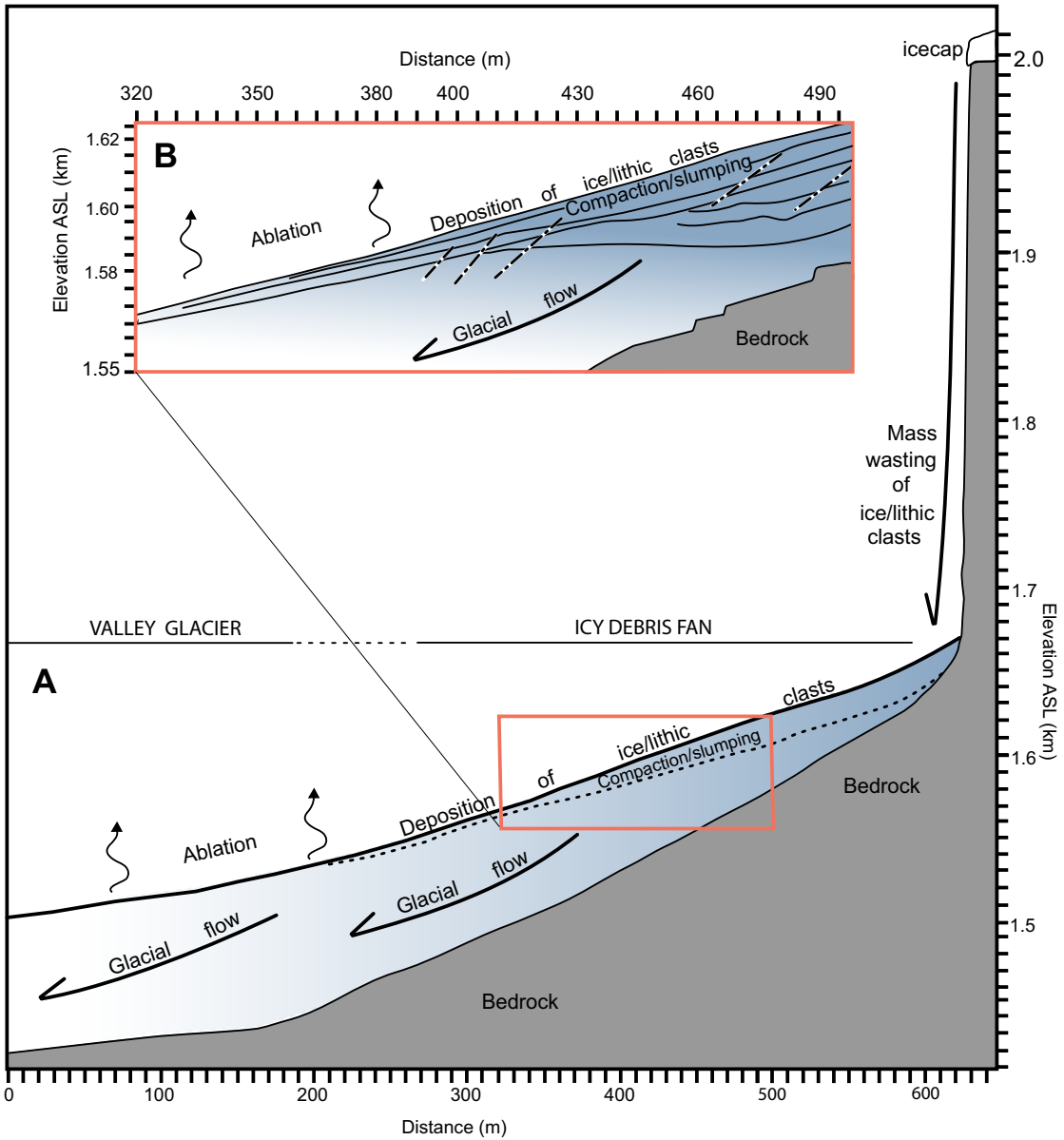

Figure 29. Schematic cross section highlighting the spatial transition between an icy debris fan (IDF) (dark blue) and subjacent valley glacier (white) in a cirque glacier where the fan axis is parallel to glacier flow. (A) Cross section with inset (B) is based on ground penetrating radar–derived interpretations and time-lapse imagery at McCarthy Glacier, Alaska (Fig. 28). McCarthy is the longest monitored IDF (2006–2015) and has yielded the greatest amount of high-resolution data; other sites exhibit different internal architecture and relationships between the axis of the fans and the direction of valley glacier flow. Importantly, axes of other fans are approximately perpendicular to valley glacier flow.

TABLE 8. ANNUAL CONTRIBUTION OF ICY DEBRIS FANS (IDFs) TO VALLEY GLACIERS

IDF site	Estimated glacier volume (m^3)[1]	Annual IDF volume contribution (m^3)	Annual IDF contribution to glacier (%)
McCarthy Glacier	11,000,000–18,000,000	1,518,000	8.4–13.8
La Perouse Glacier	147,000,000–200,000,000	937,000	<1
Douglas Glacier	50,000,000–85,000,000	3,275,000	3.9–6.6
Mueller Glacier[2]	27,000,000–33,000,000	6,607,000	20.0–24.4

[1]Range derived from two methods of estimating glacier volume: DeBeer and Sharp (2007); Bahr et al. (1997).
[2]Glacier volume estimated only for lower Mueller Glacier (below moulin).

This process may be especially important during early portions of the paraglacial interval. Additional field studies are needed to evaluate whether or not IDF deposits may be preserved in the stratigraphic record (Kochel and Trop, 2012). Based on our observations, IDF sediments are remobilized and transported into more distal environments (i.e., valley glacier till and pro-glacial outwash). We speculate that once the icecap and valley glacier have melted, IDF deposits may be incorporated into talus cones or preserved as unorganized, poorly sorted, coarse-grained accumulations of lithic fragments.

First-order findings from our 2013–2015 study of IDFs are as follows:

1. Depositional Variability

Icy debris fans received ice and sediment from an array of mass flow depositional processes originating from the overlying icecap and bedrock walls of their catchments. Depositional processes, in order of frequency, included ice avalanches, slush avalanches, slush flows, icy debris flows, hyperconcentrated flows, and rockfall and ice-rock avalanches.

Slush flows and slush avalanches dominated during transitional months (spring and fall) when rain-on-snow events were most common. Most slush flows probably originated from seasonal snow within their catchments and were mobilized by rainfall or rapid snowmelt. Icy debris flows, occurring only on fans below catchments with geomorphic complexity and abundant bedrock exposure, accounted for <5% of deposits at those fans. Icy debris flows occurred mostly during transitional and summer months in Alaska and transitional and winter months in more temperate New Zealand, mostly following rainfall, snowmelt, rain-on-snow, and outbursts (jökulhlaups). At McCarthy Glacier, slush avalanches and slush flows were nearly equal to the pace of ice avalanches during winter and transitional months. At Mueller Glacier, slush flows and slush avalanches also dominated during winter and transitional months. Rockfalls were rare on IDFs although quite common in larger, more complex catchments; one exception was the catastrophic rockfall and icy rock avalanche at Douglas Glacier. Days with the largest number of events and the highest areal extent of IDF deposits typically followed large rainfall. At all sites studied, depositional activity occurred throughout the year, but the pace of activity and the dominant depositional process varied seasonally. Most sites had a slower pace of activity during winter. Peak activity rates occurred during transitional and summer months. Process dominance differed seasonally at some locations. Ice avalanches occurred throughout the year, but occurred at higher rates during winter and summer.

2. Pace and Areal Extent of Deposition

Icy debris fans experienced vastly higher rates of annual resurfacing by new deposits compared to alluvial fans. Icy debris fans experienced annual resurfacing rates ranging from 226% to 4308%. Rates exceeding 2000% were common on half of the fans studied. The high rates of depositional activity on IDFs have implications in the management of hazards for visitors to these alpine regions (Allen et al., 2008, 2009). Better characterization of the nature and frequency of these poorly understood processes and landforms will help mitigate the impacts of these hazardous phenomena.

3. Volume of Deposition

Large volumes of ice and sediment accumulated on IDFs, in some cases >50% of the fan volume. Volume contributed to IDFs varied between sites but often exceeded 1,000,000 m^3 annually. For example, >5,000,000 m^3 of ice were delivered to Fan 1 at Mueller Glacier in one year.

4. Influence of Catchments on Deposition

Variations in depositional process dominance and volume of IDFs are attributable to variations in catchment morphology and connectivity to the icecap. Fans with small, geomorphically simple catchments as well as larger ones with limited bedrock exposure almost exclusively received deposits from ice avalanches, slush avalanches, and slush flows. Fans with large, geomorphically complex catchments were constructed by a wider array of processes, including icy debris flows and hyperconcentrated flows. Geomorphically complex catchments typically had more bedrock exposed and numerous locations where ice and sediment could be temporarily stored. Subsequent entrainment of stored sediments by ice avalanches and floods resulted in a mixture of ice and sediment delivered to the fans. Rich in sediment, icy debris flows and hyperconcentrated flows appeared initially darker compared to avalanche deposits. Icy debris flows were observed only on IDFs with complex geomorphic catchments and abundant bedrock exposure.

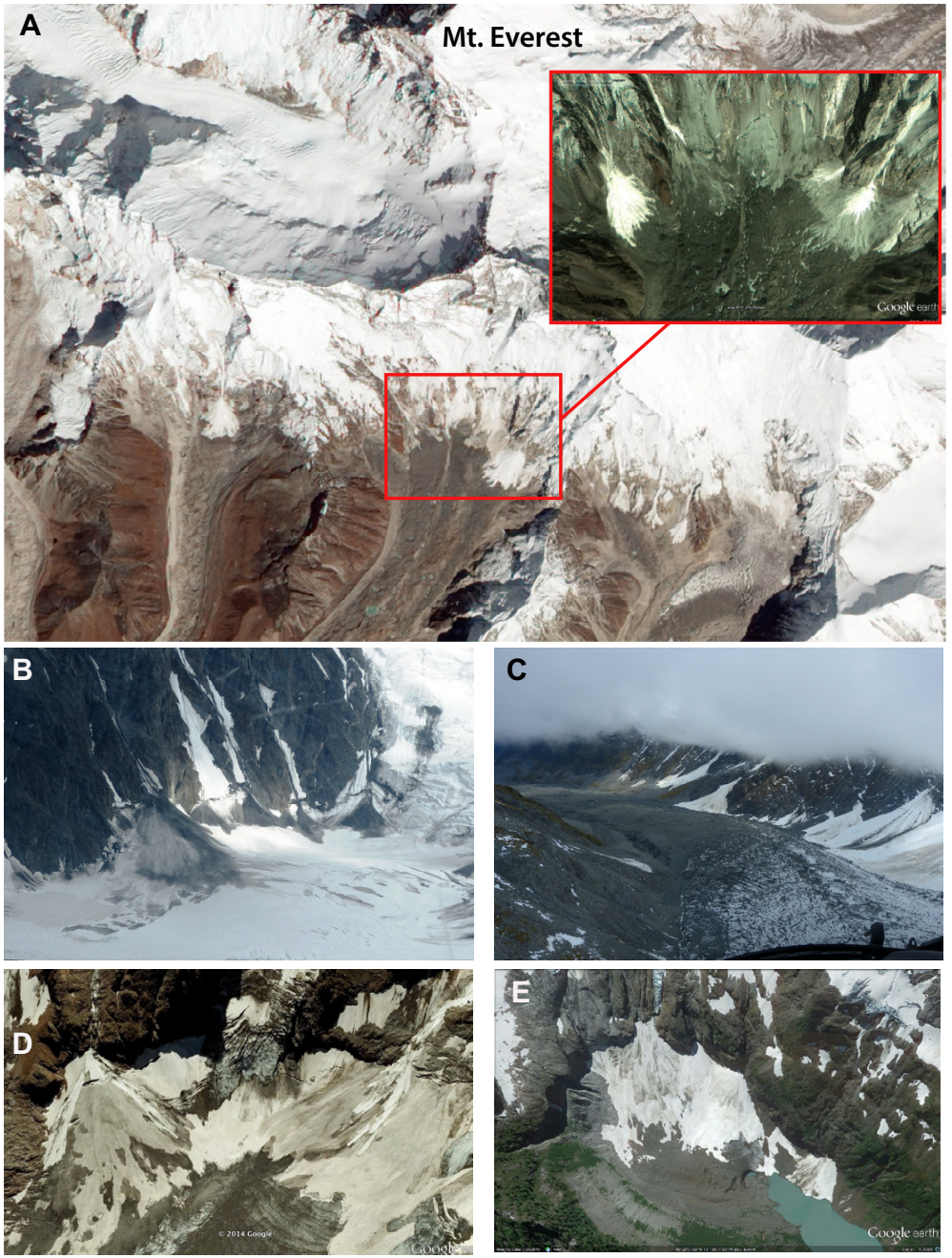

Figure 30. Photographs showing icy debris fans (IDFs) in diverse glaciated settings, including (A) Himalayan Mountains (NASA Earth Observatory image–Everest_ali_2012290 10/25/11); (B) Chugach Mountains, Alaska; (C) Balfour Glacier, Southern Alps, New Zealand; (D) Mount Hubel, Alps, Switzerland (Google Earth image); and (E) Mount Baker, Cascade Mountains, Washington, USA (Google Earth image). Not shown are examples we have mapped in Western British Columbia, Canada; Peru and Chile, Andes Mountains, South America. Variable resolution of imagery precludes mapping IDFs given their relatively small areal extent.

5. Influence of Icecap Connectivity on Deposition

The degree of connectivity to icecap supply also affected IDF depositional processes. Fans with abundant icecap exposure tended to be larger and dominated by ice avalanches. In contrast, IDFs with less icecap exposure tended to be smaller and experienced a wider range of processes, including icy debris flows and hyperconcentrated flows.

6. Controls on Fan Size

Unlike alluvial fans, there is a variable relationship between fan size and catchment size. There is a less variable relationship between fan size and the pace and volume of depositional events. Because ice-rich mass flows dominated depositional processes, IDFs with the largest area of exposed icecap face above their catchments were typically largest. Secondarily, IDFs with less geomorphically complex catchments tended to be larger.

7. Impact of IDF Deposition on Valley Glacier Budgets

Icy debris fans served as major contributors to ice budgets of associated valley glaciers. Annual contributions of ice from IDFs to valley glaciers ranged from <1% to >20% of glacier volume during the study interval. Glaciers lacking any direct upslope connection to icecaps via icefalls were more affected by IDF contributions; these include Douglas Glacier and McCarthy Glacier. Projections of glacier change and mass balance should include ice and/or sediment contributions from IDFs, especially for glaciers decoupled from icecaps.

In summary, this study better documents and quantifies the processes operating on IDFs, an essentially unexplored landform common in deglaciating alpine environments. We describe a new class of alluvial fans composed chiefly of ice emplaced by ice-dominated ice flows, illustrating the role of ice in alluvial fan dynamics in alpine environments. Finally, IDFs contribute important amounts of ice and sediment to valley glaciers; these volumes of ice have not been included in mass balance models.

ACKNOWLEDGMENTS

Keith Williams, UNAVCO, was instrumental in our field studies; he acquired repeat TLS surveys and made important contributions to other aspects of our field work. The following Bucknell University students helped collect and analyze data: Ben Bliss, Chris Duda, Steve Grune, Stew Kabis, Kim Lapsznski, Sandy Logan, Seamus McLaughlin, Brian Moretti, Alex Pellicciotti, Mattie Reid, Darin Rockwell, Erica Rubino, Charles Scales, Tracey Smith, Katherine Wagner, and Liz Wills. Trevor Chinn provided helpful insights on New Zealand glaciology. We thank Travis Kochel for help with fieldwork and for introducing us to new IDFs in New Zealand. The National Science Foundation Geomorphology and Land Program (grant EAR-1224720) provided primary funding. Grants from the National Geographic Society–Waitt Foundation Discovery Grant Program and Bucknell University supported earlier research. We thank the following parks and agencies for their collaboration and support: Wrangell–St. Elias National Park and Preserve in Alaska (Eric Veach and Mike Loso); New Zealand Department of Conservation, Westland/Tai Poutini (Ingrid Gruner) and Aoraki/Mount Cook National Parks in New Zealand (Ray Bellringer); Brad Jordan and Carilee Dill (Bucknell University) for logistical assistance; Last Frontier Air Ventures (Alaska) and The Helicopter Line (New Zealand) for air support accessing backcountry field sites. Constructive reviews by Drs. Noel Potter, Joseph Levy, and Shanaka de Silva helped us improve the manuscript.

REFERENCES CITED

Alean, J., 1985a, Ice avalanche activity and mass balance of a high-altitude hanging glacier in the Swiss Alps: Annals of Glaciology, v. 6, p. 248–249, https://doi.org/10.1017/S026030550001048X.

Alean, J., 1985b, Ice avalanches: Some empirical information about their formation and reach: Journal of Glaciology, v. 31, p. 324–333, https://doi.org/10.1017/S0022143000006663.

Allen, S.K., Owens, I., and Sirguey, P., 2008, Satellite remote sensing procedures for glacial terrain analyses and hazard assessment in the Aoraki Mount Cook region, New Zealand: New Zealand Journal of Geology and Geophysics, v. 51, p. 73–87.

Allen, S.K., Schneider, D., and Owens, J.F., 2009, First approaches towards modeling glacial hazards in the Mount Cook region of New Zealand's Southern Alps: Natural Hazards and Earth System Sciences, v. 9, p. 481–499.

Bahr, D.B., Meier, M.F., and Peckham, S.D., 1997, The physical basis of glacier volume-area scaling: Journal of Geophysical Research, v. 102, no. B9, p. 20,355–20,362.

Barnhart, T., and Crosby, B., 2013, Comparing two methods of surface change detection on an evolving thermokarst using high-temporal-frequency terrestrial laser scanning, Selawik River, Alaska: Remote Sensing, v. 5, p. 2813–2837, https://doi.org/10.3390/rs5062813.

Benn, D.I., and Evans, D.J.A., 1998, Glaciers and Glaciation: London, Arnold, 734 p.

Benn, D.I., and Owen, L.A., 2002, Himalayan glacial sedimentary environments: A framework for reconstructing and dating the former extent of glaciers in high mountains: Quaternary International, v. 97–98, p. 3–25, https://doi.org/10.1016/S1040-6182(02)00048-4.

Benn, D.I., Kirkbride, M.P., Owen, L.A., and Brazier, V., 2003, Glaciated valley land systems, *in* Evans, D.J., ed., Glacial Land Systems: London, Edward Arnold, p. 372–406.

Blair, T.C., and McPherson, J.G., 1994, Alluvial fans and their natural distinction from rivers based on morphology, hydraulic processes, sedimentary processes, and facies assemblages: Journal of Sedimentary Research, v. 64, p. 450–489.

Bradford, J.H., Harper, J.T., and Brown, J., 2009, Complex dielectric permittivity measurements from ground-penetrating radar data to estimate snow liquid water content in the pendular regime: Water Resources Research, v. 45, p. W08403, https://doi.org/10.1029/2008WR007341.

Bull, W.B., 1964, Geomorphology of segmented alluvial fans in western Fresno County, California: U.S. Geological Survey Professional Paper 352-E, 128 p.

Chinn, T.J., Heydenrych, C., and Salinger, M.J., 2005, Use of ELA as a practical method of monitoring glacier response to climate in New Zealand's Southern Alps: Journal of Glaciology, v. 51, p. 85–95, https://doi.org/10.3189/172756505781829593.

Chinn, T.J., Kargel, J.S., Leonard, G.J., Haritashya, U.K., and Pleasants, M., 2014, New Zealand's Glaciers, *in* Kargel, J.S., Leonard, G.J., Bishop, M.P., Kääb, A., and Raup, B.H., eds., Global Land Ice Measurements from Space: Berlin, Springer, p. 675–715.

Church, M.A., and Ryder, J.M., 1972, Paraglacial sedimentation: A consideration of fluvial processes conditioned by glaciations: Geological Society of America Bulletin, v. 83, p. 3059–3071, https://doi.org/10.1130/0016-7606(1972)83[3059:PSACOF]2.0.CO;2.

Cox, S.C., McSaveney, M.J., Spencer, J., Allen, S.K., Ashraf, S., Hancox, G.T., Sirguey, P., Salichon, J., and Ferris, B.G., 2015, Rock avalanche on 14 July 2014 from Hillary Ridge, Aoraki/Mount Cook, New Zealand: Landslides, v. 12, p. 395–402, https://doi.org/10.1007/s10346-015-0556-7.

Das, I., Hock, R., Berthier, E., and Lingle, C.S., 2014, 21st-century increase in glacier mass loss in the Wrangell Mountains, Alaska, USA, from airborne laser altimetry and satellite stereo imagery: Journal of Glaciology, v. 60, p. 283–293, https://doi.org/10.3189/2014JoG13J119.

DeBeer, C.M., and Sharp, M.J., 2007, Recent changes in glacier area and volume within the southern Canadian Cordillera: Annals of Glaciology, v. 46, p. 215–221.

Decaulne, A., and Saemundsson, T., 2006, Geomorphic evidence for present-day snow-avalanche and debris-flow impact in the Icelandic Westfjords: Geomorphology, v. 80, p. 80–93, https://doi.org/10.1016/j.geomorph.2005.09.007.

Decaulne, A., and Sæmundsson, T., 2010, Distribution and frequency of snow-avalanche debris transfer in the distal part of colluvial cones in central north Iceland: Geografiska Annaler. Series A. Physical Geography, v. 92, p. 177–187, https://doi.org/10.1111/j.1468-0459.2010.00388.x.

Giardino, J.R., and Vitek, J.D., 1988, Rock glacier rheology: A preliminary assessment, *in* Senneset, K., ed., Proceedings of the 5th International Conference on Permafrost: Trondheim, Tapir Publishers, p. 744–748.

Grune, S., 2016, Dynamics of icy debris fans on the McCarthy Glacier, Wrangell Mountains, Alaska: Analysis of two years of time-lapse imagery [B.S. thesis]: Lewisburg, Pennsylvania, Bucknell University, 184 p.

Hamilton, S.J., and Whalley, W.B., 1995, Rock glacier nomenclature: A re-assessment: Geomorphology, v. 14, p. 73–80, https://doi.org/10.1016/0169-555X(95)00036-5.
Hancox, G.T., and Thomson, R., 2013, The January 2013 Mt. Haast rock avalanche and ball ridge rock fall in Aoraki/Mt Cook National Park, New Zealand: GNS Science Report 2013/33, August 2013, 27 p.
Jacob, R.W., Trop, J.M., Kochel, R.C., Smith, T.D., and Rubino, E.M., 2017, GPR to image subsurface characteristics of icy debris fans in New Zealand and Alaska: Edinburgh, 9th International Workshop on Advanced Ground Penetrating Radar (IWAGPR), p. 1–6.
Johnson, A.M., and Rodine, J.R., 1984, Debris flow, *in* Brunsden, D., and Prior, D.B., eds., Slope Instability: Chichester, UK, Wiley, p. 257–361.
Kerr, T., Owens, I., Rack, W., and Gardner, R., 2009, Using ground-based laser scanning to monitor surface change on the Rolleston Glacier, New Zealand: Journal of Hydrology. New Zealand, v. 48, p. 59–71.
King, C.A.M., 1959, Geomorphology in Austerdalen, Norway: The Geographical Journal, v. 125, p. 357–369, https://doi.org/10.2307/1791119.
King, C.A.M., and Ives, J.D., 1956, Glaciological observations on some of the outlet glaciers of south-west Vatnajokull: Part 11: Ogives: Journal of Glaciology, v. 2, p. 646–651, https://doi.org/10.3189/S0022143000033098.
Kochel, R.C., and Trop, J.M., 2008, Earth analog for high-latitude landforms and recent flows on Mars: Icy debris fans in the Wrangell volcanic field, Alaska: Icarus, v. 196, p. 63–77, https://doi.org/10.1016/j.icarus.2008.03.006.
Kochel, R.C., and Trop, J.M., 2012, Morphology and dynamics of icy debris fans: Landform evolution along degrading escarpments undergoing rapid deglaciation in Alaska and New Zealand: Geomorphology, v. 151, p. 59–76, https://doi.org/10.1016/j.geomorph.2012.01.014.
Martin, E.H., and Whalley, W.B., 1987, Rock glaciers. Part 1, Rock glacier morphology: Classification and distribution: Progress in Physical Geography, v. 11, p. 260–282, https://doi.org/10.1177/030913338701100205.
Masiokas, M.H., Luckman, B.H., Villalba, R., Ripalta, A., and Rabassa, J., 2010, Little Ice Age fluctuations of Glacier Rio Manso in the northern Patagonian Andes of Argentina: Quaternary Research, v. 73, p. 96–106, https://doi.org/10.1016/j.yqres.2009.08.004.
Matthews, J.A., and McCarroll, D., 1994, Snow-avalanche impact landforms in Breheimen, Southern Norway: Origin, age, and paleoclimatic implications: Arctic and Alpine Research, v. 26, p. 103–115, https://doi.org/10.2307/1551773.
Owen, L.A., and Derbyshire, E., 1989, The Karakoram glacial depositional system: Zeitschrift für Geomorphologie, v. 76, p. 33–73.
Picco, L., Mao, L., Cavalli, M., Buzzi, E., Rainato, R., and Lenzi, M.A., 2013, Evaluating short-term morphological changes in a gravel-bed braided river using terrestrial laser scanner: Geomorphology, v. 201, p. 323–334, https://doi.org/10.1016/j.geomorph.2013.07.007.
Potter, N., Jr., 1972, Ice-cored rock glacier, Galena Creek, northern Absaroka Mountains, Wyoming: Geological Society of America Bulletin, v. 83, p. 3025–3058, https://doi.org/10.1130/0016-7606(1972)83[3025:IRGGCN]2.0.CO;2.
Rapp, A., 1995, Case studies of geoprocesses and environmental change in mountains of northern Sweden: Geografiska Annaler, v. 77, p. 189–198, https://doi.org/10.1080/04353676.1995.11880439.
Rapp, A., and Nyberg, R., 1981, Alpine debris flows in northern Scandinavia: Morphology and dating by lichenometry: Geografiska Annaler, v. 64A, p. 183–196.
Reid, M.M., 2015, Mass wasting processes, geomorphic response, and seasonal variation of icy debris fans on the La Perouse Glacier and Douglas Glacier, Tai Poutini, Westland National Park, Southern Alps, New Zealand [Undergraduate Honor's thesis]: Lewisburg, Pennsylvania, Bucknell University, 132 p.
Ritter, D.F., Kochel, R.C., and Miller, J.R., 2011, Process Geomorphology (fifth edition): Long Grove, Illinois, Waveland Press, 652 p.
Salinger, J., Chinn, T.J., Willsman, A., and Fitzharris, B., 2008, Glacier response to climate change: Water and Atmosphere, v. 16, p. 16–17.
van der Woerd, J., Owen, L.A., Tapponnier, P., Xiwei, X., Kervyn, F., Finkel, R.C., Barnard, P.L., 2004, Giant, ~M8 earthquake-triggered ice avalanches in the eastern Kunlun Shan, northern Tibet: Characteristics, nature and dynamics: Geological Society of America Bulletin, v. 116, p. 394–406, https://doi.org/10.1130/B25317.1.
Vaughan, D.G., Comiso, J.C., Allison, I., Carrasco, J., Kaser, G., Kwok, R., Mote, P., Murray, T., Paul, F., Ren, J., Rignot, E., Solomina, O., Steffen, K., and Zhang, T., 2013, Observations: Cryosphere, *in* Stocker, T.F., Qin, D., Plattner, G.K., Tignor, M., Allen, S.K., Boschung, J., Nauels, A., Xia, Y., Bex, V., and Midgley, P.M., eds., Climate Change 2013: The Physical Science Basis, Contribution of Working Group I to the Fifth Assessment Report of the Intergovernmental Panel on Climate Change: Cambridge, UK and New York, NY, USA, Cambridge University Press, p. 317–382.
White, S.E., 1976, Rock glaciers and block fields, review and new data: Quaternary Research, v. 6, p. 77–97, https://doi.org/10.1016/0033-5894(76)90041-7.